Analysis of site-directed mutants of the F_X-binding region of photosystem I and second site revertants in *Chlamydomonas reinhardtii*

A thesis submitted by
DEREK WILLIAM WRIGHT
for the degree of Master of Philosophy.

Department of Biology
University College London
February 1999.

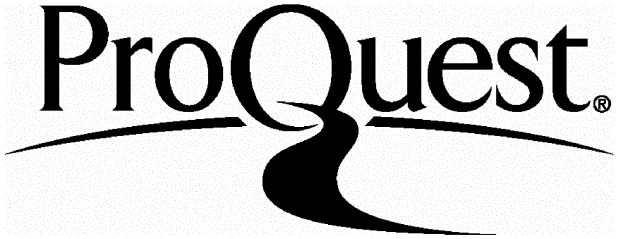

ABSTRACT

This thesis reports structural, biochemical and biophysical analyses of photosystem I (PSI), using site-directed mutants and second-site revertants of *Chlamydomonas reinhardtii*. The principal techniques used were non-denaturing gel electrophoresis, biochemical assays of electron transport, continuous wave and pulsed electron paramagnetic resonance spectroscopy (EPR) and electron-nuclear double resonance spectroscopy (ENDOR).

Site-directed mutants of the conserved region of PsaA which is thought to form the F_X binding site have been previously generated (Hallahan *et al.*, 1995): C575D, C575H, C575S and D576L, all of which are non-photosynthetic. Photosynthetic second-site revertants have been generated from D576L (Evans *et al.*, 1999). The secondary mutations are in nuclear genes.

Non-denaturing polyacrylamide gel electrophoresis of thylakoid membranes indicated that PSI did not assemble in C575D. C575H, C575S and D576L assembled PSI at reduced levels.

Continuous wave EPR showed no photoreduction of iron-sulphur centres in C575H. Spectra of F_A/F_B in D576L and the revertants showed an altered electron distribution.

$NADP^+$ photoreduction was abolished in the site-directed mutants and restored in the revertants.

Photoreduction of methyl viologen took place with thylakoid membranes of C575S and D576L. Photoreduction of neutral red but not of methyl viologen took place with C575H.

EPR and ENDOR spectra of $A_1^{\cdot -}$ indicated no significant differences in electronic structure or binding site structure between wild type and D576L, and only very small differences between *C. reinhardtii* and spinach. Rates of electron transfer were determined using time-resolved pulsed EPR. Forward electron transfer from A_1 did not take place in C575H and C575S. The rate of forward electron transfer from A_1 was considerably slower in D576L than in wild type. The revertants showed rates similar to wild type.

C575H and C575S do not bind F_X. In D576L, PsaC is incorrectly bound. The structure of the F_X binding site is incorrect in D576L, and is corrected in the revertants.

DEDICATION

This thesis is dedicated to Dr. I. Shirley.

ACKNOWLEDGEMENTS

I would like to thank Prof. Mike Evans for his supervision and advice. I would also like to thank my second supervisor Dr. Saul Purton and postgraduate advisor Prof. Jonathan Nugent.

I acknowledge Prof. Mike Evans, Dr. Peter Heathcote and Dr. Stephen Rigby for their collaboration in the spectroscopic work presented in this thesis.

I am also grateful to my other colleagues in the Photosynthesis Research Group, in particular Daniel Emlyn-Jones and Vaishali Patel and technicians Angela Ivison and Susan Carter.

This work was funded by BBSRC.

Table of Contents **Page**

List of Tables and Figures

ABBREVIATIONS

% v/v	concentration as percentage volume to volume
%w/v	concentration as percentage weight to volume
A_0	photosystem I primary acceptor
A_1	photosystem I secondary acceptor
$A_\perp$	perpendicular axial hyperfine coupling component
$A_\parallel$	parallel axial hyperfine coupling component
A_{iso}	isotropic hyperfine coupling constant
ATP	adenosine triphosphate
A. variabilis	*Anabaena variabilis*
C. limicola	*Chlorobium limicola*
C. reinhardtii	*Chlamydomonas reinhardtii*
DAD	diaminodurol
DCMU	3-((3,4-dichlorophenyl)-1,1-dimethylurea)
DCPIP	2,6-dichlorophenolindophenol
dH_2O	distilled water
ddH_2O	double distilled water
DEPC	diethylpyrocarbonate
DNA	deoxyribonucleic acid
ΔH_{ptp}	peak to peak linewidth
E_m	midpoint redox potential
E. coli	*Escherichia coli*
EDTA	ethylenediaminetetraacetic acid

ENDOR	electron nuclear double resonance
EPR	electron paramagnetic resonance
ESEEM	electron spin echo envelope modulation
ESP	electron spin polarised
F_A	iron-sulphur centre A of photosystem I
F_B	iron-sulphur centre B of photosystem I
F_X	iron-sulphur centre X of photosystem I
FCCP	carbonylcyanide p-fluoromethoxy-phenylhydrazone.
FNR	ferredoxin $NADP^+$ oxidoreductase
H. chlorum	*Heliobacterium chlorum*
HEPES	N-2-hydroxyethylpiperazine-N-2-ethanesulphonic acid
hfc	hyperfine coupling
kb	kilobases
kDa	kilodaltons
LHCI	light-harvesting complex of photosystem I
$LiDodSO_4$	lithium dodecyl sulphate
$NaDodSO_4$	sodium dodecyl sulphate
NADP	nicotinamide adenine dinucleotide phosphate
P680	primary electron donor of photosystem II
P680*	excited state of above
P700	primary electron donor of photosystem I
P798	primary donor of heliobacteria
PAGE	polyacrylamide gel electrophoresis

Pheo	pheophytin
ps	picoseconds
PSI	photosystem I
PSII	photosystem II
r.f.	radio frequency
rpm	revolutions per minute
SDS	sodium dodecyl sulphate
sp.	species
TAP	tris acetate phosphate medium
TEMED	N,N,N',N' tetramethyl-ethylenediamine

Symbols for Amino Acids

C	cysteine
D	aspartate
H	histidine
G	glycine
L	lysine
P	proline
R	arginine
S	serine
T	threonine
Y	tyrosine

1.0 INTRODUCTION

1.1 Historical background

One of the most important steps towards the modern biochemical understanding of photosynthesis was made by van Niel in the 1920's (reviewed in van Niel, 1941), who formulated a view of photosynthesis as a light-driven separation of oxidant and reductant.

Bacterial photosynthesis may be described by the equation

$$CO_2 + 2H_2A \rightarrow (CH_2O) + H_2O + 2A$$

where CO_2 is reduced to (CH_2O) and H_2A is an oxidizable substrate such as H_2S.

The overall equation for higher plant photosynthesis

$$6CO_2 + 6H_2O \rightarrow C_6H_{12}O_6 + 6O_2$$

may be rewritten as the analogous equation

$$CO_2 + 2H_2O \rightarrow (CH_2O) + H_2O + O_2.$$

Van Niel wrote the primary photochemical reaction as a splitting of water into reducing and oxidizing equivalents which reduce CO_2 and oxidize H_2A.

Elements of this scheme were later verified experimentally. Hill (1939) showed that CO_2 assimilation could be separated from photochemistry by adding an

oxidizing agent such as Fe^{3+} to a chloroplast suspension which is reduced in place of CO_2. Gaffron (1940) showed that incubation with H_2 in anaerobic conditions in algae led to CO_2 assimilation without O_2 evolution, with H_2 replacing H_2O as the oxidizable substrate.

According to van Niel's scheme, four water molecules are split to provide four reducing equivalents which reduce one CO_2 molecule. However, eight quanta are required to evolve one O_2 molecule, implying the co-operation of two quanta. This can be explained in a model involving two distinct photochemical systems, and a strong line of evidence for this was the discovery of the "red drop" and enhancement effects. For single wavelengths, the quantum efficiency of photosynthesis drops sharply at wavelengths longer than 680 nm, although chlorophyll absorbs in the 680 to 700 nm range. However, if light of wavelength longer than 680 nm is used together with shorter wavelength light, enhancement occurs: the quantum yield is greater than the sum of the yields for the two wavelengths given separately. This implied that there are two photochemical systems, only one of which can operate with wavelengths longer than 680 nm. These experiments are reviewed by Emerson (1958).

Hill and Bendall (1960) outlined a new framework which elaborated on van Niel's ideas and was consistent with recent findings, known as the "Z-scheme", in which the reducing equivalents are produced by photosystem I (PSI) and the oxidizing equivalents are produced by photosystem II (PSII), with flow of electrons from PSII to PSI.

Duysens *et al.* (1961) provided experimental support for the Z-scheme using differential absorption spectrometry. Absorption of cytochrome at 420 nm in a suspension of *Porphyridium cruentum* was measured . Exciting light of 680 nm or

562 nm was applied. 680 nm light alone led to oxidation of the cytochrome and superposition of 562 nm light caused partial rereduction. Addition of the herbicide DCMU, known to abolish photosynthetic oxygen evolution, abolished the reducing effect but not the oxidizing effect. These findings backed up the Z-scheme model, suggesting that electrons pass from PSII to PSI via a cytochrome, and electron flow from PSII to the cytochrome is blocked by DCMU.

A model for the formation of ATP was postulated in the chemiosmotic hypothesis of Mitchell (1961). It was proposed that electron transport was vectorial, leading to the generation of a proton gradient across the thylakoid membrane. The electromotive force generated by this gradient drives the formation of ATP by the ATPase complex.

Experimental evidence for Mitchell's hypothesis was obtained in the "acid bath" experiment of Jagendorf and Uribe (1966), which showed that the artificial imposition of a pH gradient across the thylakoid membrane leads to ATP synthesis in the dark.

The historical background of photosynthesis is very well reviewed in Clayton (1980).

Work over the past 30 years has elucidated the details of the framework laid out in these historical discoveries. Advanced biochemical and biophysical analyses have been combined with powerful modern molecular genetic techniques experimentally. In addition, three dimensional structures, at increasingly detailed levels of resolution, are becoming available for the reaction centres and light harvesting complexes of oxygenic photosynthetic organisms, and of their counterparts in anoxygenic photosynthetic bacteria. The first photosynthetic reaction centre

structure to be resolved to atomic detail, by x-ray crystallographic analysis, was that of *Rhodopseudomonas viridis* (Deisenhofer *et al.*, 1985). The ATPase and cytochrome b_6f complexes may also be compared with their respiratory homologues. Through the combination of these complementary approaches we have built up detailed picture of the structural and functional basis of photosynthesis.

1.2 Photosynthetic prokaryotes

The higher plant photosystems are considered to be evolved from those of ancient photosynthetic prokaryotes; the study of the modern relatives of these organisms can therefore give us insights into higher plant photosynthesis.

There are three classes of photosynthetic prokaryotes:

(i) *Rhodospiralles*

(ii) *Cyanobacteriales*

(iii) *Prochlorophyta*

Classification is by pigment content and ability to perform oxygen evolving photosynthesis. All are gram-negative bacteria, with the exception of *Heliobacterium chlorum.*

(i) *Rhodospiralles.* These are divided into *Rhodospirillineae* (purple bacteria) and *Chlorobiineae* (green bacteria). *Rhodospirillineae* are subdivided into *Chromatiaceae* (purple sulphur bacteria) and *Rhodospirillaceae* (purple non-sulphur bacteria). The purple sulphur bacteria are obligate anaerobic phototrophs and facultative heterotrophs. They will grow heterotrophically with organic substrates and sulphur compounds, or autotrophically, using hydrogen sulphide as an photosynthetic electron donor. Most species of purple non-sulphur bacteria are facultative

phototrophs, growing photosynthetically in anaerobic conditions, or heterotrophically in aerobic conditions using an external organic carbon source.

Chlorobiineae are subdivided into *Chlorobiaceae* (green sulphur bacteria) and *Chloroflexaceae* (green non-sulphur bacteria). The green sulphur bacteria are obligate anaerobes, growing photoautotrophically using sulphur compounds as electron donors. The green non-sulphur bacteria are facultative aerobes and may only photosynthesise during anaerobic conditions.

(ii) *Cyanobacteriales* (cyanobacteria). These are mostly aerobic photoautotrophs. They contain both photosystems and perform oxygenic photosynthesis. The phycobilisome, the cyanobacterial light harvesting complex, contains phycobilins. The combination of chlorophyll *a* and phycobilins imparts a blue-green appearance; the cyanobacteria were hence formerly known as blue-green algae.

(iii) *Prochlorophyta.* These organisms contain the two photosystems and both chlorophylls *a* and *b.* Phycobilins are absent. Genetically, there are close similarities to cyanobacteria. The phylum is represented by the genera *Prochloron, Prochlorothrix* and *Prochlorococcus.*

1.3 Evolutionary Relationships

1.3.1 The Chloroplast

The plastid organelles of higher plants are generally agreed to have evolved from cyanobacteria (reviewed by Douglas, 1994). However, there is dispute over whether plastid origins are monophyletic (from a single cyanobacterial ancestor) or polyphyletic (from multiple cyanobacterial ancestors).

There are several lines of evidence for this evolutionary relationship. The chloroplast has its own complete protein synthetic system with a genome of bacterial type in terms of both its plastidic structure and coding, and ribosomes of bacterial type. Homologues of several cyanobacterial genes have been found in the plastid genome. Most of the genes of plastid genome have counterparts in cyanobacteria. Some gene clusters are conserved between cyanobacteria and plastids.

There is also evidence of gene transfer from the endosymbiont to the nucleus. Where cytosolic and chloroplastic isoenzymes exist, the chloroplastic enzyme is generally has higher similarity to the cyanobacterial counterpart. Cyanobacterial genes with eukaryotic nuclear homologues have been sequenced, in particular glyceraldehyde 3-phosphate dehydrogenase.

1.3.2 Reaction Centres

Photosynthetic reaction centres are classified as Type I or Type II. Type II includes photosystem II and the purple bacterial reaction centre. The first reaction centre to be crystallised and structurally analysed to atomic resolution was that of *Rhodopseudomonas viridis* (Deisenhofer *et al.*, 1985). The purple bacterial reaction centres are useful models for photosystem II, as they are easier to crystallise and structurally simpler.

Type I centres operate at low potential, contain iron-sulphur centres and combine light-harvesting and electron transfer components; these include photosystem I and the reaction centres of green sulphur bacteria and heliobacteria.

Nitschke and Rutherford (1991) propose a scheme whereby both reaction centre types have evolved from a single ancestor. In this scheme, PSI is evolved from a fusion of an early type II reaction centre with a light harvesting protein.

1.4 The Z-Scheme

The modern elaboration of the Z-scheme, including the currently known electron donors and carriers is shown in figure 1.1. The redox potentials of the carriers also reflect the order of their physical arrangement within the thylakoid membrane; electron flow is thus vectorial, with the formation of a proton gradient. Electron flow from H_2O to $NADP^+$ is endergonic with a difference in potential of about 1.1V and is driven by absorption of light energy to PSI and PSII.

1.5 Photosystem II

The photosystem II complex consists of more than 20 protein subunits, some encoded by the nuclear genome and others by the chloroplast genome (reviewed in Nugent, 1996). The electron transfer components are bound by the core proteins D1 , D2 and cytochrome b_{559}. D1 and D2 also have the modern nomenclature PsbA and PsbF respectively). D1 and D2 are thought to form a twofold symmetry as in the L and M subunits of the purple bacterial reaction centre (Deisenhofer *et al.*, 1985), which has been used to model the PSII core (e.g. Ruffle *et al.*, 1992).

The chlorophyll *a* binding proteins CP47 (PsbB) and CP43 (PsbC) form an inner antenna, stabilise the core and modify quinone binding. CP47 is involved in stabilising the water-oxidising complex via a hydrophilic loop (Gleiter *et al.*, 1995). There is an outer light harvesting complex of chlorophyll *a/b* binding proteins.

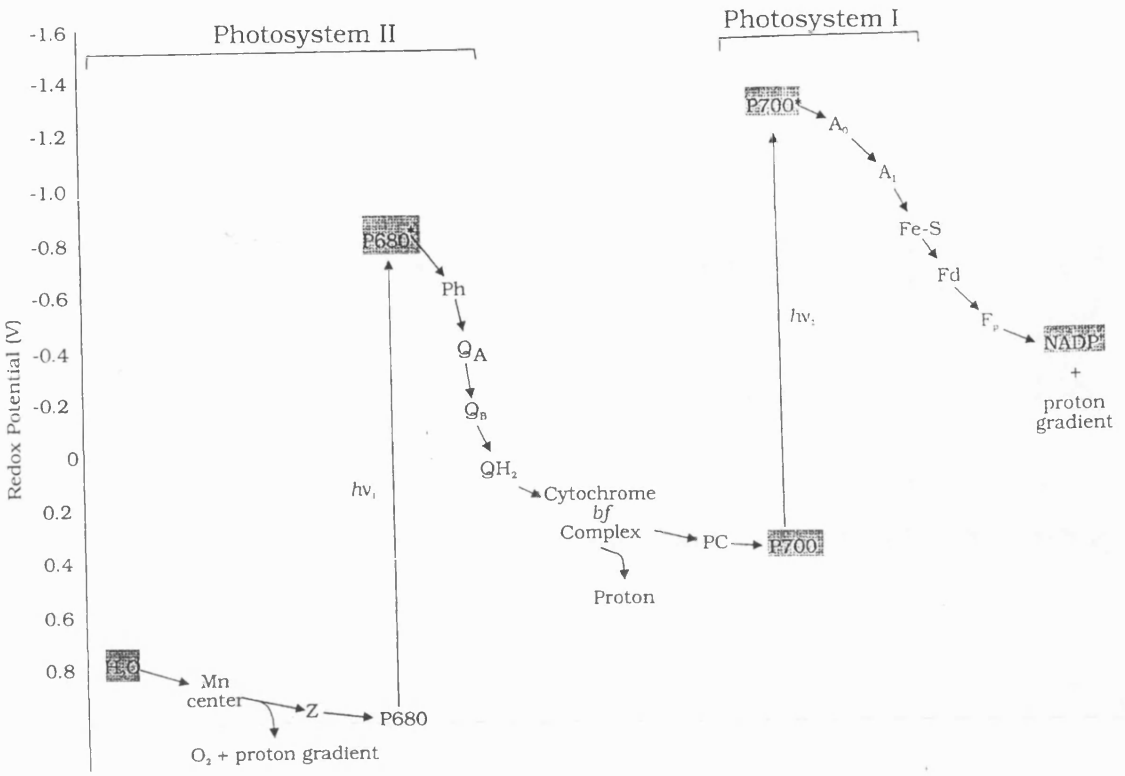

Figure 1.1

The Z-Scheme

The Z-scheme shows the pathway of electron transfer from water to $NADP^+$ in oxygenic photosynthesis. P680, the primary donor of PSII, is energised to P680*, which transfers an electron to pheophytin (Ph) and then to the quinones Q_A andQ_B. Q_B is double reduced to the quinol form (QH_2), which is mobile in the tylakoid membrane and donates electrons to the cytochrome b_6f complex. Electrons pass through this complex to the soluble electron carrier plastocyanin (PC) in the lumen. Plastocyanin donates electrons to the oxidised form of the primary donor of PSI, P700. P700 is energised to P700* and electrons pass through the acceptors A_0, A_1 and three iron-sulphur centres. Electrons pass out of PSII to the soluble electron carrier ferredoxin (Fd) in the stroma. Electrons are then passed via the enzyme ferredoxin $NADP^+$ oxidoreductase, a flavoprotein (F_p). P680 is rereduced by donation of electrons from the splitting of water. Water oxidation involves a Mn centre. Electrons are passed to $P680^+$ via a redox-active tyrosine (Z). Electron flow is in a lumenal to stromal direction, accompanied by proton pumping by the cytochrome b_6f complex. Electron transport brings about acidification of the thylakoid lumen.

The water-oxidising complex is located on the lumenal side of the thylakoid membrane. The manganese cluster is stabilised by three proteins: OEE1, OEE2 and OEE3 (PsbO, PsbP and PsbQ, respectively). H_2O is split in the water-oxidising complex in a reaction involving the manganese cluster which passes through five oxidation states, S_0 to S_4, with O_2 evolved at S_4.

Electrons are donated to the reaction centre primary donor P680 via tyrosine Z, tyrosine 161 of the D1 protein. Alternative donors tyrosine D (tyrosine 161 of D2) (Evans and Nugent, 1993) and chlorophyll Z (Koulougliotis *et al.*,1994) function when electron transfer through tyrosine Z is blocked. P680 is energised to the excited state P680* by energy funnelled from the light-harvesting proteins of PSII. $P680^+$/P680 has a highly oxidising E_m of +1150mV. The precise nature of P680 is unclear: there is evidence for a dimeric chlorophyll as in the purple bacterial reaction centre but also evidence for a chlorophyll monomer, possibly equivalent to an accessory chlorophyll in the purple bacterial reaction centre. A possible explanation is that P680 may be a weakly interacting dimer or multimer.

From P680*, an electron passes to pheophytin I (Pheo I) to form a charge separation. Two Pheo *a* molecules are present in the PSII reaction centre, but only Pheo I is involved in charge separation, suggesting that electron transfer passes along only one arm of the reaction centre, as in purple bacteria (Cogdell and Malkin, 1992). The E_m of Pheo I/Pheo I^- is more negative than -450mV.

The bound plastoquinone Q_A is reduced 200-400ps after charge separation. The E_m of Q_A/Q_A^- is about 0mV. The second plastoquinone Q_B acts as a two electron gate. Q_B is reduced to semiquinone form by Q_A^- with a kinetic of 100-200μs. The second reduction to quinol form is slower, occurring in 300-500μs.

Plastoquinol becomes mobile in the membrane and passes electrons to the cytochrome b_6f complex. A non-haem iron is present between Q_A and Q_B, but this is not involved in normal electron flow.

1.6 The Cytochrome b_6f Complex

The cytochrome b_6f complex functions as a plastoquinol-plastocyanin oxidoreductase, passing electrons from the plastoquinone pool to the soluble carrier plastocyanin on the lumenal side of the membrane. Protons are concomitantly translocated from stroma to lumen. The complex is structurally and functionally similar to the cytochrome bc_1 complexes of bacterial and mitochondrial membranes (Hauska *et al.*, 1983).

There are four major polypeptides: cytochrome *f*, cytochrome b_6 and the Rieske [2Fe-2S] protein which carry prosthetic groups involved in electron transfer; subunit IV is involved in plastoquinone binding. The Rieske protein is nuclear encoded; cytochrome *f*, cytochrome b_6 and subunit IV are encoded by the chloroplast genome. There are also small subunits of uncertain function, three of which have been identified in *C. reinhardtii*: PetG, PetL and PetM (Schmidt and Malkin, 1993). Two of the ligands to the Rieske Fe-S centre are formed by histidine residues (Britt *et al.* 1991).

1.7 Photosystem I

Photosystem I is a heteromultimeric, membrane-spanning pigment-protein complex, which utilises light energy to drive the oxidation of plastocyanin on the lumenal side of the thylakoid membrane and the subsequent reduction of ferredoxin

on the stromal side. The strong reducing power of ferredoxin is used to generate NADPH via ferredoxin-$NADP^+$ oxidoreductase in linear electron flow, or ATP in cyclic electron flow (reviewed in Golbeck and Bryant, 1991). PSI comprises at least 11 subunits in cyanobacteria and at least 13 in chloroplasts. Cyanobacteria lack PsaH, PsaG and PsaN but additionally have PsaM. All proteins are present as one copy per reaction centre. PSI complexes can be isolated in monomeric or trimeric form (Kruip *et al.*, 1993). The reaction centre exhibits pseudo-C_2 symmetry; all of the small subunits except PsaG and PsaK are located near the symmetry plane (Jansson *et al.*, 1996).

PSI associates with with multiple LHCI light-harvesting complexes. In higher plants, LHCI consists of two components: (proteins Lhca2 and Lhca3) and LHCI-730 (proteins Lhcal and Lhca4), termed according to their fluorescence emissions (reviewed in Jansson, 1994). Bassi *et al.* (1992) propose that as many as 10 chlorophyll-binding polypeptides are present in LHCI of *C. reinhardtii*; two preparations of LHCI were obtained: LHCI-680 and LHCI-705.

A charge separation is generated on the chlorophyll *a* special pair P700, which is stabilised by a series of electron acceptors: A_0 (a chlorophyll monomer), A_1 (phylloquinone/vitamin K_1) and F_X (a 4Fe-4S centre). Electrons pass from F_X to the terminal 4Fe-4S centres F_A and F_B.

1.8 The Subunits of Eukaryotic Photosystem I

1.8.1 PsaA and PsaB

P700, A_0, A_1 and F_X are coordinated by the reaction centre heterodimer proteins PsaA and PsaB. The genes, *psaA* and *psaB,* were first sequenced in maize

(Fish *et al.*, 1985), then later for several other species, including *C.reinhardtii* (Kück *et al.*, 1987). Each protein has a genetically predicted molecular weight of about 83kD. The structure of PSI from the cyanobacterium *Synechococcus elongatus* has been resolved to 4Å by Krauss *et al.* (1996). For both proteins, 11 hydrophobic domains 19-25 residues long were predicted from sequence data to represent membrane-spanning helices. In the crystal structure, 22 transmembrane helices were found in total. 8 membrane-parallel α-helices near the membrane surface were resolved. The 10 innermost transmembrane α-helices form a spirally widening double palisade round the electron transfer components; eight peripheral transmembrane α-helices form part of an outer ring. 97±5 chlorophyll *a* molecules are bound by each PsaA and PsaB, 71 of which were identified in the electron density distribution. The core proteins of PSI therefore form a large part of the light harvesting antenna as well as forming the reaction centre, a major difference from PSII. High numbers of histidine residues are present in the transmembrane helices, suggesting involvement in chlorophyll binding.

PsaA and PsaB contain the leucine zipper motif, a motif of regularly repeated leucine residues. This motif is involved in the formation of heterodimers by DNA-binding proteins. (Landschulz *et al*, 1988). The motif has been suggested to act in the dimerization of PsaA and PsaB (Kössel *et al.*, 1990). However, conservative substitutions to two of the leucine residues in the putative zipper region of PsaB were introduced by site-directed mutagenesis of PsaB in *Synechosystis* PCC6803 with no effects on growth or electron transport from P700 to F_A/F_B (Smart *et al.*, 1993), indicating that the motif may not be functional.

Subunit	Gene/Coding	Molecular Weight (kDa)	Properties	Function/Cofactors
PsaA	psaA chloroplast	~83	11 transmembrane and 4 membrane-parallel α-helices	Light-harvesting, electron transport. ~100chl a, ~15 β-carotene, P700, A_0, A_1, F_X.
PsaB	psaB chloroplast	~83	11 transmembrane and 4 membrane-parallel α-helices	Light-harvesting, electron transport. ~100chl a, ~15 β-carotene, P700, A_0, A_1, F_X.
PsaC	psaC chloroplast	8.9	stromal extrinsic, acidic	Electron transport. F_A, F_B.
PsaD	psaD nucleus	17.9	stromal extrinsic, basic	Ferredoxin docking. Stabilisation of PsaC.
PsaE	psaE nucleus	8.1	stromal extrinsic, 5-stranded β-sheet	Ferredoxin interaction. FNR binding.
PsaF	psaF nucleus	~17	1 surface (lumenal) and 2 transmembrane α-helices	Plastocyanin and cytochrome c_6 docking.
PsaG	psaG nucleus	10.0	2 transmembrane α-helices	Interaction with light harvesting complex?
PsaH	psaH nucleus	11.0	stromal extrinsic	Unknown.
PsaI	psaI chloroplast	~4	1 transmembrane α-helix	Stabilisation of PsaL?
PsaJ	psaJ chloroplast	~4	1 transmembrane α-helix	Unknown.
PsaK	psaK nucleus	8.4	2 transmembrane α-helices	Interaction with light harvesting complex?
PsaL	psaL nucleus	~18	2 transmembrane α-helices	Trimerization of PSI?
PsaN	psaN nuclear	~9	lumenal extrinsic	Unknown.

Table 1.1

The Subunit Composition of Photosystem I in *C. reinhardtii*

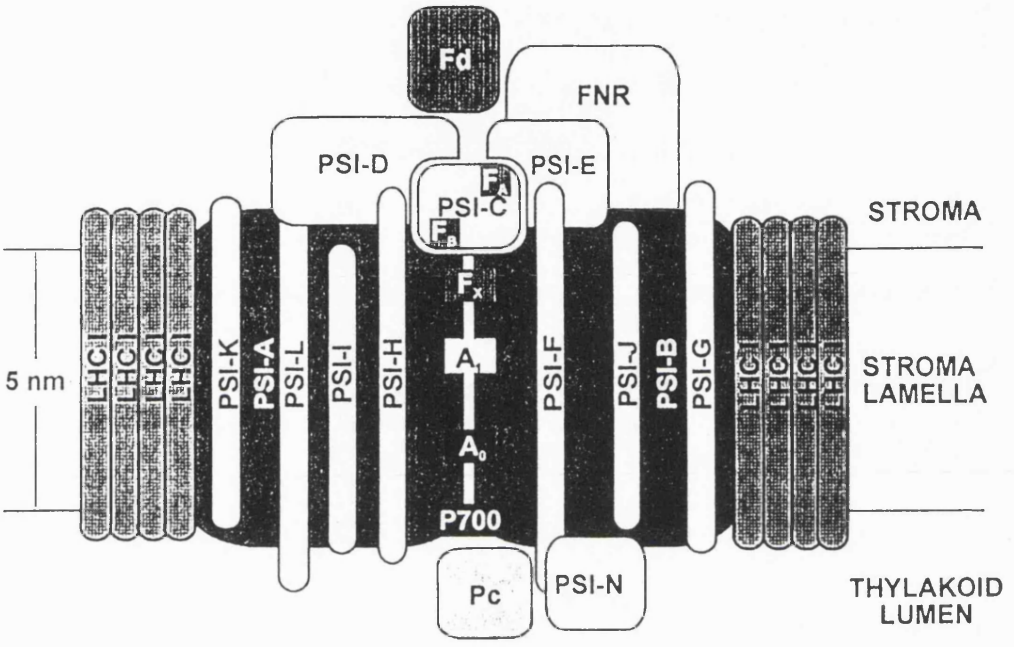

Figure 1.2

Schematic Model of the Photosystem I Complex in Higher Plants

Subunits prefixed "Psa" in the text are prefixed "PSI" in this figure. Pc, Fd and FNR are plastocyanin, ferredoxin and ferredoxin-$NADP^+$ oxidoreductase, respectively. [Diagram from Scheller *et al.*, (1997).]

In both PsaA and PsaB, there is an identical sequence of twelve amino acids FPCDGPGRGGTC, completely conserved in all photosynthetic eukaryotes so far examined (Golbeck and Bryant, 1991). A very similar amino acid sequence is also found in green bacteria (Lockau and Nitschke, 1993). This sequence contains two cysteine residues which are thought to form the ligands to F_X. The sequence is located in a hydrophilic extramembrane loop between α-helices XIII and IX, which are helices *j*,*k* and *j'*,*k'* in the crystal structure, two of the inner transmembrane α-helices. Transmembrane helices *m*,*m'* are connected to P700 by electron density. These helices each contain one histidine and probably coordinate P700. This histidine of PsaB was changed to asparagine by site-directed mutagenesis in *C.reinhardtii*, producing changes in redox potential, optical difference spectra and ENDOR spectra of P700 (Webber *et al.*, 1996).

PsaA and PsaB are encoded by the genes *psaA* and *psaB* of the chloroplast genome. In all species examined, with the exception of *C. reinhardtii, psaA* and *psaB* are adjacent and are cotranscribed as a 4.9 kb RNA (Golbeck and Bryant, 1991).

1.8.2 PsaC, PsaD and PsaE

A ridge of 35Å height projects from PSI on the stromal side of the thylakoid membrane and is assigned to subunits PsaC, PsaD and PsaE (Krauss *et al.*, 1996). These proteins may be chaotropically removed, and rebound in the presence of $FeCl_3$, Na_2S and β-mercaptoethanol, restoring electron flow to F_A and F_B (Parret *et al.*, 1990). F_A and F_B are required to be intact for rebinding of PsaC, PsaD and PsaE (Li *et al.*, 1991a). In a mutant of *C. reinhardtii* with the *psaC* gene insertionally inactivated, PSI did not accumulate, due to rapid turnover of the subunits (Takahashi

et al., 1991). A mutant with the *psaC* gene insertionally inactivated was generated in *Anabaena variabilis* (Mannan *et al.*, 1994). This mutant did not assemble PsaD or PsaE into the PSI complex. A similar mutant, also with the *psaC* gene insertionally inactivated, was generated in *Synechocystis* sp. PCC6803. This mutant assembled the PSI core, but binding of PsaD and PsaE required the addition of PsaC (Yu *et al.*, 1995a).

1.8.2.1 PsaC

PsaC is an acidic, hydrophilic protein, of 8.9 kD and 81 amino acids in length. There is a high degree of amino acid conservation throughout species, with most residues completely conserved and mainly conservative replacements in the central and N-terminal regions. There are nine conserved cysteines, eight of which ligate F_A and F_B each with the motif CxxCxxCxxCP (Golbeck, 1992).

PsaC is homologous to the bacterial ferredoxins. The structure of ferredoxin from *Peptococcus aerogenes* has been solved to 2Å (Adman *et al.*, 1976) and has proved to be a useful model for PsaC (Oh-Oka *et al.*, 1988a). PsaC contains two short α-helices and the two 4Fe-4S centres are separated by 12Å. PsaC differs from the bacterial ferredoxins by having an enlarged internal loop. The loop is suggested to interact with the core since deletion alters binding properties. PsaC also differs by having a C-terminal extension, thought to interact with PsaD (Naver *et al.*, 1996). There are two possibilities for fitting the structure into the electron density of PSI. Although the locations of F_A and F_B cannot be resolved directly, Krauss *et al.* (1996) propose a model with the termini pointing outwards: F_B would be the F_X proximal cluster in this model. The results of Rodday *et al.* (1996) are also compatible with

such a model. However, Vassiliev *et al.* (1998) present spectroscopic data for rates of electron transfer from F_X to ferredoxin best compatible with the orientation of PsaC in which F_A is proximal to F_X.

Intactness of the iron-sulphur centres is essential for the assembly of PsaC into the PSI complex, presumably due to their structural importance. Insertion of iron-sulphur centres into the PsaC apoprotein and the presence of PsaD were found by Zhao *et al.* (1990) to be necessary for the rebinding of PsaC. Mehari *et al.* (1995) found that C34 is the cysteine not involved in iron sulphur centre coordination and that two iron-sulphur centres are necessary for functional PsaC reconstituion. Yu *et al.* (1995b) found that the C51D mutation produces a mixture of 3Fe-4S and 4Fe-4S centres and that 4Fe-4S proteins are selectively rebound. Chemical rescue of 3Fe-4S mutants with the incorporation of a thiolate from added β-mercaptoethanol allows functional reconstitution of PsaC (Jung *et al.*, 1996).

The F_X domain of the core heterodimer is important in the binding of PsaC to the core, forming a loop which interacts electrostatically with PsaC. This interaction was studied in a a series of papers by Rodday, Biggins and co-workers. Chemical modification of core arginine residues or trypsin treatment of the core prevented functional reconstitution of PsaC and PsaD (Rodday *et al.*, 1993). Site-directed mutagenesis of R561 of PsaB in *Synechocystis* sp. PCC6803 affected electrostatic interaction with PsaC (Rodday *et al.*, 1994). In a site-directed mutagenesis study of *C. reinhardtii,* substitution of residues P560 and P564 impaired interaction between PsaC and the reaction centre core (Rodday *et al.*, 1995). Similar work on residue D576 of PsaA in *C. reinhardtii* is presented in this thesis. The creation of the site-directed mutant and initial analysis are presented in Hallahan *et al.* (1995). Rodday *et*

al. (1996) expressed PsaC proteins with site-directed changes in acidic residues in *E. coli.* The mutant PsaC proteins were reconstituted onto PSI cores. Results confirmed that PsaC interacts electrostatically with the PSI core.

1.8.2.2 PsaD

PsaD is a nuclear-encoded basic protein of 15.5kDa in in cyanobacteria and 17.9kDa in eukaryotes, due to an N-terminal extension (Golbeck, 1992). PsaD may be chemically cross-linked with PsaC (Oh-Oka *et al.*, 1989), PsaE and PsaH (Andersen *et al.*1992), PsaL (Xu *et al.*, 1994a) and ferredoxin (Zilber and Malkin, 1988).

PsaD stabilises the binding of PsaC and modifies the spectroscopic properties of F_A and F_B (Li *et al.*, 1991b). In a mutant of *Synechocystis* sp. PCC6803 lacking PsaD, PsaC is more easily removed chaotropically or with detergent, implying a role in stabilisation of PsaC (Chitnis *et al.*, 1996).

PsaD functions in the docking of ferredoxin to PSI. In the mutant lacking PsaD, ferredoxin-mediated $NADP^+$ reduction is inhibited (Xu *et al.*, 1994b). The lysine residue at position 106 is considered to be of particular importance in the interaction with ferredoxin. This residue may be chemically cross-linked to glutamine 93 of ferredoxin (Lelong *et al.*, 1994). Site-directed mutagenesis of lysine 106 reduces but does not abolish rates of ferredoxin-mediated $NADP^+$ reduction. Flavodoxin is an alternative physiological electron acceptor of PSI, and the mutations do not affect rates of flavodoxin-mediated $NADP^+$ reduction, implying that this acceptor has a different docking site (Chitnis *et al.*, 1996).

1.8.2.3 PsaE

This protein is nuclear-encoded, with a molecular mass of 8.1kDa in *C. reinhardtii* (Golbeck, 1992). NMR spectroscopy reveals a five-stranded β-sheet structure (Falzone *et al.*, 1994).

While PsaD forms a docking site for ferredoxin, PsaE improves the efficiency of interaction of PSI with ferredoxin. Selective removal of PsaE by cationic detergent treatment reduces electron transfer to ferredoxin. Ferredoxin suppresses the F_A/F_B to P700 backreaction. Following removal of PsaE, the extent of this suppression correlates with the amount of PsaE bound (Sonoike *et al.*, 1993). Incubation with an antibody raised against PsaE inhibits electron transport to $NADP^+$, suggested to be due to steric hindrance of ferredoxin access (Weber and Strottman, 1993). Deletion of the *psaE* gene in *Synechocystis* sp. PCC6803 greatly reduces the rate of ferredoxin reduction; site-directed mutagenesis of the termini of PsaE leads to incorrect integration and a similar phenotype to the deletion mutant, suggesting that PsaE has a role in maintaining the correct structural integrity of the ferredoxin docking site of PSI (Rousseau *et al.*, 1993).

The ferredoxin:$NADP^+$ oxidoreductase may be found bound to the thylakoid membrane, and PsaE forms the binding site. PsaE may be cross-linked to this enzyme (Andersen *et al.*, 1992). PsaE has a role in mediating cyclic electron transport. The *psaE* gene was insertionally inactivated in *Synechococcus*, the mutant grew slowly under conditions favouring cyclic electron transport (reduced light intensity or reduced CO_2) and would not grow under photoheterotrophic conditions, where PSII is inhibited with DCMU and electrons from respiration of glycerol are fed into the electron transfer chain (Zhao *et al.*, 1993). These experiments were elaborated upon

by Yu *et al.* (1993). Mutants were generated which lacked PsaE or NdhF (the $NADP^+$ dehydrogenase involved in feeding respiratory electrons into the photosynthetic chain). A double mutant lacking both proteins was also generated. Biochemical experiments on these mutants indicated that PsaE is essential for cyclic electron transport around PSI.

1.8.3 PsaF

PsaF is a nuclear encoded protein of about 17 kDa, highly charged with a pI of 9.1 (Golbeck, 1992). One surface and two transmembrane α-helices are assigned to PsaF, with the surface part on the lumenal side of the thylakoid membrane (Krauss *et al.*, 1996). PsaF occupies the same side of PSI as PsaE and PsaJ, indicated by cross-linking experiments which also prove its transmembrane structure (Jansson *et al.*, 1996). PsaF cannot be removed chaotropically (Li *et al.*, 1991a) and partitions into Triton X-114 (Tjus and Andersson, 1991), indicating a large degree of hydrophobicity.

The exact function of PsaF is still uncertain, although a function in the interaction of plastocyanin with PSI is indicated. Plastocyanin may be cross-linked to PSI and the cross-linked complex is still functional in the reduction of $P700^+$ by plastocyanin (Hippler *et al.*, 1989). In cyanobacteria, however, PsaF may be removed by cationic detergent treatment and the oxidation of the cyanobacterial cytochrome *c* electron donor is unaffected (Hatanaka *et al.*, 1993). Targeted inactivation of the gene in cyanobacteria, permitted normal photoautotrophic growth and did not affect $NADP^+$ photoreduction from cytochrome *c* (Xu *et al.*, 1994b). PsaF is therefore not necessary for docking of cytochrome *c* in cyanobacteria. Farah *et al.* (1995) described

the PsaF-deficient mutant strain 3bF of *C. reinhardtii*, which was capable of photoautotrophic growth but had greatly reduced electron transfer from plastocyanin to $P700^+$, indicating a role in plastocyanin docking in eukaryotes. This mutant was examined in more detail by Hippler *et al.* (1997), using cross-linking and flash absorption spectroscopy. In the mutant, neither plastocyanin nor cytochrome c_6 could be cross-linked to PSI . PsaF was found to be required for efficient electron transfer to $P700^+$ from plastocyanin or cytochrome c_6. In a site-directed mutagenesis study of the 3bF mutant, Hippler *et al.* (1998) found the lysine residue at position 23 in PsaF to be particularly important for interaction between PsaF and plastocyanin or cytochrome c_6.

1.8.4 PsaG and PsaK

These subunits are nuclear encoded, with a degree of homology to one another, and hydrophobic. In *C. reinhardtii*, PsaG and PsaK have molecular weights of 10.0kDa and 8.4kDa respectively. (Golbeck, 1992). PsaK forms two α-helices (Krauss *et al.*, 1996) and forms cross-links with PsaA and PsaB (Fromme, 1996). PsaK has differing detergent solubility in monomers and trimers, suggesting a location in the region adjoining trimers (Jekow *et al.*, 1995). Cross-linking suggests that PsaG may interact with LHCI and a model with PsaK and PsaG symmetrically located on either side of the PSI complex and linked to light-harvesting proteins has been proposed (Jansson *et al.*, 1996).

1.8.5 PsaL and PsaI

PsaL is a nuclear encoded protein of about 18kDa in higher plants, hydrophobic and forming two α-helices (Golbeck, 1992). PsaL has been suggested to be involved in trimerization of PSI: in a cyanobacterial mutant lacking PsaL, only monomers may be isolated (Schluchter *et al.*, 1996).

PsaI is chloroplast encoded, of about 4kDa, and hydrophobic, forming one α-helix (Golbeck, 1992). In a cyanobacterial mutant lacking PsaI, only monomers also lacking PsaL could be isolated with Triton X-100, although thylakoids contained almost wild type levels of PsaL, suggesting a role for PsaI in stabilisation of PsaL (Schluchter *et al.*, 1996).

1.8.6 PsaH, PsaJ and PsaN

PsaH is nuclear encoded, with a molecular weight of 11.0 kDa in *C. reinhardtii*. The amino acids are predominantly polar. A cross-link is formed with PsaD. PsaH is thought to be extrinsically located on the stromal side of the thylakoid membrane (Golbeck, 1992).

PsaJ is chloroplast encoded, of about 4kDa, and hydrophobic, forming one α-helix (Golbeck, 1992). PsaJ shares an open reading frame with PsaF, and the two proteins can be cross-linked (Jansson *et al.*, 1996). PsaJ has a large C-domain, thought to be located on the stromal side, interacting with PsaE (Chitnis *et al.*, 1995).

PsaN is nuclear encoded, with a molecular weight of about 9 kDa, and is the only lumenal extrinsic subunit of PSI (Chitnis *et al.*, 1995).

PsaH, PsaJ and PsaN are of unknown function.

1.9 The Redox Cofactors of Photosystem I

1.9.1 P700

P700, the primary electron donor of photosystem I, is a chlorophyll *a* pair forming a symmetric dimer parallel to the pseudo-C_2 axis of the core heterodimer, with weak electron density connecting to helices *m* and *m'* (Krauss *et al.*, 1996). P700 is named according to the 700 nm maximum of the oxidised-reduced difference spectrum. The midpoint potential was originally measured as +430mV, but more recently this value has been found to be sensitive to detergent or solvent treatment (Golbeck and Bryant, 1991).

The question of the monomeric or dimeric nature of P700 has been a source of dispute, and the consensus of current opinion is for a dimer. The spectroscopic features of $P700^+$ or the triplet state have a monomeric appearance, but this would be consistent with P700 exhibiting the optical properties of an excitonically coupled dimer (Brettel, 1997).

The unpaired spin of $P700^+$ is distributed asymmetrically over the two chlorophylls with a spin density ratio of 3:1or higher. Käβ *et al.* (1995) calculated 85% of spin density on one chlorophyll from ENDOR and ESEEM spectroscopy data. Davis *et al.* (1993), in ESEEM experiments on $P700^+$, found a damping of hyperfine interactions, indicative of a dimer with a spin density of 3:1 or 4:1 or a monomer.

Histidine ligates the primary donor of the purple bacterial reaction centre (Deisenhofer *et al.*, 1985). The ligands to P700 had been suggested to be conserved histidines in helix VIII of PsaA and PsaB. However, this has been disproved experimentally. Mutants of PSI with site-directed mutations of these histidines in PsaB were generated in *C. reinhardtii.* In ENDOR and ESEEM experiments, the

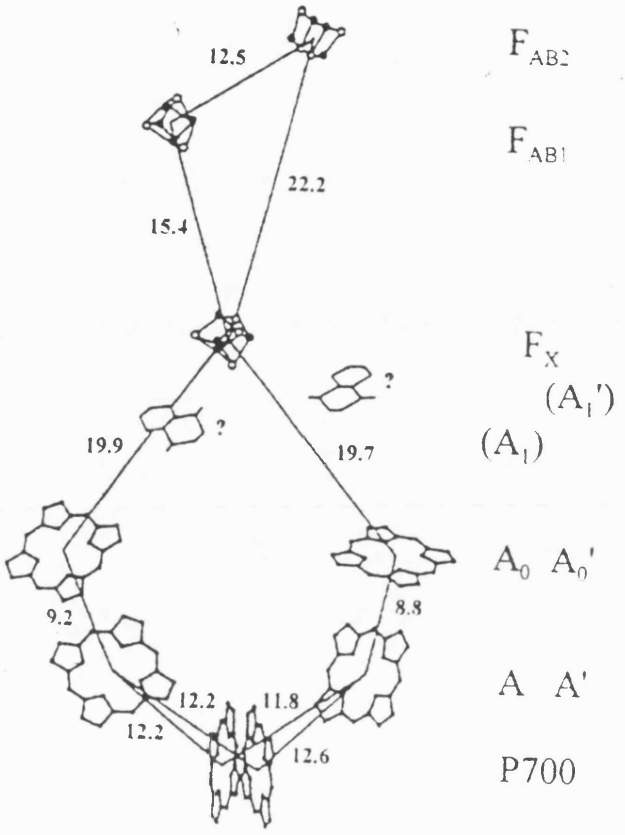

Figure 1.3

Model of the Arrangement of the Redox Cofactors of Photosystem I

Model for the Arrangement of the Redox Cofactors of Photosystem I from *Synechococcus elongatus* based on X-ray diffraction data at 4.5Å. The membrane plane is perpendicular to the connection between the centres of P700 and F_X. Distances are given in Å. [Diagram from Brettel (1997)].

spectroscopic characterisitics of $P700^+$ were unchanged by these mutations. In addition, the spectra from *C. reinhardtii* were identical to those from cyanobacteria, suggesting the protein enviroment around P700 has been highly conserved between prokaryotes and eukaryotes (Cui *et al.*, 1995). H656 in helix X of PsaB in *C. reinhardtii* was mutated to asparagine by site-directed mutagenesis and modifications of the ENDOR spectrum of $P700^+$ and the optical $P700^+/P700$ suggested this histidine to be the true ligand (Krabben *et al.*, 1995). Histidine has been spectroscopically identified as the axial ligand to the chlorophyll Mg^{2+} of P700, from ENDOR and ESEEM spectroscopy data on a histidine-tolerant mutant with specific ^{15}N labelling of histidine (Mac *et al.*, 1996).

1.9.2 A_0

A_0, the primary acceptor of photosystem I, is generally thought to be a chlorophyll monomer and the midpoint potential has been indirectly measured as -1.01V (Golbeck and Bryant, 1991).

An A_0^-/A_0 difference spectrum has been obtained, but the preparation had been subjected to very harsh ethyl ether treatment, which extracted A_1, the carotenoids and most of the antenna chlorophyll (Mathis *et al.*, 1988). A difference spectrum has also been obtained in a Triton X-100 detergent preparation of PSI under highly reducing conditions (Nuijs *et al.*, 1986). A difference spectrum has been obtained in a detergent preparation from *C. reinhardtii*. This spectrum had a maximum bleaching around 686nm. The spectrum was similar to that of spinach, but different to a cyanobacterial spectrum (Hastings *et al.*, 1995). A fraction of the charge recombination between A_0^- and $P700^+$ is seen to occupy the triplet state, which is

insensitive to magnetic fields up to 60G (Brettel and Sétif, 1987). Using time-resolved optical absorption, Mathis *et al.* (1988) detected a bleach at 690nm assigned to a chlorophyll acceptor. Much of the evidence for a monomeric chlorophyll is still inconclusive, mostly based on results from very harsh preparations, and the nature of the primary acceptor is still under debate.

1.9.3 A_1

A_1 is the secondary electron acceptor of PSI, a phylloquinone (vitamin K_1) with a redox potential of about -800mV (Golbeck, 1992).

Bonnerjea and Evans (1982), in pea Triton X-100 PSI illuminated under reducing conditions, detected an anisotropic EPR signal centred at g=2.0040 and 10.3mT wide consistent with a reduced quinone. This signal correlates with an optical absorption change with a maximum of 278nm (Mansfield and Evans, 1986).

Two phylloquinone molecules are present per PSI complex. Solvent removal of one phylloquinone does not disrupt photoreduction of F_A/F_B and $NADP^+$ (Malkin, 1986). Removal of both molecules blocks electron transfer (Itoh *et al.*, 1987).

Destruction of the quinones by exposure to UV radiation did not alter the EPR signal attributed to A_1 (Ziegler *et al.*, 1987). A possible explanation could be that PSI is extensively modified by UV, suggested by Brettel (1997). Golbeck (1992) suggests that the quinones may not be completely destroyed, or may become cross-linked to the complex. A reduced quinone EPR signal may also be photoaccumulated in green bacteria, although there is strong evidence against the involvement of an A_1 analogue

in the green bacterial electron transfer chain, indicating that photoaccumulation may produce a side reaction (see section 1.10).

Double reduction of phylloquinone to the semiquinone form removes the ESP (electron spin polarised) signal attributed to the radical pair of $P700^{\cdot+}$ and $A_1^{\cdot-}$ (Snyder *et al.*, 1991). Double reduction also removes the ability to photoaccumulate A_1^- (Heathcote *et al.*, 1993).

Deuteration of the quinone in the cyanobacterium *Anabaena variabilis* leads to a narrowing of the photoaccumulated EPR signal attributed to A_1 and also a narrowing of the ESP signal attributed to the $P700^{\cdot+}/A_1^{\cdot-}$ radical pair (Heathcote *et al.*, 1996). This identification allowed further characterisation of A_1 by ENDOR and special triple resonance spectroscopy by Rigby *et al.* (1996). Results indicated a phylloquinone anion radical with a distorted electron spin density distribution. The protein environment produces an altered electronic structure, which may explain the very low midpoint potential of the quinone.

The first observation of A_1 under physiological conditions was reported by Klughammer and Pace (1997). A saturating light pulse following dark adaptation produced an A_1^- signal detected by time-resolved EPR in *Synechococcus* and spinach chloroplasts.

1.9.4 F_X

F_X is a 4Fe-4S centre, with a midpoint potential of -730mV, a very low value for a 4Fe-4S centre (Golbeck, 1992). When F_A and F_B are chemically reduced, illumination at low temperature gives rise to an EPR signal with the characteristics of a modified iron-sulphur centre (Evans *et al.*, 1975). This signal has unusually broad

resonances and low g values of 2.04, 1.88 and 1.78 . The residues of PsaA and PsaB which form the ligands to F_X are discussed in section 1.8.1.

PsaC, the subunit which contains F_A and F_B may be removed chaotropically, leaving F_X intact. The preparation has an optical difference spectrum characteristic of a 4Fe-4S centre (Parret *et al.*, 1989). EXAFS spectroscopy of the core preparation indicate that F_X is a 4Fe-4S cluster (McDermott *et al.*, 1989). Results from Mössbauer spectroscopy also provide evidence for the 4Fe-4S nature of F_X (E. H. Evans *et al.*, 1981). Further Mössbauer experiments using a PSI core preparation lacking F_A and F_B confirmed these findings (Petrouleas *et al.*, 1989).

1.9.5 F_A and F_B

The terminal electron acceptors of PSI, F_A and F_B, are located in the PsaC protein. The midpoint potentials of F_A and F_B have been measured as -530mV and -580mV respectively (Evans *et al.*, 1974). F_A and F_B are 4Fe-4S centres and can be distinguished by low temperature EPR. The EPR signal of F_A has resonances g_x=1.86, g_y=1.94, g_z=2.05 (Evans *et al.*, 1974). F_B has resonances g_x=1.89, g_y=1.92, g_z=2.07 (Evans *et al.*, 1972). When both centres are reduced, the spectrum is different from the superposition of the two spectra, indicating magnetic interaction and a short distance between the two centres (Evans *et al.*, 1974). The amino acid ligands to F_A and F_B are discussed in section 1.8.2.1.

F_A and F_B are seen as a bleach at 430nm in an oxidised minus reduced optical difference spectrum. This feature, termed P430, had a backreaction with a half-time of 30ms at room temperature (Hiyama and Ke, 1971). Oh-Oka *et al.* (1988b) reported EPR spectra of isolated spinach PsaC, which had similar characteristics to bacterial

ferredoxins, and indicated the presence of 2Fe-S centres. When isolated PsaC is exposed to air, F_A and F_B are destroyed, and anaerobic techniques gave improved results (Oh-Oka *et al.*, 1991).

1.9.6 Pathway of Electron Transfer in Photosystem I

A second pair of chlorophylls exists between P700 and A_0. A pair of bacteriochlorophylls are present in a similar arrangement in the purple bacterial reaction centre which participate in intermediate electron transfer. It is therefore possible that these chlorophylls are involved in electron transfer in PSI (Fromme, 1996).

The path of forward electron transfer from A_0 has been questioned. The redox potentials of A_0 and A_1 have only been measured indirectly. EPR data indicates a strong interaction of F_X with A_0 rather than A_1 (Mansfield and Evans, 1988). Also, F_X photoreduction has been reported in UV-treated PSI with A_1 destroyed (Biggins *et al.*, 1989) and there is recent evidence of direct electron transfer from A_0 to F_X in green bacteria (Lin *et al.*, 1995; Brettel *et al.*,1998).

However, strong evidence for the involvement of A_1 has accumulated. Double reduction of A_1 blocks forward electron transfer (Sétif and Bottin, 1989). Brettel (1988), using time-resolved optical absorption spectroscopy of cyanobacterial PSI, reported a kinetic of 250ns for electron transfer from A_1. Bock *et al.* (1989), using transient EPR spectroscopy of cyanobacterial PSI, reported two consecutive ESP (electron spin polarised) signals with a 260ns kinetic, attributed to $P700^+/A_1^-$ and $P700^+/F_X^-$. Low temperature is required to observe F_X by EPR and forward electron transfer from A_1 is inefficient at cryogenic temperatures, but this problem has

been overcome by the use of pulsed EPR. Moënne-Loccoz *et al.* (1994), using time-resolved pulsed EPR spectroscopy of spinach PSI, reported an out-of-phase electron spin echo signal attributed to $P700^+/A_1^-$ which decayed with $t_{1/e}$=23μs at cryogenic temperatures, indicative of a recombination reaction, and decayed with $t_{1/e}$=200ns at room temperature. The latter kinetic was unchanged by removal of F_A/F_B but was lost with destruction of F_X, leading to attribution of this kinetic to electron transfer from A_1^- to F_X, and indicating a sequence of electron transfer from A_1 to F_X to F_A/F_B. Related data were obtained by Lüneberg *et al.* (1994), using optical absorption difference spectroscopy. Forward electron transfer from A_1^- had a half-life of 180ns, unchanged by removal of F_A/F_B. The kinetic reported by Bock *et al.* (1989) was further investigated by van der Est *et al.* (1994) with a variety of samples from cyanobacteria and spinach. The second ESP signal was not observed when iron-sulphur centres were removed, but was observed in core particles with F_X intact, leading to unambiguous assignment of this signal to $P700^+/F_X^-$. The photoelectric response of PSI in oriented cyanobacterial membranes was studied by Leibl *et al.* (1995). A kinetic phase of about 220ns was observed. There was little change in this kinetic with removal of F_A/F_B, but the kinetic was lost with reduction of all the iron-sulphur centres, in support of a pathway of electron transfer with F_X between A_1 and F_A/F_B.

The pathway of electron transfer through the iron-sulphur centres of PSI is unclear, and it is unclear which electron density assigned to F_A/F_B should be assigned to each cluster, although recent data is in favour of F_B as the F_X-distal cluster and the immediate donor to ferredoxin. F_B may be selectively destroyed with $HgCl_2$. Flash absorption spectroscopy of $HgCl_2$ treated spinach PSI indicated electron transfer to

F_A (Sakurai *et al.*, 1991), although F_B-reconstituted complexes were incompetent in $NADP^+$ photoreduction, suggesting $HgCl_2$-induced structural changes (He and Malkin, 1994). However, in a similar experiment with *Synechococcus*, $HgCl_2$ treatment reduced rates of $NADP^+$ photoreduction to 1/8 of original levels, restored by reconstitution of F_B, indicating the requirement of intact F_B for photoreduction of $NADP^+$. The ease of destruction of F_B by $HgCl_2$ also suggested a location of F_B nearer the protein surface than F_A (Jung *et al.*, 1995). It should be noted, however, that this is not evidence for an indispensible involvement of F_B in physiological electron flow, as destruction of an iron-sulphur cluster in a 9kDa protein would be expected to significantly alter structure. Díaz-Quintana *et al.* (1998) addressed this problem with the finding that the affinity of ferredoxin binding is not affected by $HgCl_2$-induced destruction of F_B. Photoreduction of ferredoxin by F_B-less PSI is inefficient and fast reduction is recovered by reconstitution of F_B. Vassiliev *et al.* (1998) examined kinetics of $P700^+$ reduction in $HgCl_2$-treated F_B-less complexes, and found that a very high concentration of the artificial electron acceptor methyl viologen was required for oxidation of F_A^-, implying diffusion through a protein shell. Rate versus distance estimates of electron transfer were also consistent with F_A as the F_X-proximal cluster and F_B as the F_X-distal cluster.

1.10 Green Bacteria

The reaction centres of prokaryotic green bacteria exhibit remarkable similarities to PSI (reviewed in Lockau and Nitschke, 1993).

A reaction centre protein with an apparent molecular mass of 65kDa produces a prominent band on SDS-PAGE is observed in a reaction centre preparation from

Chlorobium (Hurt and Hauska, 1984). PsaA and PsaB produce bands of similar apparent molecular mass (Golbeck and Bryant, 1992).

A gene cloned from *Chlorobium* by Büttner *et al.* (1992) was suggested to code for a protein equivalent to PsaC. The sequence had homology to *psaC* and coded for residues theoretically able to ligate two 4Fe-S centres; also, the gene was located immediately downstream of the gene for the core protein.

The conserved dodecapeptide sequence from PsaA and PsaB thought to be involved in F_X binding was found in slightly modified form in *Chlorobium* (Büttner *et al.,* 1992) and *Heliobacillus* (Trost *et al.*, 1992), providing strong evidence of a relationship to PSI and of the existence of F_X in green bacteria.

PsaA and PsaB have a remarkable degree of homology to one another and it has been suggested that they evolved from a single protein which formed a homodimer. Only a single reaction centre protein has been found in green bacteria (Büttner *et al.,* 1992, Liebl *et al.*, 1993) and it appears that these reaction centres are indeed homodimeric with a gene duplication occuring after the branching off of the Gram-positive phylum from the cyanobacterial line (Lockau and Nitschke, 1993).

Nitschke *et al.* (1990a) assigned EPR signals for iron-sulphur centres from *Chlorobium* to the equivalents of F_A, F_B and F_X due to their similar characteristics. Magnetic interaction was also observed between F_A and F_B, as in PSI. However, F_A and F_B were not chemically reducible by dithionite at pH 11, indicating lower redox potentials of these species in *Chlorobium* than in PSI . Evidence for the existence of F_A and F_B in heliobacteria was also presented by Nitschke *et al.* (1990b). These acceptors may be chemically reduced in heliobacteria, as performed in Lin *et al.*

(1995), who also observed an absorption difference spectrum similar to that of F_X in higher plants.

Spectroscopic evidence for the existence of A_0 in green bacteria was found with the observation of bleaching in reaction centres of green sulphur bacteria (Nuijs *et al.*, 1985b) and heliobacteria (Nuijs *et al.*, 1985a). Modified bacteriochlorophyll molecules very similar to chlorophyll *a* have been isolated from heliobacteria and green sulphur bacteria (van de Meent *et al.*, 1991, 1992); these are good candidates for the identity of A_0 in green bacteria. An absorption difference spectrum similar to that of A_0 in higher plants was observed by Lin *et al.* (1995) in *Heliobacillus mobilis.*

The question of the existence of A_1 in green bacteria has been a controversial subject. Some recent evidence indicates that this carrier is not part of the green bacterial electron transfer chain. As in PSI, a reduced quinone may be photoaccumulated and observed by EPR (e.g. Nitschke *et al.*, 1990a). Trost *et al.* (1992) proposed the involvement of an A_1 analogue based on the redox titration behaviour of the recombination kinetics of the primary donor $P798^+$. However, menaquinone is the only quinone present in the heliobacterial reaction centre and extraction did not impair electron transfer (Kleinherenbrink *et al.*, 1993). Lin *et al.* (1995) observed a 600ps kinetic assigned to forward electron transfer from A_0 and found no evidence spectroscopically or kinetically for the formation of $P798^+A_1^-$. Strong evidence against the presence of A_1 in heliobacteria was provided by Brettel *et al.* (1998): a menaquinone anion could not be detected using flash absorption spectroscopy and photovoltage measurements indicated direct electron transfer from A_0^- to F_X. However, the photoaccumulated menaquinone anion radical was studied by Muhiuddin *et al.* (1999) using ENDOR and special triple resonance spectroscopy.

The electronic structure was found to be very similar to that of phylloquinone anion radical in PSI, suggesting evolutionary conservation of the structure of the binding site. It was suggested that the 600ps kinetic observed by Lin *et al.* (1995) might reflect electron transfer from A_0^- to A_1, rather than to F_X.

1.11 *Chlamydomonas reinhardtii* as a Model Organism.

Chlamydomonas reinhardtii is a unicellular, biflagellate green alga. It is the first photosynthetic eukaryote in which transformation of the chloroplast genome can be performed. The first report of this was by Boynton *et al.* (1988), in which deletion mutants of the chloroplast *atpB* gene were complemented. *C. reinhardtii* has become popular for studies on photosynthesis as it may dispense with photosynthesis and grow heterotrophically, using an external carbon source such as acetate, allowing the generation of a mutant photosynthetic apparatus. Higher plant species are absolute autotrophs *C. reinhardtii* may be grown either on solid media, for maintenance or selection, or in liquid media, allowing generation of the large amounts of protein which may be required for biochemical and biophysical analyses (Boynton and Gillham, 1993). In addition, the nuclear and mitochondrial genomes may be transformed, allowing manipulation of all three genomes (Kindle and Sodeinde, 1994).

C. reinhardtii has a single, large, cup-shaped chloroplast which lies adjacent to the plasma membrane along most of the cell periphery. The chloroplast may be transformed by bombardment with DNA-coated microparticles of tungsten or gold. The 196 kb circular chloroplast genome is present in about 80 copies (Boynton and Gillham, 1993). Chloroplast transformation may also be performed using glass beads,

which is less efficient but does not require specialised equipment (Kindle *et al.* 1991). Post-transformation the chloroplast is therefore heteroplasmic, with a mixture of host and introduced plastids. The experimental system may allow for means of selection of the introduced plastid and identification of the heteroplasmic or homoplasmic state. A selectable marker for antibiotic resistance may be introduced, such as the bacterial *aadA* sequence (Goldschmidt-Clermont, 1991). Alternatively, a non-photosynthetic deletion mutant may be used as the receptor strain. This mutation may be complemented, followed by selection for photosynthetic growth on minimal medium (e.g. Boynton *et al.*, 1988). Other possibilities include selection for herbicide resistance conferred by mutations of the *psbA* gene (Przibilla *et al.*, 1991).

1.12 Background and Aims of this Project

1.12.1 Mutation of C575 of PsaA

Fe_X is thought to exist as an interpolypeptide 4Fe-4S cluster, coordinated by the cysteine residues of the conserved dodecapeptide sequence found in PsaA and PsaB. Cysteine forms the ligands to 4Fe-4S clusters in most cases, but there are some exceptions. In the 4Fe-4S centre of the ferredoxin of the thermophilic bacterium *Pyrococcus furiosus*, aspartate acts as a ligand. Other examples include the hydrogenase from *Desulfovibrio gigas*, in which a histidine residue forms one of the ligands to the cluster. Nitrogenase contains two bridged 4Fe-4S clusters, known as the P-cluster pair. It is thought that serine may form a ligand to one of these irons. Serine is thoretically able to ligate Fe-S clusters via an oxygen atom. Non-cysteinyl ligation of Fe-S clusters is covered in the review of Moulis *et al.* (1996).

Webber *et al.* (1993) showed that replacement of one of the conserved cysteines of *psaB* with histidine in *C. reinhardtii* prevented assembly of the PSI RC, providing evidence that the cysteines may function as ligands to F_X. In a study involving site-directed mutagenesis of *psaB* in *Synechocystis* sp. PCC6803, Smart *et al.* (1993) showed that replacement of cysteine by serine, histidine or aspartate greatly reduced PS1 accumulation and stopped autotrophic growth. However, a cysteine to serine change did produce a significant, if greatly reduced accumulation of PS1. Warren *et al* (1993b) suggested that this mutant formed both non-functional 3Fe-4S clusters and mixed-ligand 4Fe-4S clusters which were capable of electron transfer to Fe_A and Fe_B. Mutation of either one of the conserved cysteines of PsaB to serine in *Synechocystis* sp. PCC6803 can support a 4Fe-4S cluster, although efficiency of reduction of F_A and F_B is greatly reduced (Vassiliev *et al.*, 1995).

Site-directed mutants C575D, C575H, C575S (and D576L) have been previously generated in *C. reinhardtii* by B.J. Hallahan . In addition to the site-directed mutation, these mutants contain the *aadA* cassette (Goldschmidt-Clermont, 1991) which confers resistance to the antibiotic spectinomycin. The plasmid used in the construction of these mutants is shown in figure 1.4. These mutants are non-photosynthetic.

This thesis reports the analysis of these site-directed mutants of the proximal conserved cysteine C575 of PsaA in *C. reinhardtii*. Aims were to confirm the identity of C575 as a ligand to F_X, and to examine the effects of mutation of C575 on assembly, electron transport and spectroscopic characteristics of PSI.

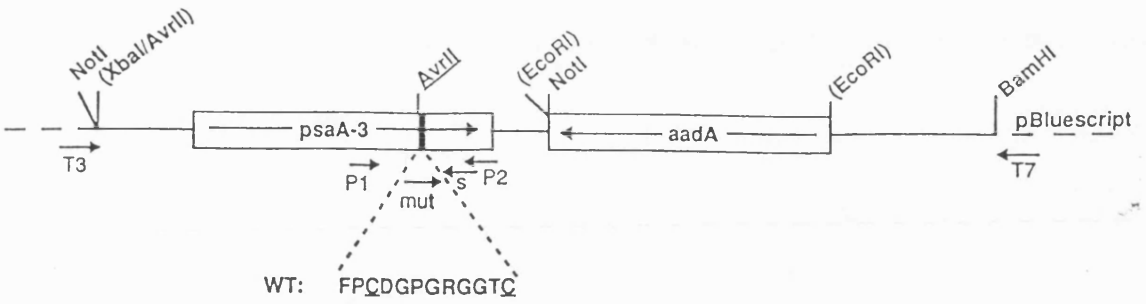

Figure 1.4

Plasmid pBev1-Avr: the Plasmid Used to Introduce Site-Directed Changes in *C. reinhardtii*

The bacterial gene conferring resistance to spectinomycin was cloned downstream of *psaA*-3 and in the opposite orientation. An *Avr*II restriction site was introduced into *psaA*-3. Restriction sites destroyed during cloning are in brackets. Primers used in the generation of the site directed changes are shown as arrows: T3 and T7 are from the pBluescript polylinker region; "mut" carries the *Avr*II site and the site-directed change; P1 and P2 are used to amplify this region and "s" is used to confirm the change by sequencing. Site directed changes were made to the proximal cysteine residue (the first underlined "C") or the adjacent aspartate residue "D". [Diagram from Hallahan *et al.*, (1995).]

1.12.2 Mutation of D576 of PsaA

The intercysteinyl region of the conserved dodecapeptide has been shown to be important in the interaction of the PSI core with PsaC. Experiments have been performed using chemical modification (Rodday *et al.* 1993), site-directed mutagenesis of *psaB* in *Synechocystis* (Rodday *et al.* 1994), and site-directed mutagenesis of *psaB* in *C. reinhardtii* (Rodday *et al.* 1995).

The function of the aspartate residue in position 576 of PsaA was examined in this project. The polar nature of this residue is likely to be significant. A function in interaction with PsaC is likely. However, it is also possible to model the formation of a salt bridge between the aspartate and arginine residues (J.Nugent, unpublished). Site-directed mutant D576L has been generated in *C. reinhardtii* by B.J. Hallahan. This mutant contains the *aadA* cassette as in the cysteine mutants. In this mutant, the polar aspartate residue has been substituted by a neutral leucine residue. The mutant is non-photosynthetic.

This thesis report studies on the effects of mutation D576L on assembly, electron transport and the spectroscopic characteristics of PSI. These include ENDOR spectra of $A_1^{\cdot -}$ in *C. reinhardtii* wild type and mutant D576L. This represents the first report of the ENDOR spectrum of $A_1^{\cdot -}$ in *C. reinhardtii.*

1.12.3 Second Site Revertants of Mutant D576L

If the effects of mutation in a non-functional mutant are not overly drastic, it is possible for secondary mutations to correct the effects of the first mutation, producing functional second site revertants. Lee *et al.* (1996) analysed second site revertants which had arisen spontaneously from PSI C-terminal extension and deletion mutants.

Second site revertants of mutant D576L were selected by photosynthetic growth on minimal medium. Four strains were selected for further study. The secondary mutations were shown by segregation to be in nuclear gene(s). The reversion mutations were therefore not in PsaA or PsaB. Sequencing also showed PsaC to be unchanged. These experiments are reported by Patel (1996).

This thesis reports spectroscopic analyses of the four revertants, including pulsed EPR kinetic measurements.

2.0 MATERIALS AND METHODS

2.1 Growth and Maintenance of *Chlamydomonas reinhardtii*

The strain of wild type *Chlamydomonas reinhardtii* used was CC1021. Site-directed mutants C575D, C575H, C575S and D576L were supplied by Dr. B.J. Hallahan. The procedures used to create these mutants have been described previously (Hallahan *et al.*, 1995).

The isolation of second-site suppressor mutants from site-directed mutant D576L was performed by V. Patel, using the following procedure. About 4 x 10^8 cells of mutant D576L were spread on a 20 x 20cm plate of HSM medium (Rochaix *et al.*, 1988). HSM is a minimal medium with no carbon source. The plate was incubated at 25°C under 45μE $m^{-2}s^{-1}$ illumination for two weeks. Phototrophic colonies were recovered to fresh HSM plates and were taken through three rounds of single colony isolations, in light as above. A more detailed description of this procedure and a molecular biological analysis of the suppressor mutants are presented in Patel (1996) and Evans *et al.* (1999). The latter has recently been submitted for publication.

C. reinhardtii cells were maintained and grown using TAP (Tris acetate phosphate) medium (Rochaix *et al.*, 1988). Cells were maintained on solid plates of TAP medium, solidified with the addition of 2% bacto-agar. Solid medium was supplemented with 100μg ml^{-1} spectinomycin, for all cell types other than wild type. Liquid TAP medium was used to grow cells in large volumes for biochemical and biophysical analysis. Liquid medium starter cultures were supplemented with 30 μg ml^{-1} spectinomycin, for all cell types other than wild type. Media were sterilised

dH_2O	975 ml
Tris	2.42 g
4x Beijerink Salts*	25 ml
1M $(K)PO_4$ ph7.0#	1 ml
Trace Elements†	1 ml
Glacial Acetic Acid	~1 ml to pH 7.0

* 4x Beijerink Salts

16 g NH_4Cl
2 g $CaCl_2.2H_2O$
4 g $MgSO_4.7H_2O$
dissolve in 1 litre distilled H_2O

1 M $(K)PO_4$

250 ml 1 M K_2HPO_4
170 ml 1 M KH_2PO_4 (titrate to pH 7.0)

– 2x PO_4 for HSM.

0.08 M K2HPO4
0.05 M KH2PO4
adjust to pH 6.9 with KOH.

† Trace Elements

(i) Dissolve in 550 ml distilled water in the order indicated below, then heat to 100C

11.4 g H_3BO_4
22 g $ZnSO_4.7H_2O$
5.06 g $MnCl_2.4H_2O$
4.99 g $FeSO_4.7H_2O$
1.61 g $CoCl_2.6H_2O$
1.57 g $CuSO_4.4H_2O$
1.1 g $(NH_4)_6 Mo_7O_{24}.4H2O$

(ii) Dissolve 50 g $EDTA.Na_2$ in 250 ml H_2O by heating and add to the above solution. Reheat to 100C. Cool to 80 - 90C and adjust to pH6.5 - 6.8 with 20% KOH.
(iii) Adjust to 1 litre. Incubate at room temperature for two weeks and allow a rust coloured precipitate to form. The solution changes from green to purple.
(iv) Filter through three layers of Whatman No.1 paper under suction until the solution is clear. Store at 4^oC.

Table 2.1
Composition of TAP medium (1 litre).

by autoclaving at 121°C for 20 minutes, with 15 lbs in^{-1} pressure. Spectinomycin was added post-autoclaving, once the medium had cooled to below 50°C. The composition of TAP medium is listed in table 2.1.

Plates were stored at 17°C and restreaked to fresh plates of solid TAP every 6-8 weeks. Working stocks were restreaked weekly. Wild type cells were grown at 50$\mu Em^{-2}s^{-1}$ illumination. Photosynthetic mutants were maintained in darkness, with the plates wrapped in aluminium foil.

Liquid cultures were grown in Erlenmeyer flasks, in the appropriate light conditions, at 25°C and aerated by shaking at 150 rpm. A loopful of working stock cells was used to inoculate a 25 ml starter culture of TAP, which was grown to stationary phase (~$2x10^7$ cells ml^{-1}). An appropriate amount of starter culture was used to inoculate a larger volume of medium. This was then grown to the cell density required. Aseptic technique was used throughout.

2.2 Verification of the Insertion of the *aadA* Cassette in Mutant C575S by Southern Blotting

The insertion of the *aadA* cassette (Goldschmidt-Clermont, 1991) into *Bam* HI fragment III of chloroplast DNA in mutant C575S was verified by Southern blotting. Chloroplast DNA was extracted and digested with restriction enzyme *Bam* HI. Fragments were separated by agarose gel electrophoresis. DNA in the gel was then transferred to a nylon membrane. The membrane was then probed with radiolabelled DNA fragments. The first probe contained exon III of the *psaA* gene of chloroplast. The second probe contained the *aadA* cassette. Binding of the radioactive probes was detected by autoradiography.

2.2.1 Extraction of DNA from *C. reinhardtii*

Small scale preparation of total DNA from *C. reinhardtii* was carried out according to the 'miniprep' method of Rochaix *et al.* (1988). Cells from a 25ml culture at a density of $1x10^7$ cells ml^{-1} were placed in a 30ml Sterilin sample bottle. Cells were harvested by centrifugation at 3000 rpm for 5 minutes, in a Mistral 3000 centrifuge. The supernatant was discarded. The following centrifugation steps were carried out using a MSE benchtop microcentrifuge, set at full speed (13 000 rpm). The cell pellet was resuspended in 1ml of TAP medium, then transferred to a 1.5ml microfuge tube and repelleted by centrifugation for 1 minute. The resulting supernatant was discarded and the cell pellet was resuspended in 0.35ml of TEN buffer (50mM EDTA pH 8.0, 20mM Tris-HCl pH 8.0, 0.1 M NaCl). 50µl of pronase at 10 mg ml^{-1} and 25µl of 20% SDS were added and the cells were incubated at 55°C for two hours in a water bath. 2µl of diethylpyrocarbonate (DEPC) were added and incubation continued for a further 15 minutes at 70°C in a fume hood. The tube was briefly cooled on ice, then 50µl of 5 M potassium acetate was added. The contents of the tube were mixed by shaking thoroughly. The tube was then incubated on ice for a further 30 minutes. The precipitate which formed was removed by centrifuging the tubes for 15 minutes and transferring the supernatant to a fresh microfuge tube. Contaminating proteins were removed by phenol extraction. One volume of TE saturated phenol was added and the phases were mixed by vortexing. Following centrifugation for 2 minutes, the upper, aqueous phase was transferred to a fresh microfuge tube and the extraction repeated three times. Phenol was removed from the solution by a final extraction with one volume of chloroform. The DNA in the recovered aqueous phase was subsequently precipitated by adding 2.5 volumes of cold (-20°C) absolute ethanol and incubating at -20°C for 30 minutes. The DNA was recovered by centrifuging the tubes for 10 minutes to pellet the DNA.

The supernatant was discarded and the pellets were washed with 70% (v/v) ethanol and then dried in a Rotovac vacuum drier. DNA pellets were finally resuspended in 50µl TE pH 8.0, 1µg ml^{-1} RNase A.

2.2.2 Restriction Enzyme Digestion of DNA and Electrophoretic Separation of DNA Fragments

The following molecular biological methods were based on those described in Maniatis *et al.* (1989).

3µl *BamHI*, 5µl of 10 x NEBuffer 4 (both supplied by New England Biolabs) and 15µl of miniprep DNA were made up to 50µl with ddH_2O in an eppendorf tube. This mixture was incubated at 37°C for 2 hours in a water bath.

DNA fragments were separated on a gel, using a midigel system. The gel was made with 1% agarose in 100ml TAE buffer (40mM Tris-acetate, 10mM EDTA, pH 8.0). The gel was run in a reservoir of 700ml TAE buffer. Prior to loading, samples were mixed with loading buffer (final composition, 0.1M EDTA, 40% glycerol, 0.001% SDS, 0.02% bromophenol blue). 30µl of sample was loaded in each well. The gel was run at 100V for about 2 hours.

2.2.3 Southern Blotting and Hybridisation

Following electrophoresis, the gel was soaked in alkali denaturing solution (1.5M NaCl, 0.5M NaOH) for 20 minutes, to denature double-stranded DNA to single-stranded DNA. The gel was then soaked in neutralising buffer (1.5M NaCl, 1M Tris-Cl pH 8.0). 2 strips of Whatman 3MM filter paper were soaked in 20 x SSC solution (3M NaCl, 0.3M Na citrate) and then placed on top of a supported glass plate, with the ends soaking in a reservoir of 20 x SSC. The gel was placed on top of the

paper. A piece of Hybond-N nylon filter, cut to the size of the gel, was placed on top of the gel. 3 sheets of 3MM paper, cut to the size of the gel, were placed on top of the nylon filter. A stack of paper towels, approximately 5cm high, was placed on top of these filter papers. A glass plate was placed on top of the paper towels and a 0.5kg weight was placed on top. This set-up was left overnight for 16 hours. The apparatus was dismantled. The position of the wells was marked through the wells onto the nylon filter using a soft pencil. The nylon filter was washed in 2 x SSC to remove any adhering agarose. The nylon filter was then sandwiched between two sheets of 3MM paper. The sheets of paper were stapled together, to retain the nylon filter, and then placed in an oven at 80°C for two hours to immobilise the DNA on the filter.

The nylon filter was probed with ^{32}P-labelled fragments of DNA. The first probe contained DNA of exon III of *psaA*, supplied by Dr. Saul Purton. The second probe contained the DNA of the *aadA* cassette. DNA for this probe was prepared as follows. 2µl of plasmid pUC-atpX-aadA, was digested with the addition of 1µl *NcoI* and 1µl *PstI* and 23µl ddH_2O. This mixture was incubated overnight for 16 hours at 37°C. The fragment was separated out by agarose gel electrophoresis. DNA was recovered from the gels using the GeneClean II kit, as described in the manufacturers' protocol (Biolabs 101). The probes were made from the DNA fragments immediately prior to use, using the Prime-It random primer labelling kit, as described in the manufacturers' protocol.

Hybridisation of the probe to the DNA on the nylon filter was carried out as follows. The filter was soaked in 25ml of pre-hybridisation solution (6 x SSC, 5 x Denhardt's solution, 0.5% SDS, 50µg ml^{-1}) in a hybridisation bag. The bag was sealed and was shaken at 65°C for 1 hour. The radiolabelled probe was denatured by

heating at 100°C for 5 minutes. The probe was added to the prehybridisation solution, the bag was re-sealed and was shaken at 65°C for 1 hour. The filter was washed by incubation in 2 x SSC, 0.1% SDS for 20 minutes at room temperature. The filter was then incubated in 1 x SSC, 0.1% SDS at 65°C for 30 minutes. A used X-ray film was wrapped in cling film and the filter was placed on top. A piece of filter paper with 5µl radioactive ink was placed in one corner. All were wrapped in cling film. In a dark room, a new X-ray film was placed on top and these were placed in a cassette. The cassette was incubated at -70°C overnight. The X-ray film was developed the next day.

For re-probing, the filter was stripped as follows. 400ml of 0.05 x SSC, 0.01M EDTA pH 8 was heated to boiling point, then removed from heat. SDS was added to a concentration of 0.1%. The filter was immersed in the hot solution for 15 minutes. This procedure was repeated with fresh solution. The filter was rinsed in 0.01 x SSC at room temperature. The filter was prehybridised and probed as before.

2.3 Measurement of Chlorophyll Concentration

Concentrations of chlorophyll *a* and chlorophyll *b* were calculated by the method of Arnon (1949) using the extinction coefficients for chlorophyll extracted in 80% acetone. The contributions to absorbance at 663 and 645 nm are as follows:

$$A663 = 82.04\ [\text{Chl } a] + 9.27\ [\text{Chl } b]$$

$$A645 = 16.75\ [\text{Chl } a] + 45.6\ [\text{Chl } b]$$

where Chl = chlorophyll concentration in mg/ml.

When the above equations are solved:

$$[\text{Chl } a] = 0.0127\ A663 - 0.00259\ A645$$

$$[\text{Chl } b] = 0.0229\ A645 - 0.00467\ A663$$

Total chlorophyll a and b may be calculated from absorbance at 652 nm:

$$[\text{Chl } a] + [\text{Chl } b] = 0.029\ A652$$

10µl of sample was added to 0.99ml of 80% acetone in an eppendorf tube. The mixture was vortexed and debris was removed by pulse centrifugation. Absorbance in a 1ml cuvette was measured at 645, 652 and 663nm against an 80% acetone blank using a Phillips PU 8740 or Unicam UV2 UV/VIS scanning spectrophotometer.

2.4 Preparation of thylakoid membranes from *Chlamydomonas reinhardtii*

Thylakoid membranes were fractionated from *C. reinhardtii* using the procedure of Diner and Wollman (1980). Liquid cultures were concentrated using a Millipore harvester. The following steps were carried out at 4C. Cells were pelleted by centrifugation at 16000 x g_{max} for 5 minutes. Cells were washed and resuspended in HSM (20mM HEPES-NaOH pH 7.5, 0.35M sucrose, 2mM $MgCl_2$) to give a chlorophyll concentration of 1mg/ml. The suspension was passed through a French pressure cell at 4000 lb/in^2 then centrifuged for 40 minutes at 48000 x g_{max}. The

supernatant was retained for the preparation of ferredoxin. The pellet was resuspended in 5mM HEPES-KOH pH 7.5, 2.2M sucrose, 10mM EDTA in a ratio of 1 volume of pellet to four volumes of buffer. This suspension was overlaid with 5mM HEPES-KOH pH 7.5, 0.5M sucrose and centrifuged for 16 hours at 140000 x g_{max}. A floating pellet was obtained and the top and bottom layers of buffer were removed with an aspirator. The pellet was suspended in 20mM Tris-Cl pH 8, 0.3M NaCl and washed by centrifugation for 1 hour at 48000 x g_{max}. The resulting pellet was resuspended in 20mM Tris-Cl pH 8, 0.1M NaCl.

2.5 Preparation of thylakoid membranes from Spinach (*Spinacea oleracea*)

Spinach leaves were washed. The large leaf stems and ribs were removed. The leaves were then homogenised for 15s in a Waring blender in grinding medium (0.33M sorbitol, 20mM Mes-NaOH, 0.2mM $MgCl_2$ pH 6.5), pre-cooled to 4°C and with sodium ascorbate added to 5mM immediately prior to use. The homogenate was filtered through 8 layers of muslin and the filtrate was centrifuged for 5 minutes at 3000 x g_{max}. The chloroplast pellet was resuspended in a hypotonic solution of 5mM $MgCl_2$ for 1 minute to osmotically shock and rupture the chloroplasts. An equal volume of double strength grinding medium was added and the mixture was centrifuged at 3000 x g_{max} for 20 minutes. The resulting supernatant was retained for use in the preparation of ferredoxin and FNR. The thylakoid pellet was resuspended in 20mM Mes-NaOH, 25mM NaCl, 5mM $MgCl_2$ pH6.3 (resuspending medium).

2.6 Electrophoretic Separation of Chlorophyll-Protein Complexes.

The method is a modification of that of Delepelaire and Chua (1979).

The entire procedure was carried out at 4°C. A Biorad Protean 2 minigel kit was used.

Thylakoid membrane samples were first diluted to the chlorophyll concentration of the least concentrated sample, then solubilized for 30 minutes in a concentrated stock solution of sample buffer containing 250mM Na_2CO_3, 250mM dithiothreitol, 10% $LiDodSO_4$, 10% sucrose to give a chlorophyll / $LiDodSO_4$ ratio of 1:20.

The composition of the gel is listed in table 2.2. The upper and lower reservoir buffers contained 50mM Tris, 40mM glycine pH 8.3. In addition, the upper reservoir buffer contained 0.1% $LiDodSO_4$, 1mM EDTA. 15µl of sample was added per well. Markers were not required as the PSI core migrates clearly as the highest green band, and mobility was not examined. Electrophoresis was performed at 4°C in the dark at 75V constant voltage for 2-3 hours. Gels were photographed immediately after electrophoresis. A blue filter was used for black and white photography.

2.7 Preparation of Digitonin Photosystem I

TEM buffer (50mM Tris-Cl pH8, 2mM EDTA, 5mM $MgCl_2$) and a stock solution of 2.5% digitonin dissolved in TEM were added to the thylakoid preparation to give final concentrations of 1mg/ml chlorophyll and 0.5% digitonin for spinach, or 1% digitonin for *C. reinhardtii*. The mixture was left on ice for 30 minutes, then centrifuged for 30 minutes at 15800g. The supernatant was retained, then centrifuged

	Resolving gel	Stacking gel
30% acrylamide/ 0.08% bisacrylamide	1.32ml	110µl
1.5M Tris-Cl pH 8.9	1.88ml	-----
0.5M Tris-Cl pH 6.7	-----	375µl
dH_2O	4.3ml	1.015ml
TEMED	3.5µl	1µl
10% ammonium persulphate	18.75µl	15µl

Table 2.2

Composition of the LiDodSO_4-polyacrylamide gel.

The minigel, with a resolving gel of 7% acrylamide and stacking gel of 3% acrylamide was cast with the above mixtures.

at 144000g, for 1.5 hours for spinach PSI or for 2.5 hours for *C. reinhardtii* PSI. The resulting pellet was resuspended in TEM.

2.8 Removal Of PsaC: Preparation of P700/F_X PSI Core Particles

The chaotropic removal of PsaC to produce an intact reaction centre was originally performed by Golbeck *et al.* (1988) using 6.8M urea. Parret *et al.* (1989) used a variety of chaotropes and found the concentration of chaotrope required for PsaC removal to be inversely related to the strength of the chaotrope. found that 6.8M urea removes all three stromal extrinsic proteins PsaC, PsaD and PsaE.

The PsaC protein of spinach digitonin PSI was removed chaotropically using urea. A Beckmann benchtop ultracentrifuge was used for the centrifugation step. All solutions were thoroughly degassed with nitrogen prior to use. A stock solution of 9M urea, 50mM Tris-Cl pH 8.0 was made up and was added dropwise with vortexing (to avoid high local concentrations of urea) to a digitonin PSI preparation in an ultracentrifuge tube, to give a final concentration of 6.8M urea (i.e. 3 volumes urea solution to 1 volume PSI). and β-mercaptoethanol was added to the reaction mixture to a final concentration of 0.1% v/v. The tube was overlaid with nitrogen, then was covered with Nescofilm and left to stand at room temperature for 30 minutes. The mixture was then diluted with TEM / 0.1% β-mercaptoethanol (50mM Tris-Cl pH8, 2mM EDTA, 5mM $MgCl_2$) to fill the ultracentrifuge tube. If a dilution of at least threefold was too high a volume for a single tube, the mixture was divided between two tubes and then filled with TEM / 0.1% β-mercaptoethanol. Tubes were

centrifuged at 144000g, at 10°C and for 2 hours. The resulting pellet was retained and resuspended in TEM, pre-cooled to 4°C.

2.9 Removal of F_X from P700/F_X PSI Core Particles to Prepare P700/A_1 "Apo-F_X" Particles

Chemical oxidative destruction of F_X was originally performed by Warren *et al.* (1990) using 3M urea and 5mM potassium ferricyanide which denatures F_X to the level of zero-valence sulphur.

Spinach PSI core particles were prepared by incubating PSI core particles for 2 hours with 3M urea and 5mM potassium ferricyanide at room temperature. In practice a stock solution of 9M urea and 15mM potassium ferricyanide was added dropwise with vortexing to the sample in an ultra centrifuge tube. The mixture was then diluted with TEM to fill the centrifuge tube. Tubes were centrifuged at 144000g, at 10°C and for 2 hours using a Beckmann benchtop ultracentrifuge. The resulting pellet was retained and resuspended in TEM, pre-cooled to 4°C.

2.10 Preparation of Ferredoxin and FNR

The methods are based on those of Buchanan and Arnon (1973) and Shin (1973), omitting the final purification steps in both cases.

1kg of spinach leaves were washed and then ground with 1.5l ice water for 2 minutes in a Waring blender. The homogenate was filtered through 2 layers of muslin. Alternatively, the supernatant from the osmotic shock stage of spinach thylakoid membrane preparation was used. 5ml of 1M Tris-Cl pH 7.8 was added to the filtrate. Acetone, precooled to -15°C, was added to 35% volume with mechanical

stirring. The mixture was centrifuged for 10 minutes at 5000 x g_{max} and the pellet discarded. Acetone, pre-cooled to -15°C, was added to the supernatant with mechanical stirring to a final concentration of 75%, then left to settle for 30 minutes. Most of the supernatant was decanted. The remainder of the mixture was centrifuged at 3000 x g_{max} for 10 minutes and the pellet retained. The pellet was washed twice with -15°C acetone then spread on large filter paper and dried. The resulting powder was resuspended in 20mM Tris-Cl pH 8.

The following steps were performed at 4°C. A column was poured with DEAE-cellulose, pre-equilibrated with 2M Tris-Cl pH 8, then washed with distilled water until free of buffer. The dissolved powder was passed through the column to remove ferredoxin. For the preparation of *C. reinhardtii* ferredoxin, the supernatant from the centrifugation step ,which followed the French pressing of cells, was diluted four-fold with 20mM Tris-Cl pH 8, then passed through the column. In the case of spinach, the resulting extract, following passage through the column, was retained for the preparation of FNR. The column was then washed with the following, each equivalent to the hold-up volume of the column: 20mM Tris-Cl pH 8, 0.15M Tris-Cl pH 7.5, 0.2M Tris-Cl pH 7.5. Ferredoxin was eluted with 20mM Tris-Cl pH8, 0.8M NaCl and collected using a fraction collector.

The FNR-containing extract (see above paragraph) was concentrated by ultrafiltration using an Amicon Diaflo system with PM10 or PM30 filters, on ice.

2.11 $NADP^+$ photoreduction assay

This method was based on that of Terashima *et al.* (1994).

3ml of thylakoid membranes at a chlorophyll concentration of 16.7μg/ml in 0.2m sorbitol, 10Mm NaCl, 5Mm $MgCl_2$, 50mM HEPES-KOH pH 7.5, 10μM DCMU, 1μM FCCP, 0.5mM DAD, 5mM sodium ascorbate, 500mM $NADP^+$ with excess amounts of spinach ferredoxin and FNR were placed in a 1 cm path length cuvette. The spectrophotometer was set at 340 nm and zeroed using this mixture. The mixture was illuminated with saturating white light for ten minutes and absorbance at 340nm was measured immediately. The rate of $NADP^+$ photoreduction in μmol NADPH/mg chl/h may be calculated by multiplying this value by 58.068. Three replicates were measured and averaged for each strain.

Initially, we thought that the low rates of $NADP^+$ photoreduction were due to the use of spinach ferredoxin as an electron acceptor, which we thought may be physiologically inapproriate. In an attempt to increase the rates of $NADP^+$ photoreduction, the assay was tested with *C. reinhardtii* wild type thylakoid membranes and a cyanobacterial flavodoxin, in place of spinach ferredoxin. The flavodoxin was produced and purified as follows. Plasmid pSE280 (Brosius, 1989), with the *isiB* gene from *Synechococcus* sp. PCC 7002 inserted into the *Nco*I and *Eco*RI restriction sites of the plasmid, which was kindly supplied by Dr. D.A. Bryant. The *isiB* gene encodes flavodoxin. The plasmid was used to transform *E. coli* strain BL21 and expression of flavodoxin was induced using 0.6mM IPTG. The procedure of transformation and expression is described in Mühlenhoff *et al.* (1996). Flavodoxin was purified according to the method described by Bottin and Lagoutte (1992).

The $NADP^+$ photoreduction assay was also tested by using *C. reinhardtii* wild type thylakoid membranes and *C. reinhardtii* ferredoxin, in place of spinach ferredoxin.

2.12 Oxygen consumption assay of PSI electron transport

The reaction was carried out using 3ml of thylakoid membranes at a chlorophyll concentration of 16.7μg/ml in 0.2M sorbitol, 10mM NaCl, 5mM $MgCl_2$, 50mM HEPES-KOH pH 7.5, 10μM DCMU, 1μM FCCP, 0.5mM DAD, 5mM sodium ascorbate, 0.5μM sodium azide and 50 μM methyl viologen or 50 μM neutral red. The reaction mixture minus the thylakoid membranes was placed in the chamber of an oxygen electrode and sealed. Constant temperature of 25°C was maintained in the chamber using a water bath and pump. Current was set to give full scale deflection of the chart recorder, which was assumed to measure 0.28μmoles O_2/ml. Thylakoid membranes were added using a microlitre syringe under a green safety light, then the recorder was left to run in darkness for 2-3 minutes to measure the rate of basal electron flow. The chamber was then supplied saturating white light from a 650W lamp shone through a water bottle as a heat filter. Best fit straight lines were drawn through the traces, and the gradient of the dark trace was subtracted from that of the light trace. The rate of light induced oxygen consumption was calculated from this value. Three replicates were measured and averaged for each strain.

2.13 Preparation of Samples for Spectroscopic Analysis

All measurements were made using standard 3mM diameter quartz EPR tubes containing samples of 0.2-0.3 ml and 2-5 mg/ml chlorophyll concentration.

CW EPR measurements of $F_{A/B}$ were made with unfractionated thylakoid membranes from *C. reinhardtii*. Pulsed EPR measurements were made with unfractionated thylakoid membranes from *C. reinhardtii* and preparations of digitonin PSI from spinach. Samples were reduced with 10mM ascorbate in darkness for 1 hour on ice. Samples were frozen in darkness in liquid nitrogen. Samples were then wrapped in aluminum foil to maintain darkness and stored in liquid nitrogen in darkness.

CW EPR and ENDOR measurements of the phylloquinone anion radical $A_1^{\cdot -}$ were made with digitonin PSI samples. A 2% w/v solution of sodium dithionite solution was degassed with nitrogen and was added to samples to give a final concentration of 0.2%. Samples were left to stand for 30 minutes in darkness at room temperature under a flow of nitrogen gas. Samples were frozen in darkness in liquid nitrogen. Samples were then wrapped in aluminum foil to maintain darkness and stored in liquid nitrogen in darkness. Photoaccumulation of $A_1^{\cdot -}$ was performed by illumination of the sample for 2 minutes using a 650W lamp, filtered through water to reduce heating. The sample being illuminated was immersed in a bath of ethanol cooled to 205K with dry ice (solid CO_2). The sample was frozen in liquid nitrogen immediately following illumination. CW EPR was used to measure the rise of the $A_1^{\cdot -}$ signal. EPR conditions are given in figure 3.7. The sample was then used for ENDOR analysis.

2.14 Continuous Wave (CW) EPR Spectroscopy

(a) Principles

The use of EPR in the study of photosynthesis is reviewed by Evans (1977).

EPR spectroscopy is a technique used to detect paramagnetic species, i.e. molecules containing unpaired electrons. EPR is therefore very useful in the study of the cofactors involved in photosynthetic electron transfer. Microwave radiation is used to induce a change in the spin state of the paramagnetic species. A change in energy state of the sample is observed.

Electrons have both spin and charge and are magnetic. In an electron pair, the spins are opposed and the net magnetic moment is zero. However, an unpaired electron has a magnetic moment and is able to interact with a an externally applied magnetic field. Normally, the electron spins are randomly oriented, all having the same energy. In a magnetic field, the spins become oriented either parallel or antiparallel to the field direction, resulting in two populations of electrons with an energy difference. An electron can move from one energy level to the other by absorbing or emitting a quantum of energy, equal to the difference in energy ΔE between the two energy levels. The higher energy state is energetically unfavourable. The proportion of electrons occupying this state can be increased by microwave irradiation of the sample. The process of return from the higher energy state to the lower is known as relaxation.

The difference in energy between the two levels may be expressed as follows:

$$\Delta E = h.v$$

where h = Planck's constant and v = the frequency of radiation.

The energy difference is directly related to magnitude of the applied magnetic field H. Thus:

$$\Delta E = h.v = g.\beta.H$$

where β= the Bohr magneton and g = the electronic g value (a characteristic of the measured sample).

The process of transition between energy states is known as resonance. The microwave frequency required to induce resonance is dependent on the magnetic field strength. Resonance may be obtained by either varying frequency in a fixed magnetic field or vice versa. In practice, the latter is used, i.e. frequency is kept constant and the magnetic field is scanned until the correct combination of magnetic field and frequency is obtained and resonance is observed.

Irradiation induces the the transition of electrons from lower to the higher energy state. However, irradiation also induces electrons in the upper energy level to emit radiation and drop to the lower level. This process is known as stimulated emission. If there are equal numbers of electrons in a given population in each state there will be no net absorption of energy. For absorption to be observed, it is therefore desirable to maximise the difference in distribution between levels.

For a given population of electrons, the ratio of electrons distributed between the two energy levels is given by the Boltzmann distribution:

$$N_1 / N_2 = 1 - (h.v / k.T)$$

where N = the number of electrons in each energy state, T = the absolute temperature and k = the Boltzmann constant.

The largest difference between the two subpopulations of electrons is therefore obtained by the use of low temperature in experimental observations. An EPR spectrum is usually presented as the first derivative of the absorption spectrum. At low temperatures, relaxation rates are slowed, leading to a sharpening of lines in the spectrum.

A spectrum may be used to identify the paramagnetic species by comparison with spectra of isolated components. Information may also be deduced about the environment of the species. The spin lattice relaxation effect describes the interaction of the ion with its surrounding environment. The spin-spin relaxation effect describes interaction with other nearby magnetic species. These effects may lead to changes in the width of the absorbance peak.

(b) Experimental details

CW EPR spectra were recorded on a JEOL RE1X X-band spectrometer fitted with an Oxford Instruments ESR 9 liquid helium cryostat.

Wide scan EPR spectra in the g=2.00 region were obtained to show the signals of reduced $F_{A/B}$. Spectra were recorded before and after illumination, and light minus dark difference spectra were calculated. Ascorbate-reduced unfractionated thylakoid membrane samples from *C. reinhardtii* were analysed. Conditions were as follows: microwave power 10mW, modulation width 1mT, temperature 15K.

EPR spectra in the g=2.00 region were obtained to show the signal of the phylloquinone anion radical $A_1^{\cdot -}$. Dithionite-reduced *C. reinhardtii* and spinach digitonin PSI samples were analysed. Conditions were as follows: microwave power 100μW, modulation width 0.17mT (spinach) or 0.2mT (*C. reinhardtii*), temperature 60K.

2.15 Pulsed EPR Spectroscopy

(a) Principles: Electron Spin Polarised (ESP) Signals

ESP signals are high intensity EPR signals arising from interactions between the partners of a radical pair. In the $P700^+/A_1^-$ pair in photosystem I, the radical spins are correlated, producing an ESP signal. Pulsed EPR is a specialised form of EPR spectroscopy which can be used to make time-resolved measurements of ESP signals. Pulsed EPR was used in the pioneering work of Thurnauer *et al.* (1979) to observe ESP signals associated with PSI at room temperature. A signal in the out-of-phase channel with a lifetime of 200ns was observed. The decay of this signal was attributed to forward electron transfer from A_1. Pulsed EPR overcomes some of the problems associated with making kinetic measurements using time-resolved CW EPR. The time lag between the first microwave pulse and the observation of the echo can be used to temporally separate the laser artifacts from the signal.

(b) Experimental details

Pulsed EPR spectra and kinetics were measured using the method of Moënne-Loccoz *et al.* (1994), on a Bruker ESP380 X-band pulsed spectrometer with a variable Q dielectric resonator (Bruker model 1052 DLQ-H 8907) fitted with an Oxford

instruments CF935 cryostat cooled with liquid nitrogen. The resolution limit of this instrument for kinetic measurements is 8ns. Actinic illumination of the sample was supplied by a Nd-YAG laser (Spectra Physics DCR-11) with pulses of 10ns duration at 532nm.

2.16 ENDOR Spectroscopy of $A_1^{\cdot -}$

(a) Principles

ENDOR is a modifed form of EPR spectroscopy in which microwave irradiation is applied to induce resonances in the electrons of paramagnetic species, while, at the same time, radio frequency irradiation is applied to induce nuclear resonances. The nuclear spins of the hyperfine tensors which surround the radical interact with the spin of the unpaired electron of the radical. This alters the microwave absorption properties of the radical. ENDOR reveals the electronic structure of radicals.

The field values are held constant while radio frequency (r.f) radiation is applied the sample . In the case of $A_1^{\cdot -}$, the field values are set at the crossing point of the first derivative CW EPR spectrum of the radical, i.e. g=2.0048 . High microwave power is used which saturates the EPR signal. The frequencies of the r.f radiation are scanned. Nuclear interaction changes the relaxation, which decreases the microwave saturation level and increases the apparent EPR signal. The induced variations in microwave absorption produce a spectrum. Individual hyperfine coupling (hfc) constants may be calculated from the features of the ENDOR spectrum. Resonances may be assigned by comparison with spectra of *in vitro* analogues of the

radical. Deuteration of analogues and *in vivo* deuteration of groups of the radical may be used to assign resonances to particular bonds (Rigby *et al.*, 1996).

(b) Experimental details

The $A_1^{\cdot -}$ radical was photoaccumulated. The sample was frozen in liquid nitrogen. The CW EPR spectrum of the radical was obtained. ENDOR spectra were obtained as described in Rigby *et al.* (1994). ENDOR spectra were obtained using a Bruker ESP 300 spectrometer in conjunction with a Bruker EN 003 ENDOR interface, a Wavetek 3000-446 radio frequency synthesiser, an EN 370 power amplifier and an EN 801 ENDOR cavity. The Wavetek synthesiser was also used for frequency modulation of the radio frequency (r.f.) output. Temperature was controlled with an Oxford Instruments continuous flow ESR 900 cryostat with an ITC 4 temperature controller. The impedance of the radio frequency circuit was 50Ω.

Acquisition conditions were as follows: microwave power 3.0mW; r.f. power 100W; r.f. modulation depth 177kHz; scan time 84s; temperature 90K. Spectra were obtained from the sum of 200 scans.

3.0 RESULTS

3.1 Verification of the Insertion of the *aadA* Cassette in Mutant C575S by Southern Analysis

All of the site directed mutants were created by Dr. B.J. Hallahan, using the plasmid pBev1-Avr, described in Hallahan *et al.* (1995). The *aadA* cassette is inserted downstream of the stop codon of *psaA* exon III, in the opposite orientation. The verification of the insertion of the *aadA* cassette into *Bam* HI fragment III of *C. reinhardtii* chloroplast DNA, by Southern analysis has been described previously for C575D, C575H and D576L (Hallahan *et al.*, 1995). It is necessary to check that the transformation has taken place correctly. Here, the procedure is repeated for mutant C575S.

Total DNA was digested with *Bam* HI, fragments were separated by gel electrophoresis and then transferred to a nylon filter by Southern blotting. Figure 3.1 shows an autoradiograph of the filter, probed with the "Bam 13" probe (Hallahan *et al.*, 1995). This probe contains *psaA* exon III. Lane 4 shows the wild type fragment, of 6.8kb size. Lanes 1, 2 and 3 show DNA from different isolates of the C575S mutant. In these lanes, a fragment with decreased mobility, with an increased size of 8.7kb, is clearly seen. The fragment is increased in size from 6.8kb to 8.7kb, due to the insertion of the *aadA* cassette.

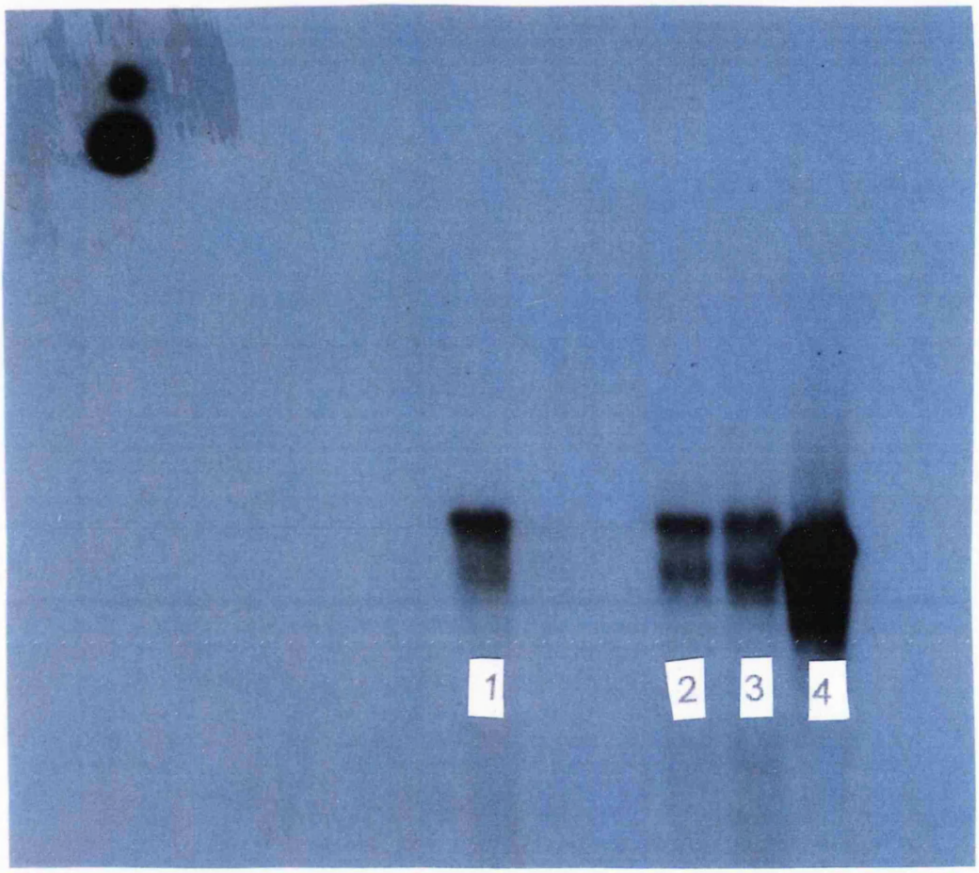

Figure 3.1

DNA analysis of Mutant C575S: Probing With *psaA* DNA

Total DNA extracted from mutant C575S was digested with *Bam* HI and probed using a fragment of Bam 13, radioactively labelled with ^{32}P. Lanes 1,2 and 3 represent DNA from different isolates of mutant C575S. Lane 4 represents DNA from *C. reinhardtii* wild type. The band of 6.8kb size in wild type is increased to 8.7kb in mutant C575S by the insertion of the *aadA* cassette. The spots in the top right hand corner represent radiolabelled ink.

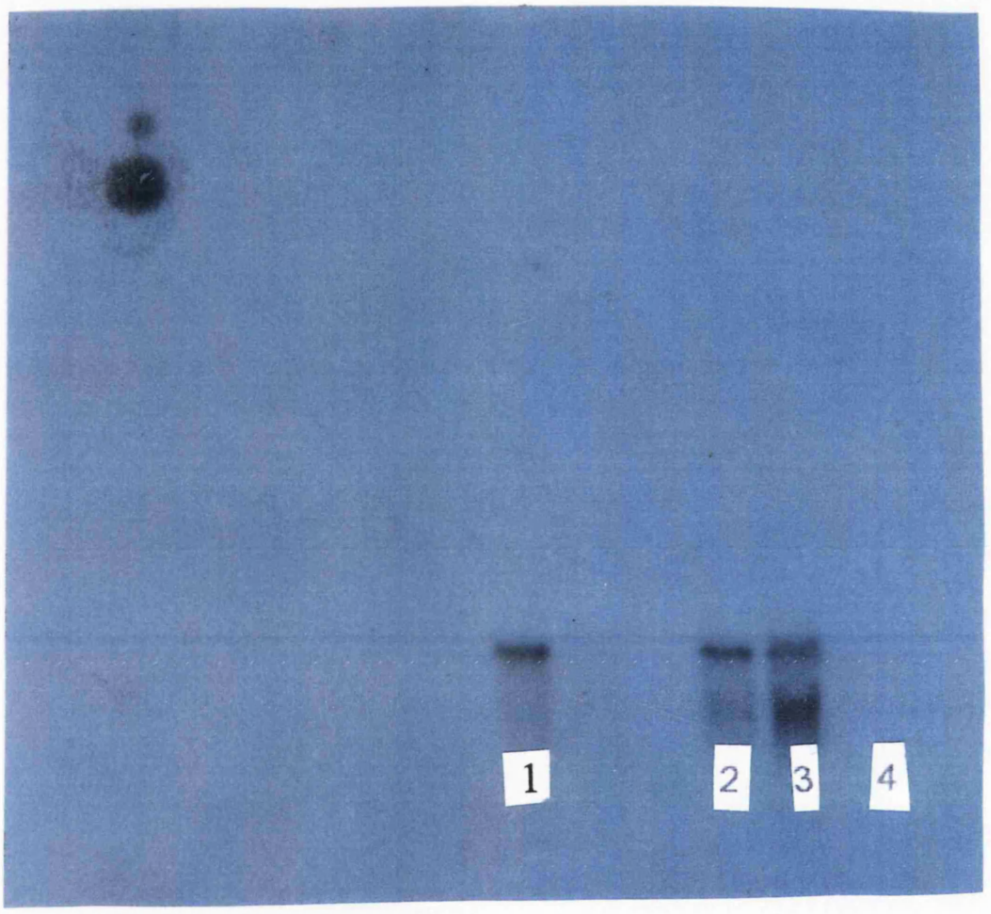

Figure 3.2

DNA analysis of Mutant C575S: Probing With *aadA* DNA

Total DNA extracted from mutant C575S was digested with *Bam* HI and probed using a fragment of DNA containing the *aadA* cassette, radioactively labelled with ^{32}P. Lanes 1,2 and 3 represent DNA from different isolates of mutant C575S. The same 8.7kb fragment is seen as in figure 3.1. Lane 4 represents DNA from *C. reinhardtii* wild type, which does not bind the probe. The spots in the top left hand corner represent radiolabelled ink.

The filter was stripped of the first probe and re-probed with *aadA* DNA. The autoradiograph showing the binding of this probe is presented in figure 3.2. The probe binds to the same fragments of C575S DNA as seen in the first probing, showing that the *aadA* cassette is present and is in the correct position: in the same *Bam* HI fragment which contains *psaA* exon III. The wild type lane is a control, showing that the probe is binding only to fragments which contain *aadA*. There is no binding of the *aadA* probe to wild type DNA.

3.2 "Green Gel" Analysis of Assembly of Photosystem I in *C. reinhardtii* Site-Directed Mutants

In general, native green gel systems are used to determine the complement of chlorophyll-protein complexes in the thylakoid membrane. All of the chlorophyll in chloroplasts is thought to exist as chlorophyll-protein complexes. Markwell *et al.* (1979) fractionated all of the photosynthetic pigments of maize as chlorophyll-protein complexes using the zwitterionic detergent Deriphat-160. Only negligible amounts of free or detergent solubilised chlorophyll were produced. Many different protocols are available, producing different sets of chlorophyll-protein complexes. A variety of detergents have been used. Other variants, such as the inclusion of urea in the gel system, have also been used. Chlorophyll-protein complexes and green gel techniques are reviewed by Green (1988). Green gel techniques are particularly useful in the study of the composition of light-harvesting complexes. Here, however, green gel electrophoresis has been used as a convenient assay to examine levels of assembly of photosystem I in mutants.

The method used here was based on the method of Delepelaire and Chua (1979). Five bands were observed by Delepelaire and Chua, designated CPI to CPV. The highest green band, CPI, contained chlorophyll *a* and no chlorophyll *b*. CPI represents the photosystem I core (Green, 1988), which binds about 100 chlorophyll *a* molecules (Golbeck, 1992). The detergent $LiDodSO_4$ is less harsh than $NaDodSO_4$, leading to enhanced stability of chlorophyll-protein complexes. The stability of the hydrophobic interaction between chlorophyll and protein is also enhanced at low temperature. The procedure is therefore performed at 4°C.

In the original paper, gradient gels were used, as a variety of bands of different mobility were examined. Here, however, as only the single highest band was of interest, a low percentage resolving gel of 7% acrylamide was used. Markers were not required for this reason, and also because the migration of chlorophyll-protein complexes is not well-related to molecular weight (Delepelaire and Chua, 1979).

Green gels which include the site-directed mutants are shown in figure 3.3. 2137::*aadA* is a transformant which incorporates the *aadA* cassette but has no site-directed amino acid changes. This transformant has growth rates indistinguishable from wild-type (Hallahan *et al.*, 1995). Gel A shows that thylakoid membranes of this transformant contain CPI. In addition, the band has a strong intensity, suggesting that introduction of the *aadA* cassette does not cause reduced levels of PSI assembly. This transformant serves as a positive control: changes in assembly of PSI in the site-directed mutants and the inability to grow phototrophically are solely due to the site-directed changes. Lane 3 of gel B contains thylakoid membranes from the B4 strain. B4 is a mutant which lacks PSI, serving as a negative control. Lane 1 of

Gel A Gel B

Figure 3.3

Qualitative green gel analysis of Assembly of Photosystem I in *C. reinhardtii*.

Unfractionated thylakoid membranes were analysed in all lanes except lane 1 of gel B. Chlorophyll-protein complexes were resolved by LiDodSO_4-PAGE (Delepelaire and Chua, 1979), using a stacking gel of 3% acrylamide and a resolving gel of 7% acrylamide, according to the procedure outlined in section 2.6. CPI, the band which represents the photosystem I core complex, is denoted. The contents of the lanes of gel A are denoted. The contents of the lanes of gel B are as follows: (1) wild type digitonin PSI; (2) C575S thylakoid membranes; (3) B4 thylakoid membranes (PSI minus strain); (4) wild type thylakoid membranes.

gel B contains a digitonin preparation from *C. reinhardtii* wild type, confirming that this preparation contains PSI.

Thylakoid membranes of site-directed mutant C575D were run in lane 3 of gel A. CPI is absent: this mutant does not assemble PSI. Mutants C575H, D579L and C575S all have a CPI band. These three non-photosynthetic mutants each assemble a non-functional PSI complex. In gel B, the CP1 band of C575S has a strongly reduced intensity relative to wild type, suggesting a reduced level of assembly compared to wild type.

EPR spectra showing the signal of photooxidised P700 in wild type, 2137::*aadA*, C575D, C575H and D579L are presented in Hallahan *et al.* (1995). These results also indicate similar levels of PSI assembly between wild type and 2137::*aadA*. Reduced P700 signal intensity was seen in C575D, C575H and D579L, reflecting decreased levels of PSI assembly relative to wild type.

3.3 CW EPR Analysis of Reduced $F_{A/B}$ in *C. reinhardtii* site-directed mutants.

Figure 3.4 shows wide scan EPR spectra of ascorbate-reduced thylakoid membranes, recorded following illumination at low temperature, under which conditions the spectra of photoreduced F_A and F_B may be observed. These results are complicated by the presence of a large signal around g=2.02, seen in thylakoid membranes of *C. reinhardtii*. This signal is attributed to non-PSI iron-sulphur centres. The NADH dehydrogenase, present in algal thylakoids, may contribute to this signal.

In wild type, the spectrum indicates that the electron is mainly associated with F_A (resonances about g=2.05, 1.94 and 1.86). Some reduction of F_B is also apparent (resonances about g=2.07, 1.90 and 1.88). These are similar to the values reported for higher plants (Evans *et al.*, 1972; Evans *et al.*, 1974) and cyanobacteria (e.g. Li *et al.*, 1991b; Vassiliev et al., 1995). Under conditions of illumination at low temperature, the electron is generally found to be mainly associated with centre F_A. Vassiliev *et al.* (1995), in a study of *Synechocystis* sp. PCC 6803, report a ratio of 5:1, of PSI complexes with photoreduction of F_A compared to PSI complexes with photoreduction of F_B. Li *et al.* (1991b), in a study of *Synechococcus* sp. PCC 6301, report a similar figure of 85% photoreduction of F_A.

In mutants C575D and C575H, no photoreduction of iron-sulphur centres was observed. For mutant C575D, this reflects the impairment of assembly of PSI observed in the green gel experiments. Mutant C575H, however, does assemble a PSI complex. This complex, therefore, has impaired electron transport, and the electron is not transported to the iron sulphur centres. The spectrum has the g=2.00 signal of $P700^+$, but no other signals. Hanley *et al.* (1992) report the spectrum of PSI core particles, with F_A and F_B removed by urea treatment, recorded with illumination at low temperature, under EPR conditions which would show the spectra of reduced F_A and F_B. Some signals are seen on either side of the g=2.00 signal, due to F_X. Warren *et al.* (1990) report the EPR spectrum of the "Apo-F_X" particle, in which PsaC has been chaotropically removed and then F_X has been oxidatively destroyed, using 5mM potassium ferricyanide. Outside of the g=2.00 region, the spectrum is flat. The spectrum presented here for mutant C575H is similar, indicating no photoreduction of iron-sulphur centres. It should be noted that this does not mean that F_A and F_B are

not present. It is possible that these centres are present but are not photoreduced, due to the absence of a redox-active F_X centre. F_X is intermediate in electron transfer between A_1 and F_A/F_B (Moënne-Loccoz *et al.* 1994). This electron transfer step is blocked in C575H. It is unlikely that an iron-sulphur centre is present at the F_X binding site of PSI in mutant C575H. Vassiliev *et al.* (1995) describe two cyanobacterial site-directed mutants in which either of the conserved cysteine residues has been substituted by serine. While these mutants have a very low quantum efficiency of electron transfer to F_X at room temperature, freezing under constant illumination photoreduces F_A/F_B, showing that a F_X centre which is not active at room temperature can permit electron flow at low temperature. This is not observed in mutant C575H. Also, ligation of F_X by histidine has never been observed in any other studies (Smart *et al.*, 1993).

The spectrum of D576L differs from wild type. g_x is obscured by the g=2.02 signal. Although the spectrum has a degree of noise, a resonance may be observed around g=1.94. This is similar to the g_y value of F_A in wild type *C. reinhardtii.* A single resonance is observed for g_z, with a shifted value of about 1.87. The spectrum appears to indicate an altered electron distribution between F_A and F_B, suggesting that the conformation of PsaC may be incorrect. The spectrum appears to indicate association of the electron with a single centre, which has altered resonances. Li *et al.* (1991b) examined the influence of the binding of PsaD on the features of EPR spectra of F_A and F_B. The *psaC* gene product of *Synechococcus* sp. PCC 7002 was reconstituted onto the PSI core of *Synechococcus* sp. PCC 6301. Without the addition of PsaD, low temperature photoreduction produced an approximately equal electron distribution between F_A and F_B. Resonances of F_A and F_B were also abnormally broad. Upon addition of the *psaD* gene product of *Nostoc*

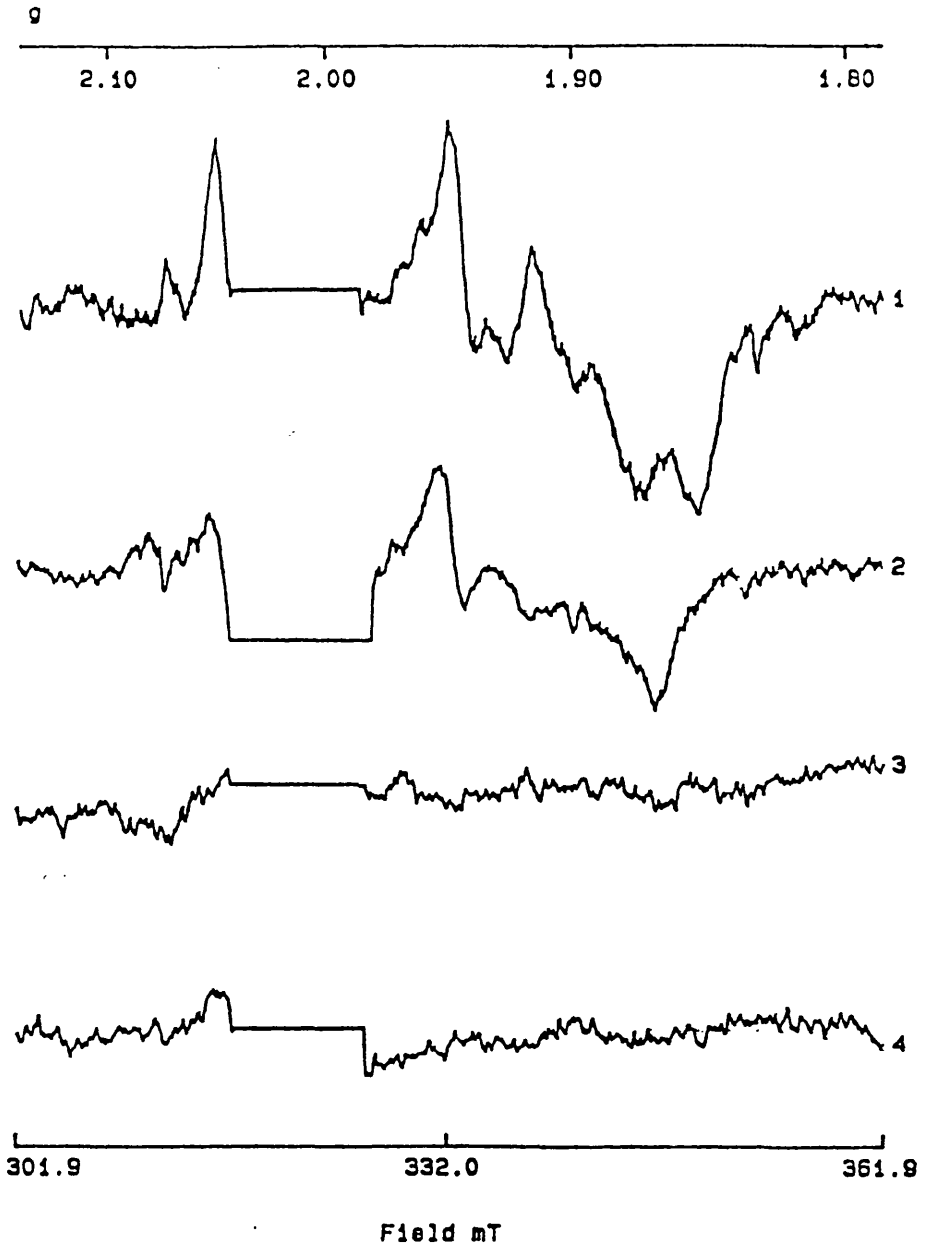

Figure 3.4

CW EPR Spectra of Photoreduction of $F_{A/B}$ in *C. reinhardtii* site-directed mutants .

Wide scan EPR spectra in the g=2.00 region of *C. reinhardtii* unfractionated thylakoid membranes. The spectra presented are light-minus-dark difference spectra. The large signals due to $P700^{\cdot+}$ in the centres of the spectra have been deleted for clarity. Spectra were recorded before and after illumination, and light minus dark difference spectra were calculated. Samples were reduced with 10mM sodium ascorbate in darkness for 1 hour and then frozen in liquid nitrogen in darkness. Spectra were recorded before and after illumination at 15K. (1) wild type. (2) D576L. (3) C575H. (4) C575D. EPR conditions: microwave power 10mW, modulation width 1mT, temperature 15K.

sp. PCC 6809, electron distribution changed to favour F_A, and resonances sharpened, producing spectra very similar to the control. PsaD was also found to stabilise binding of PsaC. This study showed that the electron distribution and resonances of F_A and F_B are sensitive to incorrect binding of PsaC. With mutant D576L, we also see that incorrect binding of PsaC to the PSI core has an effect on the low temperature electron distribution between F_A and F_B. Here, however, the effect is due to the interaction of PsaC with the conserved residues of the PSI core, not due to the influence of PsaD.

No further analyses were performed with C575D, as it had been well established that this mutant does not assemble PSI.

We were unable to obtain a useful spectrum from C575S thylakoid membranes due to the low level of assembly, the g=2.02 iron-sulphur signal and contamination by manganese. Digitonin preparations from *C. reinhardtii* had levels of contaminating signals, attributed to copper contamination, too high to obtain useful PSI spectra. The source of this copper is unlikely to be from plastocyanin, as digitonin treatment removes any bound plastocyanin (Hanley *et al.*, 1992). Copper signals have been reported which arise from the light-harvesting complex of PSII (Miller and Brudvig, 1991). A light-harvesting protein present in the digitonin preparation may be the source of this contamination.

We also attempted to analyse samples of C575H and C575S thylakoid membranes which had been chemically reduced with sodium dithionite at pH 10. This treatment can chemically reduce F_A and F_B. We aimed to resolve the question of the presence or absence of these clusters in mutants C575H and C575S.

Unfortunately, we were unable to obtain useful spectra, due to the large non-PSI iron-sulphur signal.

We attempted to obtain EPR spectra of F_X^- in *C. reinhardtii*, at 8K. A high power of 50mW was used as F_X^- has fast relaxation. These experiments were unsuccessful due to the difficulty of poor signal-to-noise caused by overlap with the signals of F_A/F_B and the problem of non-PSI signals in *C. reinhardtii*. The F_A/F_B spectra of D576L and the revertants do not show any obvious changes due to F_X in the g=1.76 region, which is outside the envelope of F_A/F_B. However, subtle changes may not have been detected.

To try to reduce the problem of non-PSI signals in EPR analysis of *C. reinhardtii* thylakoid membranes, we attempted transformation of the FuD7 mutant, which does not contain PSII. We used the same DNA constructs which were used to transform the site-directed mutant strains analysed in this thesis, according to the biolistic transformation protocol used in Hallahan *et al.* (1995). Unfortunately, the transformants were unable to grow.

3.4 Assays of $NADP^+$ Photoreduction Activity in *C. reinhardtii* site-directed mutants

In the $NADP^+$ photoreduction assay, physiological PSI activity and the subsequent reduction of $NADP^+$ is mimicked. This assay is particularly useful to examine the effects of biochemical treatments of PSI. The assay has been used to study the removal and functional reconstitution of subunits (Hanley *et al.*, 1992). The assay has also been used to study the destruction and functional reconstitution of F_B

(He and Malkin, 1994). Here, the assay is used to verify that the PSI complexes which the site-directed mutants assemble are non-functional.

In the assay, a thylakoid membrane preparation or PSI preparation is illuminated, along with added $NADP^+$, a reduced electron donor , ferredoxin or flavodoxin, and FNR. With spinach chloroplasts, DCPIP alone may act as a donor, as plastocyanin is bound to the membrane. With spinach detergent PSI, plastocyanin must be added, as it is removed in the detergent preparation. Following urea treatment of spinach PSI, DCPIP alone may donate electrons directly $P700^+$, due to donor side damage (Hanley *et al.*, 1992). However, DCPIP alone, or with higher plant plastocyanin, will not donate electrons to $P700^+$ in *C. reinhardtii* to support $NADP^+$ photoreduction. Here, this problem has been overcome by the use of an alternative electron donor, DAD. Rates of $NADP^+$ photoreduction are rather low, but that is satisfactory here, as we are only examining whether or not the thylakoid membranes are competent in $NADP^+$ photoreduction.

Rates of $NADP^+$ photoreduction are presented in table 3.1. Results are also summarised in table 3.3. Mutants C575H, C575S and D576L assemble PSI complexes incompetent in $NADP^+$ photoreduction. This was the expected result, as these mutants cannot grow photosynthetically.

$NADP^+$ photoreduction rates for D576L revertants #1 and #2 are presented. These are competent in $NADP^+$ photoreduction, with rates lower than wild type. This was the expected result, as these mutants are able to grow photosynthetically. Due to the donor side limitatation of the reaction, the reduced rates, compared to wild type, are attributed to the reduced levels of assembly

of the PSI complex. The reaction is unable to detect any changes in the efficiency of electron transfer through PSI which may be present.

Before the experimental assays of the site-directed mutants described above, assays were carried out on *C. reinhardtii* wild type digitonin PSI and *C. reinhardtii* wild type thylakoid membranes, using Synechococcus sp. PCC 7002 flavodoxin in place of spinach ferredoxin, produced from transformed *E. coli.* An assay was also carried out on *C. reinhardtii* wild type thylakoid membranes, using *C. reinhardtii* ferredoxin in place of spinach ferredoxin. Rates of $NADP^+$ photoreduction by *C. reinhardtii* wild type thylakoid membranes, with either flavodoxin or *C. reinhardtii* feredoxin, were effectively the same as with spinach ferredoxin, as shown in table 3.1. These tests with physiologically relevant electron acceptors showed that the low rates of $NADP^+$ photoreduction were due to limitation by electron donation to $P700^+$, not due to limitation by electron acceptance from the terminal iron-sulphur centres of PSI. It was therefore decided to use spinach ferredoxin for the experimental assays, as it is easily extracted in large quantities. *C. reinhardtii* wild type digitonin PSI was not competent in $NADP^+$ photoreduction. This was assumed to be due to damage to the acceptor complex of PSI, and this preparation was therefore considered unsuitable for optical flash spectroscopic measurements, which would have been useful to examine the back reaction from F_A/F_B to P700 in the D576L mutant. As ferredoxin is not photoreduced by this preparation, it is also not useful for the study of ferredoxin binding. Optical flash measurements of P700 are difficult with thylakoid membrane preparations due to the bulk chlorophyll content. The *C. reinhardtii* digitonin PSI preparation was, however, considered suitable for CW EPR and ENDOR

spectroscopy of $A_1^{\cdot -}$, as this is would be unlikely to be affected by damage to the surface of the PSI complex, due to its structurally deeper location.

3.5 Assays of Photoreduction of Artificial Electron Acceptors in *C. reinhardtii* site-directed mutants

PSI electron transport may be examined biochemically, using the artificial electron acceptor methyl viologen. This chemical may accept electrons from PSI, in turn converting water to hydrogen peroxide. PSI electron transport may therefore be measured as oxygen consumption, using an oxygen electrode.

Methyl viologen does not accept electrons from the physiological acceptor sites for ferredoxin or flavodoxin. Methyl viologen is able to penetrate the protein and accept electrons directly from the terminal iron-sulphur centres (Fujii *et al.*, 1990). In the results presented in this thesis, a methyl viologen concentration of 50mM was used. Vassiliev *et al.* (1998) found that this concentration was able to accept electrons only from the F_X-distal iron-sulphur cluster of PSI.

In this study, methyl viologen was used to examine partial electron transport in the site-directed mutants. A preparation of spinach PSI with PsaC removed was analysed. A preparation of spinach PSI with PsaC removed and F_X oxidatively destroyed was also analysed.

Rates of oxygen consumption are presented in table 3.2. Results are also summarised in table 3.3. Methyl viologen is photoreduced by site-directed mutants C575S and D576L. In D576L, this probably reflects electron transfer to the terminal iron-sulphur clusters The complex is unlikely to be extensively structurally disrupted, relative to wild type, as revertants can be generated easily. In C575S, however, this

appears to reflect direct acceptance of electrons from A_1^-, as pulsed EPR results indicate that forward electron transfer from this carrier does not occur at room temperature (see section 3.7.2). Structural disruption may permit the methyl viologen to enter the complex to accept electrons from A_1^- directly in C575S.

Both of the biochemically treated spinach preparations are competent in methyl viologen photoreduction. PSI with PsaC removed and F_X intact has previously been shown to be able to potoreduce methyl viologen (Parret *et al.*, 1989). Here, it is shown that methyl viologen can accept electrons directly from F_X or A_1, if these carriers are structurally accessible.

The thylakoid membrane preparation of C575H was the only preparation unable to photoreduce methyl viologen, at the concentration used in these experiments. This mutant was further analysed by repeating the experiment, with the more hydrophobic electron acceptor neutral red in place of methyl viologen. C575H was able to photoreduce neutral red, indicating partial electron transport, to a carrier not accessible to methyl viologen. Pulsed EPR results indicate that this mutant can photoreduce A_1, with no further forward electron transfer (see section 3.7.2). It is likely that neutral red, unlike methyl viologen, is able to penetrate the PSI complex of C575H, to accept electrons from A_1. This reflects a lesser degree of structural disruption to PSI than is found in C575S.

Boiled wild type membranes were used as a negative control for methyl viologen photoreduction. This proved to be a poor control, as this sample was able to photoreduce methyl viologen at a low rate, presumably due to free chlorophyll in the sample. The total lack of methyl viologen photoreduction activity in mutant C575H, however, indicates that the experimental rates observed are due to electron transport.

Strain	Rate of $NADP^+$ photoreduction (micromol NADPH/mg chl/h)
wild type	17.2
B4 (PSI minus)	0
C575D	0
C575H	0
C575S	0
D576L	0
Revertant #1	3.6
Revertant #2	5.1
wild type digitonin PSI	0
*wild type / flavodoxin	16.7
*wild type / *C. reinhardtii* ferredoxin	16.5

Table 3.1

$NADP^+$ Photoreduction by *C. reinhardtii* Thylakoid Membranes

$NADP^+$ photoreduction was assayed by measuring the change in absorption at 340nm following 10 minutes illumination by saturating white light. The reaction mixture contained thylakoid membranes at a chlorophyll concentration of 16.7μg/ml, 0.2M sorbitol, 10Mm NaCl, 5mM $MgCl_2$, 50mM HEPES-KOH pH 7.5, 10μM DCMU, 1μM FCCP, 0.5mM DAD, 5mM sodium ascorbate, 500mM $NADP^+$ with excess amounts of FNR and spinach ferredoxin, except where denoted*.

Sample	Rate of oxygen uptake (micromol O_2/mg chl/h)
wild type thylakoid membranes (MV)	217
boiled thylakoid membranes (MV)	47.6
C575H thylakoid membranes (MV)	1.68
C575S thylakoid membranes (MV)	84.5
D576L thylakoid membranes (MV)	128
spinach PSI (MV)	163
spinach PSI: PsaC removed (MV)	86.2
spinach PSI: F_X destroyed (MV)	98.1
wild type thylakoid membranes (NR)	155
C575H thylakoid membranes (NR)	146

Table 3.2

Oxygen Consumption Assay of PSI Electron Transport

The rate of oxygen uptake measured with an oxygen electrode at a constant temperature of 25°C, supplied with saturating white light. The reaction mixture contained thylakoid membranes/PSI at a chlorophyll concentration of 16.7μg/ml, 0.2M sorbitol, 10mM NaCl, 5mM $MgCl_2$, 50mM HEPES-KOH pH 7.5, 10μM DCMU, 1μM FCCP, 0.5mM DAD, 5mM sodium ascorbate, 0.5μM sodium azide and 50 μM methyl viologen or neutral red. MV denotes methyl viologen. NR denotes neutral red.

	NADP+ photoreduction	Oxygen uptake (methyl viologen)	Oxygen uptake (neutral red)
wild type thylakoids	+	+	+
C575H thylakoids	-	-	+
C575S thylakoids	-	+	
D576L thylakoids	-	+	
spinach PSI		+	
spinach PSI: PsaC removed		+	
spinach PSI: F_X destroyed		+	

Table 3.3

Summary of Results of Biochemical Assays of PSI Electron Transport

+ denotes that the sample performed the assay.

- denotes that the sample was incapable of performing the assay.

3.6 CW EPR Analysis of Reduced $F_{A/B}$ in *C. reinhardtii* D576L Second site Revertants.

Figure 3.5 shows wide scan EPR spectra of ascorbate-reduced thylakoid membranes, recorded with conditions under which the spectra of reduced F_A and F_B may be observed. As before, these results are complicated by the presence of a large non-PSI iron-sulphur centre signal around g=2.02, as described in section 3.3.

The characteristics of the spectra of wild type and D576L are described in section 3.3. The spectra of the four revertants are all similar to one another and similar to the spectrum of D576L. As in D576L, the spectra of the revertants appear to have a single g_x resonance, although the spectra are somewhat noisy, particularly the spectrum of revertant number 4. The abnormal electron distribution between F_A and F_B and the implied abnormal conformation of PsaC, seen in D576L, also appears to be present in the revertants. Photosynthetic growth has been restored in the revertants, apparently without correction of this abnormality.

Before the D576L revertants were generated, we thought that the abnormalities in F_A and F_B of D576L, which cause the abnormal electron distribution under low temperature illumination, also were the cause of the mutant being incompetent in photosynthesis. However, the similarity between the spectrum of D576L and the spectra of the revertants show that this is not the case. The EPR spectrum of free PsaC of spinach is reported in Hanley *et al.* (1992). The spectrum has the characteristics of a soluble 2(4Fe-4S) iron-sulphur protein. The EPR spectrum of F_A and F_B in free PsaC represents the superposition of two rhombic spectra. EPR spectra of free PsaC are virtually identical in higher plants and cyanobacteria (Li et al., 1991b). Small differences between higher plants and cyanobacteria arise when PsaC

is bound to the core. Mehari *et al.* (1991) reconstituted spinach PsaC onto the PSI core of *Synechococcus* sp. PCC 6301. This produced sharpening of the resonances of F_A and F_B to produce a spectrum virtually identical to that of spinach. In their experiment, however, the spinach PsaC protein was bound normally, as the F_X-binding loop which interacts with PsaC is completely conserved between spinach and higher plants. In D576L and the revertants, a part of the PSI core which binds PsaC is mutated. We show that the spectral characteristics of F_A and F_B in bound PsaC are not only determined by PsaC itself, but also by the nature of the interaction between PsaC and the PSI core. These appear to be the main factors determining the spectral characteristics of F_A and F_B in bound PsaC. In the revertants, secondary mutation permits the restoration of electron flow from A_1^- to ferredoxin, without altering the spectral characteristics of F_A and F_B. The DNA sequences encoding PsaC and the F_X-binding regions of PsaA and PsaB are unchanged in the revertants (Patel, 1996).

Although the EPR spectrum of the iron-sulphur centres in free PsaC differs from that of bound PsaC, the redox potentials of F_A and F_B are thought to be an intrinsic property of the protein, as the values are unchanged when PsaC is bound to the PSI core (Oh-oka *et al.*, 1991). A change in the the redox potentials of F_A and/or F_B could cause photosynthetic incompetence. The D576L revertants are able to photosynthesise, suggesting that the incorrect binding of PsaC causes little change in the normal redox potentials of F_A and F_B. This suggests that the redox potentials of F_A and F_B are determined by PsaC, even when the protein is incorrectly bound. The altered resonances of F_A and F_B in D576L and the D576L revertants are unlikely to reflect changes in the redox potentials of F_A and F_B.

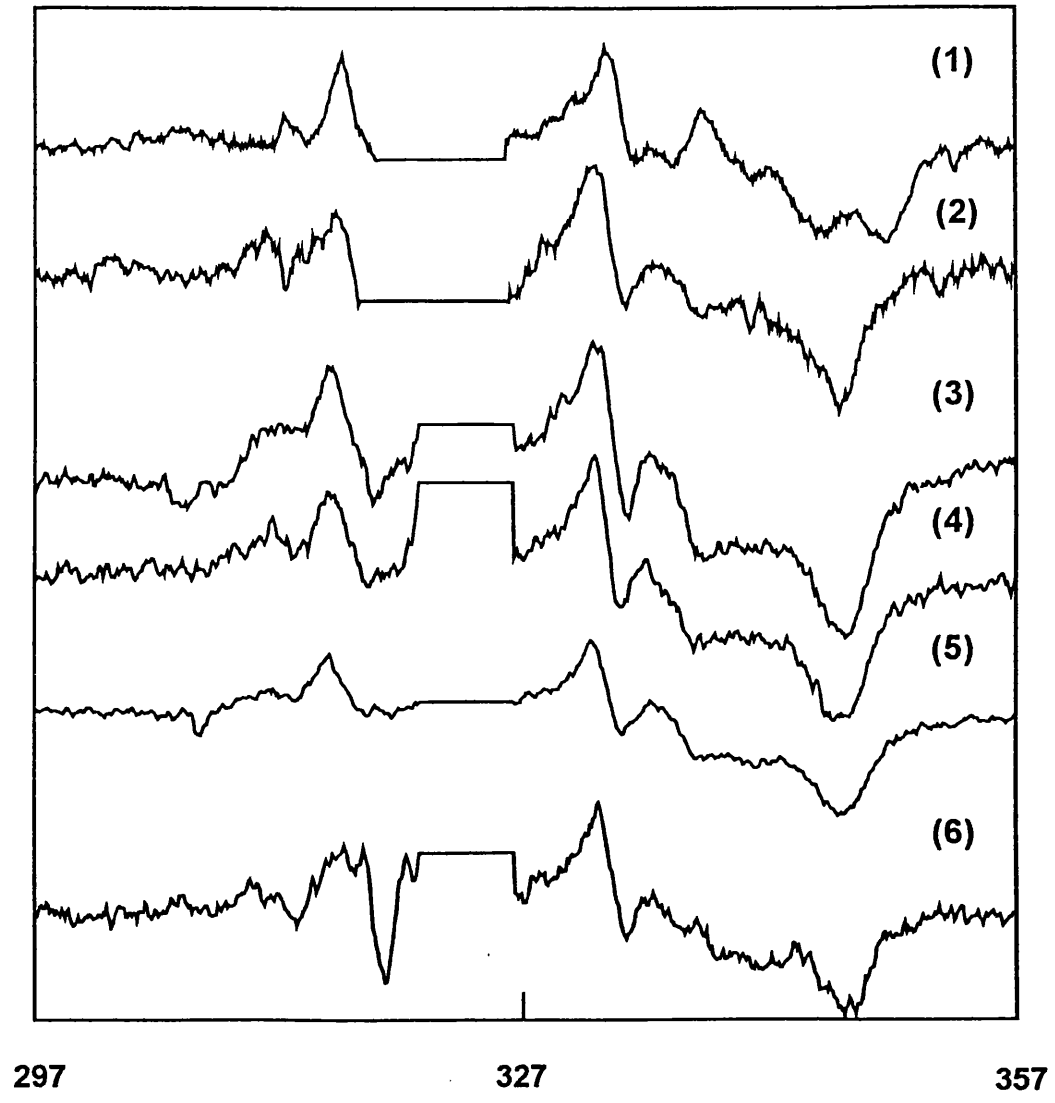

Figure 3.5

CW EPR Spectra of Photoreduction of $F_{A/B}$ in *C. reinhardtii* D576L second site revertants.

Wide scan EPR spectra in the g=2.00 region of *C. reinhardtii* unfractionated thylakoid membranes. The spectra presented are light-minus-dark difference spectra. The large signals due to $P700^{\cdot+}$ in the centres of the spectra have been deleted for clarity. Spectra were recorded before and after illumination, and light minus dark difference spectra were calculated. Samples were reduced with 10mM sodium ascorbate in darkness for 1 hour and then frozen in liquid nitrogen in darkness. Spectra were recorded before and after illumination at 15K. (1) wild type. (2) D576L. (3)-(6) revertants #1-#4. EPR conditions: microwave power 10mW, modulation width 1mT, temperature 15K.

3.7 Pulsed EPR Analysis of the Kinetics of Electron Transfer from A_1^-

The temperature dependence of forward and reverse electron transfer from A_1^- is complex, with peculiar effects of low temperature on electron transfer (Schlodder *et al.* 1998). Between 300 and 200K, A_1^- is oxidised by F_X. However, reduction of temperature to below 150K produces different fractions of PSI, which have different electron transfer behaviour. This is thought to be due to the formation of different subpopulations of PSI complexes with different conformational states. At low temperature, laser flash excitation induces, in a large proportion of centres, the formation of $P700^+/A_1^-$ with no further forward electron transfer, followed by charge recombination. This effect may be seen in about 45% of PSI centres at 77K (Schlodder *et al.* 1998).

In the results presented here, the kinetics of decay of the ESP signal attributed to the radical pair $P700^{\cdot+}/A_1^{\cdot-}$ were measured by pulsed EPR at two temperatures: 100K and 260K. At 100K, the kinetics of decay of the radical pair $P700^{\cdot+}/A_1^{\cdot-}$ due to charge recombination were measured. Moënne-Loccoz *et al.* (1994) observed a large light-induced signal at g=2.003 in the out-of-phase channel at 4K. At room temperature, two signals were observed, both around g=2.00, one in the in-phase channel and one in the out-of-phase channel. The out-of-phase signal was spectrally identical to the out-of-phase signal observed at 4K. In the results presented here, the decay kinetics of the same out-of-phase signal are analysed, at 100K and 260K.

From 300K down to 240K, there is little slowing of the rate of forward electron transfer from A_1^- to F_X (Schlodder *et al.* 1998). EPR measurements are more easily performed with the sample in a frozen state, because of microwave absorption by water. Results are presented which show the time constants of decay of

the radical pair $P700^{\cdot+}/A_1^{\cdot-}$ at 260K, due to forward electron transfer to F_X. These kinetics are very similar to the kinetics of forward electron transfer from A_1^- which would exist at room temperature.

Sample kinetic traces are shown in figure 3.6. Time constants of decay ($t_{1/e}$) of $P700^{\cdot+}/A_1^{\cdot-}$ were calculated from single exponential fits of the obtained traces.

3.7.1 Kinetics of Decay of the ESP Signal of $P700^{\cdot+}/A_1^{\cdot-}$ at 100K

Values of the time constants of decay ($t_{1/e}$) of the ESP Signal of $P700^{\cdot+}/A_1^{\cdot-}$ are presented in table 3.4. Similar rates are seen between spinach digitonin PSI and wild type *C. reinhardtii* thylakoid membrane, both with $t_{1/e}$ of about 26μs. The apparent value for wild type *C. reinhardtii* digitonin PSI is shorter, but this is averaged from only two measurements, so the error associated with this value is likely to be large, and the true value is likely to be the same as in thylakoid membranes. In D576L, the values are effectively the same between digitonin PSI and thylakoid membranes, indicating that the detergent treatment does not affect the kinetics of the backreaction. D576L has similar values to wild type with $t_{1/e}$ of about 26μs. The C575S thylakoid membrane sample also appears to have a similar value, although this value was only calculated from 2 measurements, so the degree of error is large. The time constant of decay in revertant #1 is somewhat shorter than the values in the other *C. reinhardtii* samples, with $t_{1/e}$ of about 15μs.

Moënne-Loccoz *et al.* (1994), in pulsed EPR measurements of spinach PSI, found that the ESP Signal of $P700^{\cdot+}/A_1^{\cdot-}$ decayed with $t_{1/e}$ of 23μs at 4K, reflecting charge recombination. Brettel and Golbeck (1995), in a study of the optical absorbance kinetics of A_1, observed a decay phase with $t_{1/2}$=15μs at 10K. The

kinetics of charge recombination at cryogenic temperatures which are observed for C. reinhardtii are therefore in a similar range to those observed in previous studies.

3.7.2. Kinetics of Decay of the ESP Signal of $P700^{\cdot+}/A_1^{\cdot-}$ at 260K

Values of the time constants of decay of the ESP Signal of $P700^{\cdot+}/A_1^{\cdot-}$ at 260K are presented in table 3.5, expressed as $t_{1/e}$. Wild type *C. reinhardtii* has a value of 355±136ns. This value is in the normal range for PSI, as observed in other studies. Moënne-Loccoz *et al.* (1994), also using pulsed EPR of spinach, observed a room temperature decay of $P700^{\cdot+}/A_1^{\cdot-}$ with $t_{1/e}$=200ns. Bock *et al.* (1989), using transient EPR of spin-polarised signals, observed forward electron transfer from $P700^{\cdot+}/A_1^{\cdot-}$ with $t_{1/e}$=260ns. Studies on electron transfer of cyanobacterial PSI showed similar rates. Leibl *et al.* (1995), in a study of the photoelectric response, observed a phase of $t_{1/e}$=220ns. Van der Est *et al.* (1994), using transient EPR of two consecutive spin-polarised signals, observed forward electron transfer from $P700^{\cdot+}/A_1^{\cdot-}$ with $t_{1/e}$=280ns. Lüneberg *et al.* (1994), in a study of the optical kinetics of A_1^-, observed forward electron transfer from A_1^- with $t_{1/2}$=180ns. Wild type C. reinhardtii has similar kinetics of forward electron transfer from A_1^-, at room temperature, to other organisms.

In C575H and C575S, long rates of decay, around $t_{1/e}$=2μs in both cases, are observed. The existence of the ESP signal proves that A_1 is present in C575H and C575S. Warren *et al.* (1993a), in experiments on PSI with F_X oxidatively destroyed, observed that the majority of flash-induced absorbance change of P700, followed at 820nm, decayed with a half-time of 10μs. This decay was due to charge recombination between A_1^- and $P700^+$. Brettel and Golbeck (1995) followed the

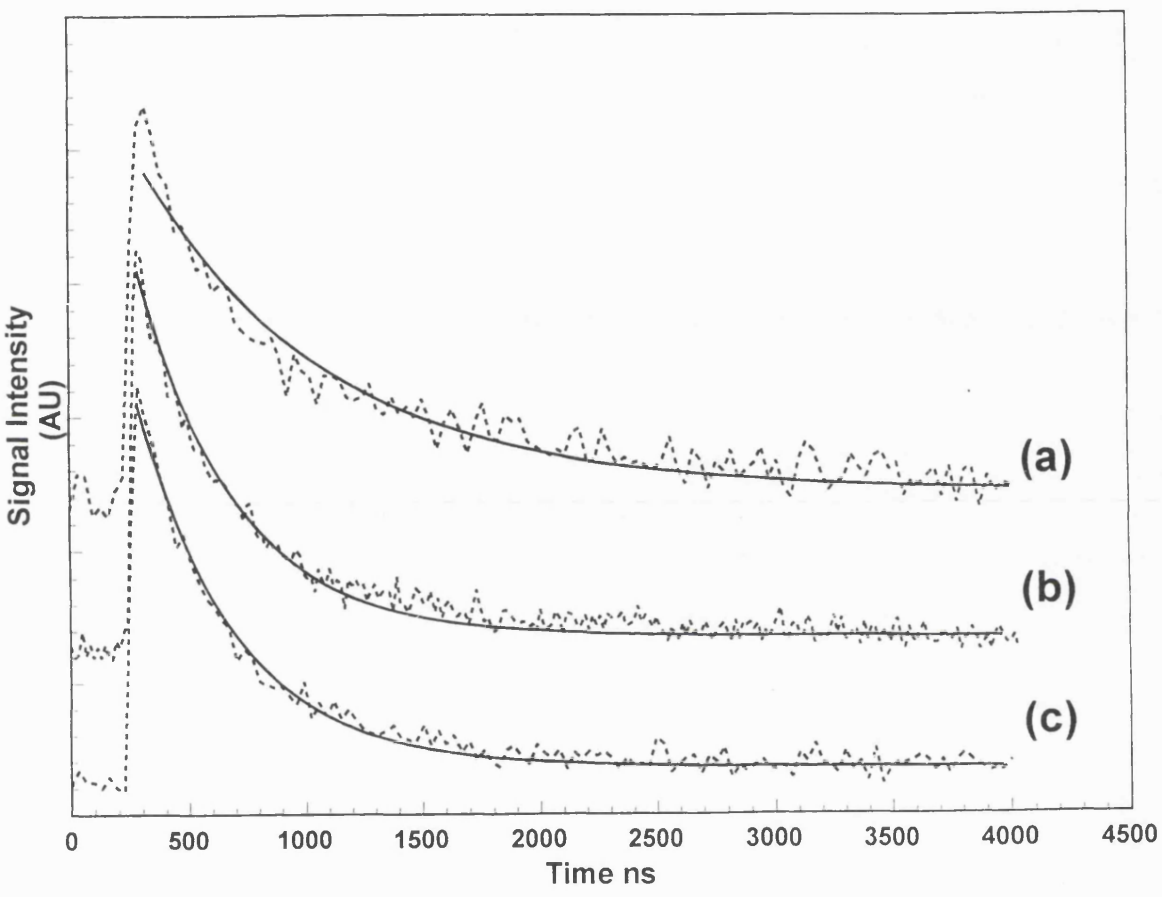

Figure 3.6

EPR Transients of Decay of the $P700^{\cdot+}/A_1^{\cdot-}$ ESP Signal in *C. reinhardtii*

Examples of EPR transients showing decay of the $P700^{\cdot+}/A_1^{\cdot-}$ ESP signal at 260K in *C. reinhardtii* unfractionated thylakoid membranes, following laser flash excitation. Samples were reduced with 10mM sodium ascorbate in darkness for 1 hour and then frozen in liquid nitrogen in darkness. Transients were recorded as described in section 2.15 The dotted lines are experimental traces. The solid lines are single exponential fits. (a) D576L, $t_{1/e}$=806ns (b) wild type, $t_{1/e}$=422ns (c) D576L revertant #1, $t_{1/e}$=417ns.

	Decay of spin polarised signal $t_{1/e}$ (μs).	standard deviation	number of measurements
Spinach digitonin PSI	26.6	3.6	8
C. reinhardtii wild type thylakoid membranes	26	1.3	16
C. reinhardtii wild type digitonin PSI	21.3	-	2
C. reinhardtii D576L thylakoid membranes	26.1	1.2	5
C. reinhardtii D576L digitonin PSI	24.8	1.5	6
C. reinhardtii D576L revertants #1 and #2 thylakoid membranes	15.1	2.25	7
C. reinhardtii C575S thylakoid membranes	25	-	2

Table 3.4

Kinetics of Decay of the ESP Signal of $P700^{\cdot+}/A_1^{\cdot-}$ at 100K

All samples were reduced with 10mM ascorbate.

The spectroscopic method is detailed in section 2.15.

	Decay of spin polarised signal $t_{1/e}$ (ns).	standard deviation	number of measurements
Spinach digitonin PSI	453	95	23
C. reinhardtii wild type	355	136	20
C. reinhardtii C575H	2199	282	12
C. reinhardtii C575S	1750	-	2
C. reinhardtii D576L	848	146	14
C. reinhardtii D576L revertant #1	293	80	10
C. reinhardtii D576L revertant #2	343	85	10
C. reinhardtii D576L revertant #3	390	64	10
C. reinhardtii D576L revertant #4	350	-	1

Table 3.5

Kinetics of Decay of the ESP Signal of $P700^{\cdot+}/A_1^{\cdot-}$ at 260K

All samples are of thylakoid membranes, except where noted.

All samples were reduced with 10mM ascorbate.

The spectroscopic method is detailed in section 2.15.

decay of A_1^- directly at 380nm, in PSI with F_X oxidatively destroyed. The room temperature back reaction from A_1^- was multiphasic in this preparation, and components with half-times of 10μs and 110μs were seen. The decay kinetics of the $P700^{\cdot+}/A_1^{\cdot-}$ radical pair in C575H and C575S are in the same time range, and are considered to reflect charge recombination. Moënne-Loccoz *et al.* (1994), using pulsed EPR, observed a room-temperature decay of the out-of phase signal with $t_{1/e}$=1.3μs in PSI which had been depleted of all iron-sulphur centres. This decay kinetic was considered to reflect either the back reaction or the decay of polarization. The results for C575H and C575S are very similar to this value. The CW EPR spectrum of C575H indicates that there is no forward electron transfer from A_1. The slow decay of $P700^{\cdot+}/A_1^{\cdot-}$ therefore cannot reflect forward electron transfer in C575H and is likely to reflect the back reaction from $A_1^{\cdot-}$ to $P700^{\cdot+}$. A similar rate of decay is seen in C575S, which also reflects the back reaction from $A_1^{\cdot-}$ to $P700^{\cdot+}$.

The rate of decay of 848±146ns which is observed in D576L is intermediate between the rates of wild type and C575H/C575S. In wild type, normal forward electron transfer takes place. In C575H and C575S, forward electron transfer from A_1^- does not takes place. The intermediate time constant of D576L can be interpreted to reflect an increased competition between the back reaction and the forward reaction from A_1^-. The ENDOR results show that no significant changes occur in the protein environment of A_1 (section 3.9) relative to wild type. The 100K back reaction rate is unaltered, suggesting that the P700-A_1 region of the reaction centre is not altered by the mutation. The slowed rate of decay of $P700^{\cdot+}/A_1^{\cdot-}$ therefore must be due to reduced efficiency of the forward reaction, caused by structural changes to the F_X binding site.

In the revertants, the rates of decay recover to values similar to wild type, indicating that the original balance of competition between the forward and reverse reactions has been restored. This suggests that the structural fault in the F_X binding site has been corrected, permitting the restoration of a normal rate of forward electron transfer.

3.8 CW EPR Spectroscopy of $A_1^{\cdot -}$ in *C. reinhardtii*

Rigby *et al.* (1996) compared the CW EPR spectra of $A_1^{\cdot -}$ in spinach and the cyanobacterium *A. variabilis* to the spectrum of the *in vitro* phylloquinone anion radical. The $A_1^{\cdot -}$ spectra were less symmetrical. In particular, the $A_1^{\cdot -}$ spectra had a shoulder on the low-field side of the spectrum which is not seen in the *in vitro* phylloquinone. The protein environment of $A_1^{\cdot -}$ therefore affects the features of the spectrum.

The EPR signal of photoaccumulated $A_1^{\cdot -}$ was originally reported by Bonnerjea and Evans (1982). Mansfield and Evans (1988) suggested that the EPR signal of photoaccumulated $A_1^{\cdot -}$ may have a narrower linewidth than had been previosly reported. When photoaccumulated samples were stored at 77K, the $A_1^{\cdot -}$ signal decayed, but the $A_0^{\cdot -}$ signal did not. A difference spectrum was thus calculated, in order to remove the contribution of $A_0^{\cdot -}$. The difference spectrum had ΔH_{ptp}=0.95mT.

The conditions used here to photoaccumulate $A_1^{\cdot -}$ were established by Heathcote *et al.* (1993). In their experiments on spinach, an asymmetric EPR signal centred at g=2.0048, with ΔH_{ptp}=0.95mT, was photoaccumulated. Double-reduction abolished this signal. The EPR signal of photoaccumulated $A_1^{\cdot -}$ in *A. variabilis* was

centred at g=2.0047, with ΔH_{ptp}=0.88mT (Heathcote *et al.*, 1996). The signal was narrowed by biosynthetic deuteration, due to loss of proton hyperfine interactions. The photoaccumulated EPR spectrum, which we observe here, has thus been unequivocally attributed to the phylloquinone radical $A_1^{\cdot -}$. The values for *A. variabilis* approach those reported for the EPR spectrum of the phylloquinone anion *in vitro*, of g=2.0047, with ΔH_{ptp}=0.85mT. The wider linewidth in spinach was suggested to be due to a small contribution from another component, possibly $A_0^{\cdot -}$.

The results presented here represent the first report of the CW EPR spectrum of $A_1^{\cdot -}$ in *C. reinhardtii*. Digitonin PSI samples were reduced with dithionite at pH 8. Reduction with dithionite at pH 8 helps to avoid double reduction of phylloquinone to the quinol form which can take place with dithionite at pH 10 (Heathcote *et al.*, 1993). Illumination of samples reduced with dithionite at pH 10 can also cause photoaccumulation of both of the phylloquinone molecules in the reaction centre. Illumination of samples reduced with dithionite at pH 8 causes photoaccumulation of only one of the phylloquinones, which is likely to represent the physiological carrier A_1 (Heathcote *et al.*, 1993). Mansfield and Evans (1988) compared pea digitonin PSI to Triton-X100 PSI. In digitonin PSI, a magnetic interaction was seen between A_0 and F_X. This interaction was lost in Triton-X100 PSI. Addition of ^2H_2O also caused a narrowing of linewidth of the EPR signal with Triton-X100 PSI, suggesting exposure of A_1 to the medium in this preparation. Deuteration did not produce new spectral features in digitonin PSI, indicating that A_1 was in an aprotic environment. Also, the orientation of redox components in digitonin preparations is similar to that in the native membrane (Rutherford and Sétif, 1990). Digitonin was therefore considered to be a suitable detergent for the spectroscopic analysis of $A_1^{\cdot -}$ presented

here. Spectra were recorded using microwave powers which were non-saturating at the recording temperature.

The CW EPR spectra of $A_1^{\cdot -}$ in spinach and *C. reinhardtii* wild type are presented in figure 3.7. The two spectra are very similar. The *C. reinhardtii* spectrum has values g=2.0047 and ΔH_{ptp}=0.875-0.9mT. The linewidth is similar to that seen in *A. variabilis* (Heathcote *et al.*, 1996). As already mentioned, the wider linewidth of spinach may be due to a contribution from a non-$A_1^{\cdot -}$ component of PSI. The shape of the *C. reinhardtii* spectrum is more like that of spinach than that of *A. variabilis*. The shoulder on the low-field side is more pronounced in *A. variabilis* (Heathcote *et al.*, 1996). The breadth of the shoulder is similar in *C. reinhardtii* and in spinach. This suggests that the A_1 binding site is very similar in spinach and *C. reinhardtii*. A high degree of conservation of the structure of the binding site throughout photosynthetic eukaryotes is suggested. The A_1 binding site was studied in greater detail by ENDOR (section 3.9).

3.9 ENDOR Spectroscopy of $A_1^{\cdot -}$ in *C. reinhardtii*

The ENDOR spectra of $A_1^{\cdot -}$ in spinach and the cyanobacterium *Anabaena variabilis* were obtained by Rigby *et al.* (1996). *In vivo* deuteration of A_1 by growth of *A. variabilis* on [*methyl*-d_3] methionine allowed assignment of features of the ENDOR spectrum to either methyl or hydrogen bonded protons. ENDOR spectra of model naphthoquinones were also obtained. The spectral features were assigned by comparison to previous studies of quinone anion radicals in frozen solution. ENDOR spectra of the menaquinone in the green bacteria *Heliobacterium chlorum* and *Chlorobium limicola* have also been obtained (Muhiuddin *et al.*, 1999). The function

of the menaquinone in green bacteria is uncertain, but the ENDOR spectra suggest a similar electronic structure to $A_1^{\cdot-}$ in higher plants. Differences in hfc's between $A_1^{\cdot-}$ and phylloquinone in vitro indicated an altered electronic structure. Van der Est *et al.* (1997) studied the ESP signal of the $P700^{\cdot+}/A_1^{\cdot-}$ radical pair by W-band (95GHz) EPR spectroscopy. Results indicated that the anisotropy of the g-tensor of phylloquinone in the A_1 binding site is larger than that in frozen isopropanol solution. The g-tensor is a measure of the effect of the environment on the orbital energies and the spin density distribution. The protein environment of $A_1^{\cdot-}$ is therefore important in determining the electronic structure of the radical.

In this study, we have used ENDOR to examine possible changes in the protein environment of A_1 caused by mutation D576L. The results presented here also represent the first ENDOR study of $A_1^{\cdot-}$ in *C. reinhardtii*. The spectra are presented in figure 3.8. The hfc's and the assignments of the spectral features are collected in table 3.6. The structure of phylloquinone and a carbon atom numbering scheme is shown in figure 3.9.

Frozen solution ENDOR spectra of radicals, taken at the crossing point of the EPR signal, typically show all orientations of the molecules in the applied field simultaneously, i.e. a powder spectrum. Features of the spectrum arise from protons and the lineshapes which are observed reflect the symmetry of the hyperfine tensors and the random orientation of the tensors in the applied field. Axially symmetric hfc's have an intense $A_\perp$ (perpendicular) component with a weaker $A_{||}$ (parallel) turning point. The hyperfine coupling constants are measured from the zero crossing points, except for the $A_{||}$ features of methyl groups, where the peak maximum is used. The couplings of each of the three protons of a methyl group are rendered equivalent by

the rotation of the group. The most intense features of frozen solution semiquinone radical ENDOR spectra arise from the $A_{\perp}$ components of the axially symmetric hfc's to protons hydrogen bonded to the quinone oxygens and the protons of methyl groups β to the delocalised π orbital system which bears the unpaired electron. These features are seen in the ENDOR spectra of *C. reinhardtii*.

The ENDOR experiment required different conditions in *C.reinhardtii.* compared to spinach. With *C.reinhardtii*, a lower microwave power and a higher temperature were used. This probably indicates contamination by paramagnetic metal ions, such as Cu^{2+} or Mn^{2+}. In all cases, hfc's were determined with a precision of ±0.1 MHz.

Feature 3 of the *C.reinhardtii* ENDOR spectra represents the $A_{\perp}$ component of the hfc to the methyl group of the quinone. This feature was assigned in *A. variabilis*, due to its lineshape and its disappearance following deuteration of the methyl group, which abolishes the proton hyperfine interactions of the group. The methyl hfc has a value of 8.8MHz, slightly lower than that of spinach or *A. variabilis*. This is the same as the value for *H. chlorum* (Muhiuddin *et al.*, 1999). However, as in these studies of other organisms, the difference between the $A_{\perp}$ and $A_{||}$ components of the methyl group is about 3.5MHz and the methyl hfc represents the largest hfc to a covalently attached proton. This is characteristic of quinone methyl groups. The isotropic hyperfine coupling constant A_{iso} is calculated as $1/3(A_{||} + 2A_{\perp})$. The methyl A_{iso} is thus 10.0MHz in wild type *C. reinhardtii*, compared to 10.2MHz in spinach. The hfc's of β methyl groups are directly related to the unpaired electron spin density at the attached ring carbon atom (ρ_C) by the equation:

$$A_{iso} = Q\rho_C$$

where Q is a constant equal to 106MHz. The spin density at C(2) of the quinone is therefore 0.094 in *C. reinhardtii*, compared to 0.096 in spinach. The spin density at C(2) of the *in vitro* phylloquinone anion radical is 0.073 (Rigby *et al.*, 1996). The increase in this spin density, relative to the *in vitro* phylloquinone anion radical, is 29% in *C. reinhardtii* and 31% in spinach. Both *C. reinhardtii* and spinach therefore have a similar degree of increase in the spin density at C(2) of $A_1^{\cdot -}$, compared to the *in vitro* phylloquinone anion radical.

Two hydrogen bonds are expected from the quinone, one to each oxygen. In the ENDOR spectrum of *A. variabilis* (Rigby *et al.*, 1996), one feature was seen, thought to arise from the degenerate hfc's to both oxygens of the quinone. The spectrum of *A. variabilis* grown on [methyl-d_3] methionine showed partial resolution of the feature into two features, suggesting a degree of but not complete degeneracy. This difference only reflected improved resolution of the spectrum, as these H-bonds should be the same in the two cases. Special triple spectra showed that this feature was indeed split into two components. In *C. reinhardtii*, two features are seen (numbers 1 and 2), confirming H-bonding to both quinone oxygens. The H-bond hfc's each depend on the spin density of the unpaired electron at the oxygen and the H-O distance. The increased H-bond hfc's of $A_1^{\cdot -}$, relative to the *in vitro* phylloquinone anion radical, reflect decreased O-H distances and/or increased spin density at the $A_1^{\cdot -}$ quinone oxygen atoms. These two effects can be related: changes in the O-H distance affect the polarisation of the C=O bond and the spin density at the oxygen.

There is a greater inequality between the two H-bond hfc's in *C. reinhardtii*, compared to spinach or *A. variabilis*. This reflects a reduced O-H distance and/or increased spin density at one of the quinone oxygens, and an increased O-H distance and/or reduced spin density the other quinone oxygen. A similar situation is seen in *H. chlorum* (Muhiuddin *et al.*, 1999). These results suggest a less symmetric H-bonding environment of $A_1^{\cdot -}$ in *C. reinhardtii*, compared to spinach or *A. variabilis*. H-bonding is seen to be important in determining the electronic structure of the quinone *in vivo*.

Other features seen in the ENDOR spectrum of *A. variabilis* (Rigby *et al.*, 1996) are absent in the in the spectrum of *C. reinhardtii*, for example the weak features which were assigned to the $A_{\perp}$ and $A_{||}$ components of a hfc to a methylene proton on C(3) of the quinone (figure 3.9). The *C. reinhardtii* preparations are probably contaminated with paramagnetic metal ions. A better PSI detergent preparation could possibly allow recording at higher power and resolution of more spectral features.

The spectrum of $A_1^{\cdot -}$ in wild type *C. reinhardtii* has the features expected from previous studies. There are only small differences between *C. reinhardtii* and spinach. H-bonding is seen to be important in determining the electronic structure of the quinone *in vivo*. Conserved histidine residues have been identified in PsaA and PsaB which are possible candidates for the formation of H-bonds to the quinone (Webber and Bingham, 1998).

The spectra and the hfc's are virtually identical between *C. reinhardtii* wild type and D576L. This indicates that the quinone binding site is structurally unchanged by the mutation. The remarkably low redox potential of A_1 is due to the

influence of the protein environment on electronic structure. Any changes would be detected by ENDOR. The redox potential of A_1 is therefore likely to be unchanged in D576L.

We attempted to obtain ENDOR spectra of $A_1^{\cdot-}$ in PSI samples of the four revertant mutants. Unfortunately, useful spectra could not be obtained due to unacceptably low signal-to-noise ratios caused by contamination.

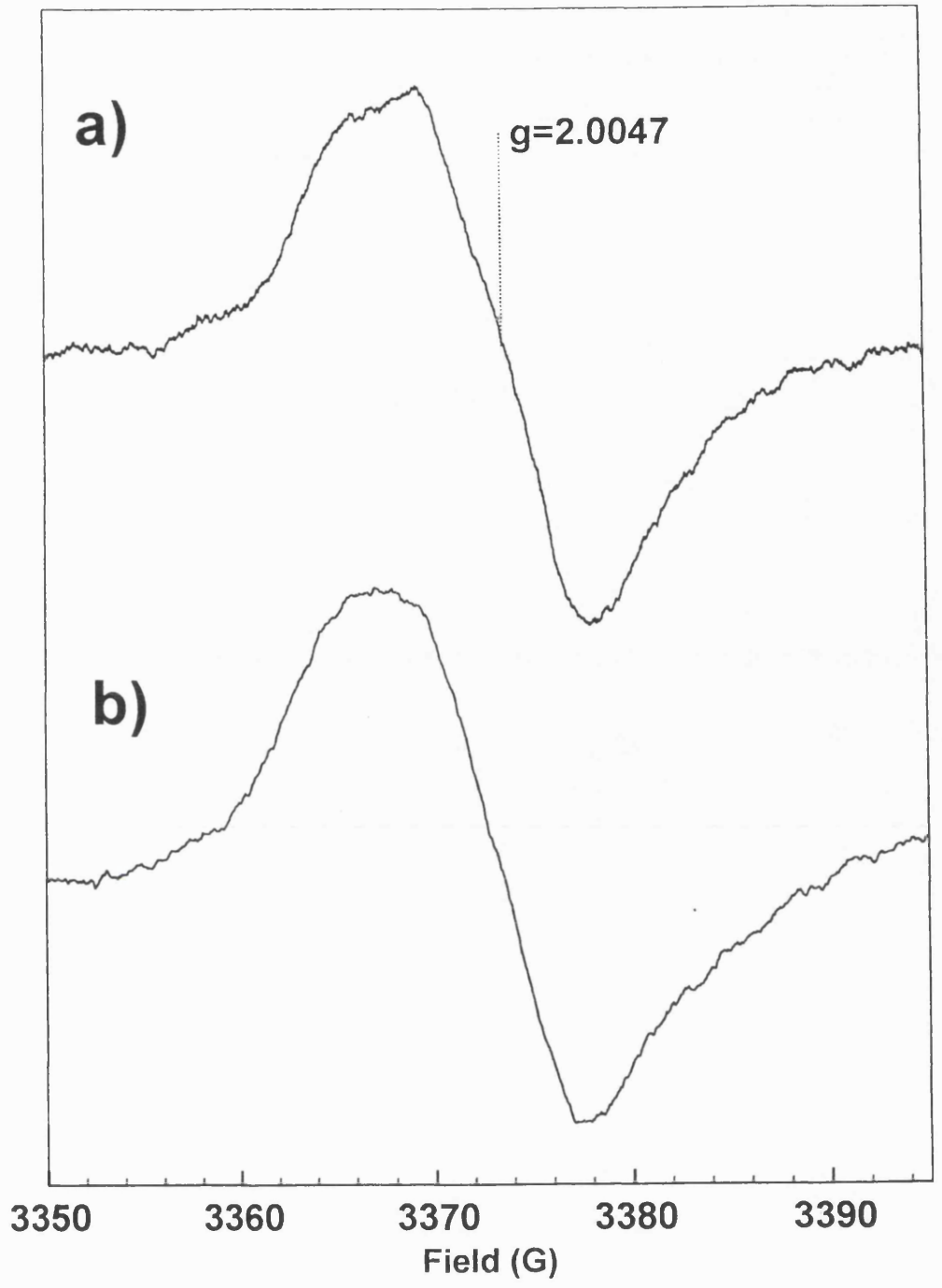

Figure 3.7

CW EPR Spectra of $A_1^{\cdot -}$ in Digitonin PSI of Spinach and *C. reinhardtii*.

EPR spectra in the g=2.00 region of *C. reinhardtii* and spinach digitonin photosystem I particles showing the signal due to photoaccumulation of $A_1^{\cdot -}$. Samples were illuminated at 205K for 2 minutes, followed by freezing in liquid nitrogen. Spectra were recorded before and after illumination. The spectra presented are light-minus-dark difference spectra. Samples were reduced with 0.2% sodium dithionite at pH 8.0 in darkness for 30 minutes and then frozen in liquid nitrogen in darkness. (a) spinach (b) *C. reinhardtii* wild type. EPR conditions: microwave power 100μW; modulation width (a) 0.17mT, (b) 0.2mT; temperature 60K.

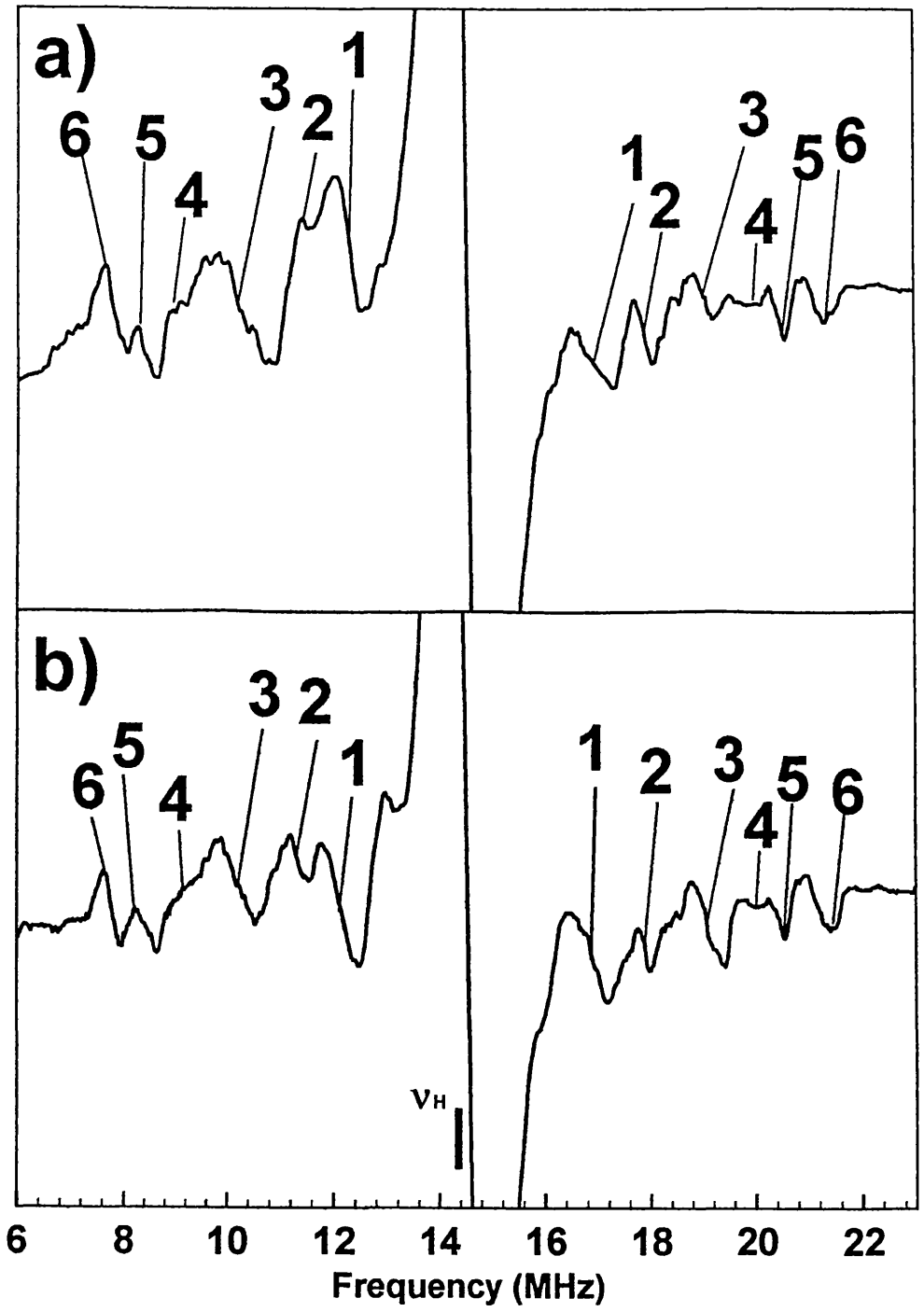

Figure 3.8

ENDOR Spectra of $A_1^{\bullet -}$ in Digitonin PSI from *C. reinhardtii* wild type and site-directed mutant D576L. ENDOR spectra of $A_1^{\bullet -}$ in *C. reinhardtii* (a) wild type and (b) D576L digitonin photosystem I particles. The spectra presented are the sum of 200 scans. Numbers refer to the features assigned in table 3.6. Samples were reduced with 0.2% sodium dithionite at pH 8.0 in darkness for 30 minutes and then frozen in liquid nirtogen in darkness. $A_1^{\bullet -}$ was photoaccumulated by illumination at 205K for 2 minutes, followed by freezing in liquid nitrogen. ENDOR conditions: microwave power 3.0mW; r.f. power 100W; r.f. modulation depth 177kHz; scan time 84s; temperature 90K.

Feature	Hyperfine coupling (MHz)					Assignment
	Wild type	**D576L**	**Spinach**	**H. chlorum**	**C. limicola**	
1	-4.6	-4.7	-5.2	-5.4	-5.0	H-bond $A_{\perp}$
2	-6.4	-6.6	-6.0	-6.2	-6.5	H-bond $A_{\perp}$
3	8.8	8.8	9.0	8.8	8.6	2-Methyl $A_{\perp}$
4	10.9	11.0	-	11.2	10.0	H-bond $A_{\|\|}$
5	12.3	12.3	12.6	12.3	12.2	2-Methyl $A_{\|\|}$
6	13.7	13.8	13.4	-	13.0	H-bond $A_{\|\|}$

Table 3.6

ENDOR Spectroscopy of $A_1^{\bullet -}$ in *C. reinhardtii*: Hyperfine Coupling Constants and Resonance Assignments

All samples are of digitonin PSI.

All samples were reduced with 0.2% w/v sodium dithionite.

The spectroscopic method is detailed in section 2.16.

Values of hyperfine coupling constants have an accuracy of ±0.1MHz.

Data for the radical in spinach are from Rigby *et al.* (1996).

Data for the menaquinone radical in *Heliobacterium Chlorum* and *Chlorobium limicola* are from Muhiuddin *et al.* (1999).

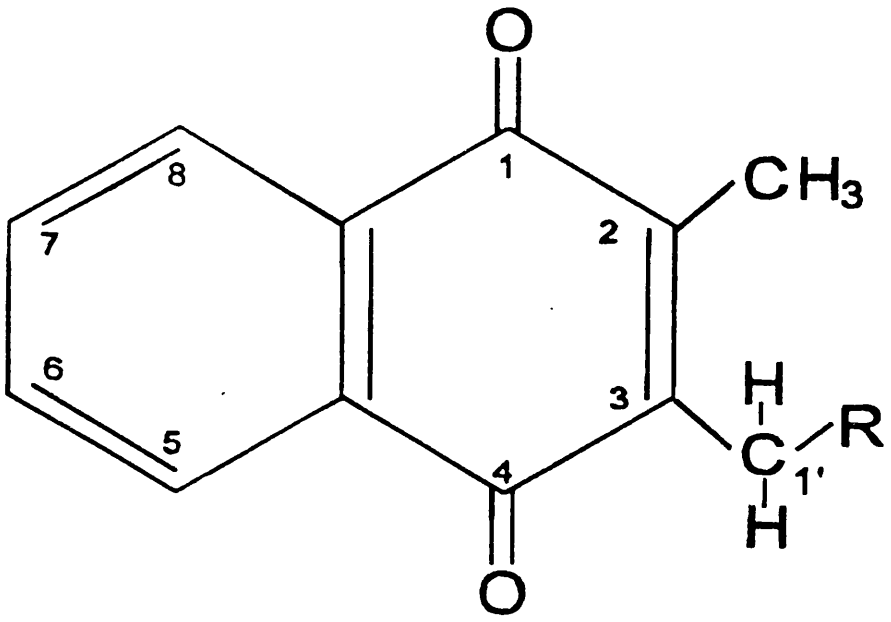

Figure 3.9

The Structure of Phylloquinone

The structure of phylloquinone is shown, with a carbon atom numbering scheme. R is $CHCCH_3CH_2(CH_2CH_2CHCH_3CH_2)_3H$. [Diagram from Rigby *et al.* (1996).]

4.0 DISCUSSION

4.1 Electron Donation to PSI of *C. reinhardtii* in Biochemical Assays of Electron Transport

In this study, the results of biochemical assays of electron transport in *C. reinhardtii* are presented. The values of the wild type rates of $NADP^+$ photoreduction and methyl viologen photoreduction are a good deal lower than those seen in thylakoid membranes of other organisms.

In $NADP^+$ photoreduction assays of the cyanobacteria *Synechococcus* sp. PCC 6301 (Jung *et al.*, 1995) and *Synechocystis* sp. PCC 6803 (Xu *et al.*, 1994b), the key to high rates of $NADP^+$ photoreduction was found to be the use of a physiologically relevant electron donor. In these cases, reduced *Spirulina maxima* cytochrome c_6 was used as the electron donor. The reaction with *Synechococcus* sp. PCC 6301 worked equally well with flavodoxin from *Synechococcus* sp. PCC 7002 or with spinach ferredoxin.

The low rates seen in the results of the biochemical assays of electron transport in *C. reinhardtii* reported in this thesis are presumably due to inefficient electron donation to PSI from the artificial donor DAD. The results of Jung *et al.* (1995) suggest that the physiological relevance of the electron acceptor in the $NADP^+$ photoreduction assay is relatively unimportant.

Like cyanobacteria, *C. reinhardtii* is able to use either plastocyanin or cytochrome c_6 as a physiological electron donor. In *C. reinhardtii*, both donors are negatively charged. The efficiency of electron transfer from plastocyanin is highly sensitive to ionic strength, showing the importance of electrostatic interactions

between plastocyanin and PsaF. The efficiency of electron transfer from cytochrome c_6 is less sensitive to ionic strength (Hippler *et al.*, 1997). In a study of the PsaF-deficient 3bF strain of *C. reinhardtii*, the *in vivo* rate constant of electron transfer from plastocyanin to PSI was decreased 20-fold. However, in *in vitro* measurements, this rate was decreased 100-fold (Farah *et al.*, 1995). This difference may reflect sensitivity to differences between ionic strength between the two environments. This suggests that for future *in vitro* measurements of electron transport, the use of reduced cytochrome c_6 as an electron donor is to be recommended.

Because the rates of $NADP^+$ photoreduction reported in this thesis are highly donor-limited, they only show whether PSI in a sample is competent or incompetent in $NADP^+$ photoreduction. The differences between the wild type rates and the reduced rates reported in the D576L revertants only reflect differences in levels of assembly of PSI. They do not reflect any reductions in the efficiency of PSI electron transport, relative to wild type, that may be present in the revertants. Future experiments, conducted with a physiologically relevant electron donor, would permit reductions in the efficiency of PSI electron transport in mutants of *C. reinhardtii* to be analysed.

4.2 The Effects of Site-Directed Mutagenesis of C575 of PsaA in *C. reinhardtii*

The effects of mutation of C575 are severe. C575D does not assemble PSI. C575H and C575S have greatly reduced levels of assembly of PSI. C575H and C575S are unable to transport electrons beyond A_1^-.

C575H and C575S both contain P700 and A_1, as shown by the detection of the ESP signal of $P700^{\cdot+}/A_1^{\cdot-}$. It is possible to chemically reduce F_A and F_B in PSI

samples with sodium dithionite at pH 10, allowing detection of these centres by CW EPR. However, the non-PSI iron-sulphur centre EPR signal, seen around g=2.02 in spectra of thylakoid membranes from *C. reinhardtii*, would make the determination of the presence of F_A and F_B by chemical reduction difficult. In C575H and C575S, photoreduction of F_A and F_B is impossible, as the results from pulsed EPR at 260K show that forward electron transfer from A_1^- to F_X does not take place, blocking electron transport to F_A and F_B, if those carriers are present. F_X has been proven to be intermediate between A_1 and F_A/F_B in the pathway of electron transport through PSI (Moënne-Loccoz *et al.*, 1994). A mutant of *C. reinhardtii* with the *psaC* gene insertionally inactivated was generated by Takahashi et al (1991). This mutant did not assemble PSI at steady-state levels, due an increased rate of turnover. The insertion of the two iron-sulphur centres into PsaC is necessary for reconstitution of PsaC onto the PSI core to take place (Zhao *et al.*, 1990). Studies involving site-directed mutagenesis of F_A and F_B have also shown that these clusters are required to be intact, as 4Fe-4S clusters, for binding of PsaC to the PSI core to take place (Mehari *et al.*, 1995; Yu *et al.*, 1995b; Jung *et al.*, 1996). The findings of these studies imply that assembly of the PSI complex would not take place without the incorporation of a PsaC protein with 2 4Fe-4S clusters. PSI complexes of mutants C575H and C575S are therefore likely to contain F_A and F_B, as it is unlikely that PSI complexes would assemble otherwise. The ENDOR results presented in this thesis indicate the presence of contaminating paramagnetic metal ions in the digitonin preparations of *C. reinhardtii* PSI which were used in this study. An improved PSI detergent preparation would remove the difficulties for EPR analysis caused by the signals of the non-PSI iron sulphur centres in the thylakoid membrane of *C. reinhardtii*. The presence or absence

of F_A and F_B in mutants C575H and C575S could then be determined by EPR of detergent PSI which had been chemically reduced by sodium dithionite at pH 10.

In mutant C575H, photoreduction of 50mM methyl viologen does not take place. Spinach digitonin PSI, with PsaC removed and F_X oxidatively destroyed, is capable of reducing methyl viologen directly from A_1^-. In C575H, electron transport to A_1^- takes place, with no further forward electron transport, as shown by pulsed EPR at 260K. Site-directed mutation of either of the conserved cysteine residues of PsaB to serine in *Synechocystis* sp. PCC 6803 produces a mixed-ligand 4Fe-4S cluster. These mutants are non-photosynthetic, but reduction of F_A/F_B at low temperature may be detected by EPR (Vassiliev *et al.*, 1995). This shows that a PSI complex with a mixed-ligand 4Fe-4S F_X cluster which is not redox-active at room temperature can still photoreduce F_A/F_B at cryogenic temperatures. A 3Fe-4S F_X cluster was detected by EPR in the C565S mutant of PsaB in *Synechocystis* sp. PCC 6803 (Warren *et al.*, 1993b). However this signal was not present in freshly isolated thylakoid membranes. The 3Fe-4S F_X cluster was considered to be an artifact caused by detergent treatment. In mutant C575H of *C. reinhardtii*, no photoreduction of iron-sulphur centres is detected by low temperature EPR. Taking into account the results of the previous studies detailed above, C575H is considered not to bind an iron-sulphur centre at the F_X-binding site. Access of methyl viologen to A_1^- is structurally blocked by protein. The more hydrophobic acceptor neutral red is able to penetrate the protein and accept electrons from A_1^-. This suggests the presence of an acceptor complex (proteins PsaC, PsaD and PsaE) which blocks access of methyl viologen to A_1^-. If these proteins were not present and only a core PSI complex was

assembled, it is likely that the structural disruption around the F_X binding site caused by the mutation would allow access of methyl viologen to A_1^-.

In mutant C575S, photoreduction of 50mM methyl viologen does take place. Taken at face value, this result would suggest electron transport to F_A/F_B. However, electron transport to A_1^- takes place, with no further forward electron transport, as shown by pulsed EPR at 260K. In this mutant, methyl viologen is therefore able to accept electrons directly from A_1^-. This suggests that the C575S mutation causes greater structural disruption around the F_X binding site than does the C575H mutation. Cysteine to serine mutants of PsaB in *Synechocystis* support a 4Fe-4S cluster which is not redox-active at room temperature (Vassiliev *et al.*, 1995). However, mutant C575H of PsaA in *C. reinhardtii* does not bind an iron-sulphur centre at the F_X-binding site and C575S has even greater structural disruption in this region. It is therefore considered highly unlikely that C575S binds an iron-sulphur centre at the F_X-binding site.

Smart *et al.* (1993) generated equivalent site-directed mutants of C565 of PsaB in *Synechocystis* sp. PCC 6803. In their study, mutation to histidine was more severe than mutation to serine. The histidine mutant had a lower level of assembly of PSI and did not photoreduce F_A/F_B. The serine mutant accumulated more PSI, and photoreduction of F_A/F_B was detected. However, mutant C575S of PsaA of *C. reinhardtii*, analysed in this thesis, does not bind a F_X cluster. This is likely to reflect the greater sensitivity of PSI assembly to mutation in *C. reinhardtii*, compared to cyanobacteria. Alternatively, it could reflect a different contribution to the binding site of the F_X cluster from C575 of PsaA, compared to the equivalent residue in PsaB. The very low redox potential of F_X, compared to other 4Fe-4S clusters, suggests that

the binding of this centre is unusual. This is the first site-directed mutagenesis study of the conserved cysteines of PsaA and the two effects cannot be differentiated.

4.3 Site-Directed Mutant D576L of PsaA and Second Site Revertants in *C. reinhardtii*

The results presented in this thesis for mutant for mutant D576L are in agreement with the results of Rodday *et al.*, who studied the importance of the intercysteinyl region of the conserved dodecapeptide sequence. Studies were performed involving chemical modification of arginine residues (Rodday *et al.*, 1993) and site directed mutagenesis of PsaB in *Synechocystis* (Rodday *et al.*, 1994) and site-directed mutagenesis of PsaB in *C. reinhardtii* (Rodday *et al.*, 1995). The results of these studies showed the importance of the intercysteinyl region of the F_X binding loops in the electrostatic interaction with PsaC. Rodday *et al.* (1995) mutated residue D562 of PsaB to asparagine in *C. reinhardtii*. This mutant did not accumulate PSI, indicating the importance of this residue, but revealing nothing about the precise function of the residue.

Mutant D576L of PsaA in *C. reinhardtii* assembles PSI, at reduced levels relative to wild type. This reduced level of assembly probably reflects the unstable binding of PsaC to the PSI core in this mutant. The incorporation of PsaC into PSI is required for stable assembly of the complex in *C. reinhardtii* (Takahashi et al., 1991). Mutation of D576 to a neutral residue destabilises the electrostatic binding of PsaC, which presumably leads to increased turnover of the complex.

The EPR spectrum of F_A/F_B is different in free and bound PsaC (Hanley *et al.*, 1992), indicating that binding to the core significantly modifies the conformation

of PsaC. Binding of PsaD also modifies the conformation of PsaC (Li *et al.*, 1991b). The low temperature electron distribution in mutant D576L is altered relative to the wild type. The electron appears to be associated with only one of the terminal iron-sulphur centres. It is impossible to discern the identity of this centre from the EPR spectrum, as the resonances are abnormal, differing from the normal resonances of either F_A or F_B. In wild type, the electron is mainly associated with F_A. In the D576L revertants, the abnormal electron distribution between F_A/F_B is retained, but the abnormal conformation of PsaC implied by this observation does not prevent photosynthetic growth. This suggests that the conformation of PsaC is not drastically altered relative to wild type. It is therefore more likely that, in D576L, the electron is associated with F_A, as association with F_B would presumably require a more extensive conformational change. The g_y resonance is similar to that of wild type F_A, in support of this postulation. An interesting experiment would be to examine the effects of $HgCl_2$ on D576L. $HgCl_2$ may be used to selectively destroy centre F_B, without significant changes to the EPR spectral properties of F_A. If $HgCl_2$ treatment did not change the EPR spectrum of D576L, this would indicate association of the electron with F_A.

In D576L, the rate of electron transfer from A_1^- to F_X is considerably slowed relative to wild type, as detected by pulsed EPR at 260K. There are no significant changes in the A_1 binding site in D576L, as detected by ENDOR. The altered rate must therefore be due to reduced competitiveness of the forward reaction from A_1^-, due to structural changes in the F_X binding site. This shows that residue D576 is not only important in the electrostatic interaction with PsaC. The residue is also important in maintaining the structural integrity of the F_X binding site. Rodday *et al.*

(1995) suggest that the conserved aspartate residue contributes to the stability of the F_X cluster, possibly by hydrogen bonding to the adjacent cysteine ligand. The results presented in this thesis are in agreement with this hypothesis.

However, although the efficiency of electron transfer from A_1^- to F_X is lowered, forward electron transfer is not abolished. The rate of decay of the quinone radical is much slower in mutants C575H and C575S which do not bind F_X. Vassiliev *et al.* (1995) described cysteine to serine mutants of PsaB in Synechocystis which bound mixed ligand 4Fe-4S clusters. These mutants were non-photosynthetic but showed low temperature photoreduction of F_A/F_B. This shows that photoreduction of F_A/F_B at cryogenic temperatures does not necessarily reflect electron transfer under physiological conditions. D576L similarly binds a F_X cluster through which electron transfer is abnormally inefficient. The characteristics of D576L are not entirely analogous, however. The results of the assays of methyl viologen photoreduction suggest that D576L is capable of photoreduction of F_A/F_B at room temperature. At 50mM, methyl viologen can only accept electrons from the F_X-distal iron-sulphur cluster (Vassiliev *et al.*, 1998). Structural disruption can permit methyl viologen to accept electrons from A_1^- or F_X^-. The donation of electrons directly from A_1^- to methyl viologen in D576L is highly unlikely. C575H has a PSI complex which is more severely altered structurally, as it does not bind F_X. PSI in C575H cannot donate electrons to methyl viologen. The reduced efficiency of electron transfer from A_1^- to F_X would be expected to severely reduce the quantum efficiency of electron transport through PSI, but, if the methyl viologen results do truly show room-temperature photoreduction of the terminal iron-sulphur clusters, there may additionally be a lesion in electron transport between F_A/F_B and

ferredoxin/flavodoxin. Binding of PsaD is necessary for PsaC to assume the correct conformation (Li *et al.*, 1991b). It is therefore conceivable that incorrect binding and conformation of PsaC could also cause PsaD to assume an incorrect conformation, disrupting the binding of the soluble electron acceptors. An alternative possibility is that a very low rate of $NADP^+$ reduction does in fact occur in D576L, but is not detected due to the insensitivity of the donor-limited assay. Improved rates in this assay with use of a better electron donor would allow this hypothesis to be tested. The other alternative is that the loose binding of PsaC does in fact allow entry of methyl viologen to the reaction centre.

The question of the interaction of ferredoxin with PsaD in D576L could be tested by optical flash spectroscopy. An improved detergent preparation would be very helpful in this type of experiment. Optical flash spectroscopy would allow the presence and rate of a F_A/F_B to P700 back reaction to be determined, resolving the question of electron transfer to the terminal iron-sulphur clusters. If this reaction did occur, the degree of abolition of the back reaction by addition of ferredoxin could be analysed. Ferredoxin binding in the revertants and wild type could also be compared. Attempts could also be made to cross-link PsaD to ferredoxin in D576L. If a cross-link was not found, this would indicate an alteration in the ferredoxin binding site.

The inefficient electron transfer from A_1^- to F_X is corrected in all four revertant strains analysed, indicating the importance of a competitive rate of forward electron transfer. This is therefore a very important lesion which is relatively easily corrected. Revertants of D576L are easily generated, suggesting that a variety of amino acid changes can compensate for the primary mutation. The D576L mutation therefore does not have drastic structural effects on PSI, and this mutant is therefore

on the "borderline" of being competent in photosynthesis. One of the factors which determines the rate of electron transfer is the distance between carriers. A_1 has not been exactly located in the current 4Å crystal structure of PSI (Krauss *et al.*, 1996). The quinone is difficult to locate in the electron density map due to its small size and its similarity to aromatic amino acid side chains. A location where influence by a subunit other than PsaA or PsaB is possible. Initially, we thought that the reversion mutations could alter the location of A_1. However we have shown that the protein environment of A_1 is unchanged by the D576L mutation, probed by ENDOR. The rate of forward electron transfer at 260K is considerably slowed in D576L, although the quinone is unchanged. This must therefore be due to changes in F_X. This is the fault which is corrected in the revertants, restoring wild type rates of forward electron transfer. The ENDOR spectrum of wild type $A_1^{\cdot -}$ is also very similar to that of spinach, suggesting a high degree of evolutionary conservation of the A_1 binding site. The quinone has a very low redox potential. Correct binding is probably very important to functionality and binding is unlikely to be altered in the revertants as this would be likely to make the quinone non-functional. The 100K rate of back reaction is slightly faster in the revertants. However, this measurement was made by combining two different samples and may not be reliable. Schlodder *et al.* (1998) attribute the peculiar low temperature behaviour of PSI partly to the formation of different fractions of PSI complexes with different conformational substates. Different freezing behaviour in the second site revertants leading to the formation of conformational states different from wild type is a possible explanation for the slightly faster back reaction rate, if it is not an artifact.

Brettel (1997) suggests that the redox potentials of A_1 and F_X are very close. One of the factors which determines rate of electron transfer is the gap in free energy. Small changes in the redox potential of F_X in mutant D576L could therefore cause large changes in the rate of electron transfer from A_1^- to F_X. Parret *et al.* (1989) report that, following removal of PsaC, the redox potential of F_X is increased by 60mV. Brettel (1997) suggests possible explanations for this change in redox potential and changes in the energetics of the $P700^+/F_X^-$ pair which are caused by removal of PsaC. One of the proposed causes is conformational changes within the PSI core complex. There is some similarity between this situation and mutant D576L. The mutation could cause abnormality in the conformation of the F_X-binding region, causing a change in redox potential of F_X. The reorganisation energy around F_X may also be altered in D576L, which could affect the rate of electron transfer. The aspartate residue obviously contributes to the structural integrity of the F_X binding site, possibly by hydrogen bonding to the adjacent cysteine, as suggested by Rodday *et al* (1995). F_X has an unusual binding site as it is an interpolypeptide cluster. The very low redox potential is thought to be due to specific qualities of its binding site. Here we show that alteration to the structure of the binding site drastically reduces the efficiency of electron transfer to F_X.

In all four revertants, a fast rate of forward electron transfer is restored, implying that the structural integrity of the F_X binding site has been restored. However, this is not accompanied by the restoration of wild type EPR resonances and electron distribution of F_A/F_B. It should be noted that the ratio of electron distribution between F_A/F_B at low temperature does not reflect the room temperature ratio. In some species, F_A is more easily reduced at low temperature, for example

spinach and *C. reinhardtii*. In some species, F_B is more easily reduced at low temperature, for example barley and *Phormidium laminosum*. The species differences in the temperature dependencies of F_A and F_B may be due to the formation of different frozen conformational substates (Brettel, 1997). The restoration of electron flow to ferredoxin in the revertants without the restoration of a wild type electron distribution illustrates the principle that the ratio of electron distribution between F_A/F_B at low temperature does not reflect the room temperature ratio. It is likely that both F_A/F_B are functional for electron flow to ferredoxin to take place, although photoreduction of only one of these centres is seen at low temperature.

In the revertants, the D576L mutation is still present and PsaC has no amino acid changes, shown by DNA sequencing (Patel, 1996). PsaC is still incorrectly bound, leading to an altered conformation and altered low temperature electron distribution between F_A/F_B. This suggests that the orientation of PsaC relative to the core may have been slightly altered by the reversion mutations, altering the structure of the F_X binding loop which electrostatically interacts with PsaC. The reversion mutation is in a nuclear encoded protein, as shown by the genetic segregation of the mutation (Patel, 1996). The most likely candidate for the location of the secondary mutation is PsaD. Li *et al.* (1991b) have shown that this protein modifies the binding of PsaC to the core. Their experiments showed changes in the EPR spectral characteristics of F_A/F_B, caused by the binding of PsaD. We do not observe changes in the EPR spectra of the revertants, relative to D576L. However, a subtle alteration in the structure of PsaD may not necessarily cause changes in the EPR spectrum, whereas Li *et al.* (1991b) were examining the effects of complete absence of PsaD, which is a much more gross alteration. If ferredoxin binding is indeed impaired, it is

conceivable that in D576L, incorrect binding of PsaC could alter the conformation of PsaD. The secondary mutation could restore the correct conformation of PsaD, simultaneously restoring the integrity of the ferredoxin binding site and changing the orientation of PsaC. However, it is not proven that ferredoxin binding is altered in D576L and this may not be the case. Mutation in subunits other than PsaD could restore the integrity of the F_X binding site. PsaC, PsaD and PsaE form a structural unit. PsaE is in close association with PsaC. PsaE also maintains the structural integrity of the ferredoxin binding site (Rousseau *et al.*, 1993). There are other possibilities. PsaF has been shown to posses a membrane-spanning region which interacts with PsaE (Jansson *et al.*, 1996). PsaC stabilises the association of PsaL with the PSI complex (Mannan *et al.*, 1994), and a mutation on PsaL may therefore affect PsaC.

The exact location of the reversion mutation could be determined by reconstitution experiments. PsaD or PsaE extracted from the revertant could be reconstituted along with PsaC onto a D576L core preparation. Electron transfer in the reconstituted sample could then be analysed by pulsed EPR. Alternatively, the genes encoding the proteins could be sequenced.

REFERENCES

Adman E. T., Sieker L. C., Jensen L. H. (1976). The structure of *Peptococcus aerogenes* ferredoxin. Refinement at 2Å. *J. Biol. Chem. 251, 3801-3996.*

Andersen B., Koch B., Scheller H. V. (1992). Structural and functional analysis of the reducing side of photosystem I. *Physiol. Plant. 84, 154-161.*

Arnon D. I. (1949). Copper enzyme in isolated chloroplasts. Polyphenol oxidase in *Beta vulgaris. Plant Physiol. 24, 1-15.*

Bassi R., Soen S. Y., Frank G., Zuber H., Rochaix J.-D. (1992). Characterization of chlorophyll *a/b* proteins of photosystem I from *Chlamydomonas reinhardtii. J. Biol. Chem. 267, 25714-25721.*

Biggins J., Tanguay N. A., Frank H. A. (1989). Electron transfer reactions in photosystem I following vitamin K_1 depletion by ultraviolet radiation. *FEBS Lett., 247, 291-296.*

Bock C. H., van der Est A. J., Brettel K., Stehlik D. (1989). Nanosecond electron transfer kinetics in photosystem I as obtained from transient EPR at room temperature. *FEBS Lett., 247, 291-296.*

Bonnerjea J. R. and Evans M. C. W. (1982). Identification of multiple components in the intermediary electron carrier complex of photosystem I. *FEBS Lett. 148, 313-316.*

Bottin H. and Lagoutte B. (1992). Ferredoxin and flavodoxin from the cyanobacterium *Synechocystis* sp. PCC 6803. *Biochim. Biophys. Acta 1101, 48-57.*

Boynton J. E. and Gillham N. W. (1993). Chloroplast transformation in *Chlamydomonas. Meth. Enzymol. 217, 510-536.*

Boynton J. E., Gillham N. W., Harris E. H., Hosler J. P., Johnson A. M., Jones A. R., Randolph-Anderson B. L., Robertson D., Klein T. M., Shark K. B., Sanford J. C. (1988). Chloroplast transformation in *Chlamydomonas* with high velocity microprojectiles. *Science 240, 1534-1538.*

Brettel K. (1988). Electron transfer from A_1^- to an iron-sulphur center with $t_{1/2}$=200ns at room temperature in photosystem I. Characterisation by flash absorption spectroscopy. *FEBS Lett., 239, 93-98.*

Brettel K. (1997). Electron transfer and arrangement of the redox cofactors in photosystem I. *Biochim. Biophys. Acta 1318, 322-373.*

Brettel K. and Golbeck J. H. (1995). Spectral and kinetic characterization of electron acceptor A_1 in a photosystem I core devoid of iron-sulfur centers F_X, F_B and F_A. *Photosynth. Res. 45, 183-193.*

Brettel K. and Sétif P. (1987). Magnetic field effects on primary reactions in photosystem I. *Biochim. Biophys. Acta 893, 109-114.*

Brettel K., Leibl W., Liebl U. (1998). Electron transfer in the heliobacterial reaction centre: evidence against a quinone-type electron acceptor functioning analogous to A_1 in photosystem I. *Biochim. Biophys. Acta 1363, 175-181.*

Britt R. D., Sauer K., Klein M. P., Knaff D. B., Kriauciunas A., Yu C. A., Yu L., Malkin R. (1991). Electron spin envelope modulation spectroscopy supports the suggested coordination of two histidine ligands to the Rieske Fe-S centers of the cytochrome b_6f ccomplex of spinach and the cytochrome bc_1 complexes of *Rhodospirillum rubrum, Rhodobacter sphaeroides* R-26, and bovine heart mitochondria. *Biochemistry 30, 1982-1991.*

Brosius J. (1989). Superpolylinkers in cloning and expression vectors. *DNA 8, 759-777.*

Buchanan B. B. and Arnon D. I. (1973). Ferredoxins from photosynthetic bacteria, algae and higher plants. *Meth. Enzymol. 23, 413-440.*

Büttner M., Xie D. L., Nelson H., Pinther W., Hauska G., Nelson N. (1992). Photosynthetic reaction centre genes in green sulphur bacteria and in photosystem I are related. *Proc. Natl. Acad. Sci. USA 89, 8135-8139.*

Chitnis P. R., Xu Q., Chitnis V. P., Nechushtai R. (1995). Function and organisation of PSI polypeptides. *Photosynth. Res. 44, 23-40.*

Chitnis V. P., Jung Y. S., Albee L., Golbeck J. H., Chitnis P. R. (1996). Mutational analysis of photosystem I polypeptides. Role of PsaD and the lysyl 106 residue in the reductase activity of photosystem I. *J. Biol. Chem. 271, 11772-11780.*

Clayton R. K. (1980). *Photosynthesis: physical mechanisms and chemical patterns. Cambridge University Press.*

Cogdell R. and Malkin R. (1992). An introduction to plant and bacterial photosystems. *The photosystems: structure, function and molecular biology. Ed. J. Barber. Elsevier Science Publishers. pp. 1-13.*

Cui L., Bingham S. E., Kuhn M., Käß H., Lubitz W., Webber A. N. (1994). Site-directed mutagenesis of the conserved histidines in the helix VIII domain of PsaB impairs assembly of the PSI reaction centre without altering spectroscopic characteristics of P700. *Biochemistry 34, 1549-1558.*

Davis I. H., Heathcote P., Maclachlan D. J., Evans M. C. W. (1993). Modulation analysis of the electron spin echo signals of in vivo oxidised primary donor ^{14}N chlorophyll centres in bacterial, P870 and P960, and plant Photosystem I, P700, reaction centres. *Biochim. Biophys. Acta 1143, 183-189.*

Deisenhofer J., Epp O., Miki K., Huber R., Michel H. (1985). Structure of the protein subunits in the photosynthetic reaction centre of *Rhodopseudomonas viridis* at 3Å resolution. *Nature 318, 618-624.*

Delepelaire P. and Chua N.-H. (1979). Electrophoretic purification of chlorophyll *a/b-* protein complexes from *C. reinhardtii* and spinach and analysis of their polypeptide compositions. *J. Biol. Chem. 256, 9300-9307.*

Díaz-Quintana A., Leibl W., Bottin H., Sétif P. (1998). Electron transfer in photosystem I reaction centers follows a linear pathway in which iron-sulphur cluster F_B is the immediate donor to soluble ferredoxin. *Biochemistry 37, 3429-3439.*

Diner B. A. and Wollman F. A. (1980). Isolation of highly active photosystem II particles from a mutant of *C. reinhardtii. Eur. J. Biochem. 110, 521-526.*

Douglas S. E. (1994). Chloroplast origins and evolution. *The molecular biology of cyanobacteria. Ed. D. A. Bryant. pp. 91-118.*

Duysens L. N. M., Amesz J., Kamp B. M. (1961). Two photochemical systems in photosynthesis. *Nature 190, 510-511.*

Emerson R. (1958). The quantum yield of photosynthesis. *Ann. Rev. Plant Physiol. 9, 1-24.*

Evans E. H., Rush J. D., Johnson C. E., Evans M. C. W., Dickson D. P. E. (1981). Mössbauer spectroscopic studies of the nature of centre X of photosystem I reaction centres from the cyanobacterium *Chloroglea fritschii. Eur. J. Biochem. 118, 81-84.*

Evans M. C. W. (1977). Electron paramagnetic studies in photosynthesis. *Primary processes of photosynthesis. Ed. J. Barber. Elsevier Press. pp. 433-464.*

Evans M. C. W. and Nugent J. H. A. (1993). Structure and function of the reaction center cofactors of oxygenic organisms. *The photosynthetic reaction centre 1. Eds. J. R. Norris and J. Deisenhofer. Academic press NY. pp. 391-415.*

Evans M. C. W., Telfer A., Lord A. V. (1972). Evidence for the role of a bound ferredoxin as the primary electron acceptor of photosystem I in spinach chloroplasts. *Biochim. Biophys. Acta 267, 530-537.*

Evans M. C. W., Reeves S. G., Cammack R. (1974). Determination of the oxidation-reduction potential of the bound iron-sulphur proteins of the primary electron acceptor complex in photosystem I. *FEBS Lett., 49, 111-114.*

Evans M. C. W., Sihra C. K., Bolton J. R., Cammack R. (1975). Primary electron acceptor complex of photosystem I in spinach chloroplasts. *Nature, 256, 668-670.*

Evans M. C. W., Purton S., Patel V., Wright D., Heathcote P., Rigby S.E.J. (1999). Modification of electron transfer from the quinone electron carrier, A_1, of photosystem I in second site suppressors of a D-L change within the Fe-S_X binding site. *In press.*

Falzone C. J., Kao Y., Zhao J., MacLaughlin K. L., Bryant D. A., Lecomte J. T. J. (1994). ^{1}H and ^{15}N NMR assignments of PsaE, a photosystem I subunit from the cyanobacterium *Synechococcus* sp. Strain PCC 7002. *Biochem. 33, 6043-6051.*

Farah J., Rappaport F., Choquet Y., Joliot P., Rochaix J.-D. (1995). Isolation of a *psaF*-deficient strain of *Chlamydomonas reinhardtii*: efficient interaction of plastocyanin with the photosystem I reaction centre is mediated by the PsaF subunit. *EMBO J. 14, 4976-4984*

Fish L. E., Kück U., Bogorad L. (1985). Two partially homologous adjacent light-inducible maize chloroplast genes encoding polypeptides of the P700 chlorophyll *a*-protein complex of photosystem I. *J. Biol. Chem. 260, 1413-1421.*

Fromme P. (1996). Structure and function of photosystem I. *Curr. Op. Struct. Biol. 4, 473-484.*

Fujii T., Yokoyama E.-I., Inoue K., Sakurai H. (1990). The sites of electron donation of photosystem I to methyl viologen. *Biochim. Biophys. Acta 1015, 41-48.*

Gaffron H. (1940). Carbon dioxide reduction with molecular hydrogen in green algae. *Am. J. Bot. 27, 273-283.*

Gleiter. H. M., Haag E., Shen J.-R., Eaton-Rye J., Seeliger A. G., Inoue Y., Vermaas W. F. J., Renger G. (1995). Involvement of the CP47 protein in stabilisation and photoinactivation of a functional water-oxidising complex in the cyanobacterium *Synechocystis* sp. PCC6803. *Biochemistry 34, 6847-6856.*

Green B. R. (1988). The chlorophyll-protein complexes of higher plant photosynthetic membranes or just what green band is that? *Photosynth. Res. 15, 3-32.*

Golbeck J. H. (1992). Structure and function of Photosystem I. *Ann. Rev. Plant Physiol. Plant Molec. Biol. 43, 293-324.*

Golbeck J. H. and Bryant D. A (1991). Photosystem I. *Current Topics in Bioenergetics 16, Academic Press Inc., pp.83-177.*

Golbeck, J. H., Parret K. G., Mehari, T., Jones, K. L., Brand, J. (1988). Isolation of the intact photosystem I reaction centre core containing P700 and iron-sulphur center F_X. *FEBS Lett. 228, 268-272.*

Goldschmidt-Clermont M. (1991). Transgenic expression of aminoglycoside adenine transferase in the chloroplast: a selectable marker for site-directed transformation of Chlamydomonas. *Nuc. Acids Res. 19, 4083-4089.*

Hales B. J. and Case E. E. (1981). Immobilized radicals IV. Biological semiquinone anions and neutral semuquinones. *Biochim. Biophys. Acta 637, 291-302.*

Hallahan B. J., Purton S., Ivison A., Wright D., Evans M. C. W. (1995). Analysis of the proposed Fe-S_X binding region of photosystem I by site directed mutation of *psaA* in *Chlamydomonas reinhardtii. Photosynth. Res. 46, 257-264.*

Hanley J. A., Kear J., Bredenkamp G., Heathcote P., Evans M. C. W. (1992). Biochemical evidence for the role of the bound iron-sulphur centres A and B in NADP reduction by photosystem I. *Biochim. Biophys. Acta 1099, 152-156.*

Hastings G., Hoshina S., Webber A. N., Blankenship R. E. (1995). Universality of energy and electron transfer processes in photosystem I. *Biochemistry 34, 15512-15522.*

Hatanaka H., Sonoike K., Hirano M., Katoh S. (1993). Small subunits of photosystem I reaction centre complexes from *Synechococcus elongatus.* I. Is the *psaF* gene product required for oxidation of cytochrome *c*-553? *Biochim. Biophys. Acta 1141, 45-51.*

Hauska G., Hurt E., Gabellini N., Lockau W. (1983). Comparative aspects of quinol-cytochrome *c* / plastocyanin oxidoreductases. *Biochim. Biophys. Acta 726, 97-133.*

He W.-Z. and Malkin R. (1994). Reconstitution of iron-sulfur center B of photosystem I damaged by mercuric chloride. *Photosynth. Res. 41, 381-388.*

Heathcote P., Hanley J. A., Evans M. C. W. (1993). Double-reduction of A_1 abolishes the EPR signal attributed to A_1^-: evidence for C_2 symmetry in the photosystem I reaction centre. *Biochim. Biophys. Acta 1144, 54-61.*

Heathcote P., Moënne-Loccoz P., Rigby S. E. J., Evans M. C. W. (1996). Photoaccumulation in photosystem I does produce a phylloquinone ($A_1^{\cdot -}$) radical. *Biochemistry 35, 6644-6650.*

Hill R. (1939). Oxygen production by isolated chloroplasts. *Proc. Roy. Soc. (London) B127, 192-210.*

Hill R. and Bendall F. (1960). Function of two cytochrome components in chloroplasts: a working hypothesis. *Nature 186, 136-137.*

Hippler M., Ratajczak R., Haehnel W. (1989). Identification of the plastocyanin binding subunit of photosystem I. *FEBS Lett. 250, 280-284.*

Hippler M., Drepper F., Farah J., Rochaix J.-D. (1997). Fast electron transfer from cytochrome c_6 and plastocyanin to photosystem I of *Chlamydomonas reinhardtii* requires PsaF. *Biochemistry 36, 6343-6349.*

Hippler M., Drepper F., Haehnel W., Rochaix J.-D. (1998). The N-terminal domain of PsaF: precise recognition site for binding and fast electron transfer from cytochrome c_6 and plastocyanin to photosystem I of *Chlamydomonas reinhardtii. Proc. Natl. Acad. Sci. USA 95, 7339-7344.*

Hiyama T. and Ke B. (1971). A further study of P430: a possible primary electron acceptor of photosystem I. *Arch. Biochem. Biophys. 147, 99-108.*

Hurt E. C. and Hauska G. (1984). Purification of membrane-bound cytochromes and a photoactive P840 protein complex of the green sulphur bacterium *Chlorobium limnicola* f. *thiosulfatophilum. FEBS Lett. 168, 149-154.*

Itoh S., Iwaki M., Ikegami I. (1987). Extraction of vitamin K_1 from photosystem I particles by diether treatment and its effects on the A_1^- EPR signal and system I photochemistry. *Biochim. Biophys. Acta 893, 508-516.*

Jagendorf A., T. and Uribe E. (1966). ATP formation caused by acid-base transition of spinach chloroplasts. *Proc. Natl. Acad. Sci. USA 55, 170-177.*

Jansson S. (1994). The light-harvesting chlorophyll *a/b*-binding proteins. *Biochim. Biophys. Acta 1184, 1-19.*

Jansson S., Andersen B., Scheller H. V. (1996). Nearest-neighbor analysis of higher-plant photosystem I holocomplex. *Plant Physiol. 112, 409-420.*

Jekow P., Fromme P., Witt H. T., Saenger W. (1995). Photosystem I from *Synechococcus elongatus*: preparation and crystallisation of monomers with varying subunit compositions. *Biochim. Biophys. Acta 1229, 1115-1120.*

Jung Y.-S., Yu L., Golbeck J. H. (1995). Reconstitution of iron-sulphur center F_B results in complete restoration of $NADP^+$ photoreduction in Hg-treated photosystem I from I *Synechococcus* sp. PCC 6301. *Photosynth. Res. 46, 249-255.*

Jung Y.-S., Vassiliev I. R., Qiao F., Yang F., Bryant D. A., Golbeck J. H. (1996). Modified ligands to F_A and F_B in photosystem I. Proposed chemical rescue of a [4Fe-4S] cluster with an external thiolate in alanine glycine and serine mutants of PsaC. *J. Biol. Chem. 270, 31135-31144.*

Käβ H., Bittersman-Weidlich E., Andreasson L.-E., Bönigk B., Lubitz W. (1995). ENDOR and ESEEM of the ^{15}N labelled radical cations of chlorophyll *a* and the primary donor P700 in photosystem I. *Chem. Phys. 194, 419-432.*

Kindle K. L. and Sodeinde O. A. (1994). Nuclear and Chloroplast transformation in *Chlamydomonas reinhardtii*: strategies for genetic manipulation and gene expression. *J. App. Phycol. 6, 231-238.*

Kindle K. L., Richards K. L., Stern D. B. (1991). Engineering the chloroplast genome: Techniques and capabilities for chloroplast transformation in *Chlamydomonas reinhardtii. Proc. Natl. Acad. Sci. USA 88, 1721-1725.*

Kleinherenbrink F. A. M., Ikegami I., Hiraishi A., Otte S. C. M., Amesz J. (1993). Electron transfer in menaquinone-depleted membranes of *Heliobacterium chlorum. Biochim. Biophys. Acta 1142, 69-73*

Klughammer C., Pace R. J. (1997). Photoreduction of the secondary photosystem I electron acceptor vitamin K_1 in intact spinach chloroplasts and cyanobacteria in vivo. *Biochim. Biophys. Acta 1318, 133-144.*

Kössel H., Döry I., Igloi G., Maier R. (1990). A leucine zipper motif in PSI. *Plant Mol. Biol. 15, 497-499.*

Koulougliotis D., Innes J. B., Brudvig G.W. (1994). Location of chlorophyll Z in photosystem II. *Biochemistry 33, 11814-11822.*

Krauss N., Schubert W.-D., Klukas O., Fromme P., Witt H. T., Saenger W. (1996). Photosystem I of photosynthesis at $4A^{o}$ represents the first structural model of a joint photosynthetic reaction centre and core antenna system. *Nat. Struct. Biol. 3, 965-973.*

Kruip J., Boekema E. J., Bald D., Boonstra A. F., Rögner M. (1993). Isolation and structural characterisation of monomeric and trimeric photosystem I complexes ($P700.F_A/F_B$ and $P700.F_X$) from the cyanobacterium *Synechocystis PCC 6803. J. Biol. Chem. 268, 23353-23360.*

Kück U., Choquet Y., Schneider M., Dron M., Bennoun P. (1987). Structural and transcriptional analysis of two homologous genes for the P700 chlorophyll *a*-apoproteins in *Chlamydomonas reinhardtii*: evidence for in vivo trans-splicing. *EMBO J. 6, 2185-2195.*

Landschulz W. H., Johnson P. F., McKnight S. L. (1988). The leucine zipper: a hypothetical structure common to a new class of DNA binding proteins. *Science 240, 1759-1764.*

Lee H., Bingham S. E., Webber A. N. (1996). Site-directed mutagenesis and analysis of second-site revertants indicates a requirement for C-terminal amino acids of PsaB for stable assembly of the photosystem I complex in *Chlamydomonas reinhardtii. Photochem. Photobiol. 64, 46-52.*

Leibl W., Toupance B., Breton J. (1995). Photoelectric characterization of forward electron transfer to iron-sulphur centers in photosystem I. *Biochemistry 34, 10237-10244.*

Lelong C., Sétif P., Lagoutte B., Bottin H. (1994). Identification of the amino acids involved in the functional interaction between photosystem I and ferredoxin from *Synechocystis* sp. PCC 6803 by chemical cross-linking. *J. Biol. Chem. 269, 10034-10039.*

Li N., Warren P. V., Golbeck J. H., Frank G., Zuber H., Bryant D. A. (1991a). Polypeptide composition of the photosystem I complex and the photosystem I core protein from *Synechococcus* sp. PCC 6301. *Biochim. Biophys. Acta 1059, 215-225.*

Li N., Zhao, J. D., Warren P. V., Warden J. T., Bryant D. A., Golbeck J. H. (1991b). PsaD is required for the stable binding of PsaC to the photosystem I core protein of *Synechococcus* sp. PCC 6301. *Biochemistry 30, 7863-7872.*

Liebl, U., Mockensturm-Wilson, M., Trost, J. T., Brune, D. C., Blankenship, R. E., Vermaas, W. (1993). Single core polypeptides in the reaction centre of the photosynthetic bacterium *Heliobacillus mobilis* - structural implications and relations to other photosystems. *Proc. Natl. Acad. Sci. USA 90, 7124-7128.*

Lin S., Chiou H.-C., Blankenship R. E. (1995). Secondary electron transfer processes in membranes of *Heliobacillus mobilis. Biochemistry 34, 12761-12767.*

Lockau W. and Nitschke W. (1993). Photosystem I and its bacterial counterparts. *Physiol. Plant. 88, 372-381.*

Lüneberg J., Fromme P., Jekow P., Schlodder E. (1994). Spectroscopic characterisation of PSI core complexes from thermophilic *Synechococcus* sp.. Identical reoxidation kinetics of A_1^- before and after removal of the iron-sulphur-clusters F_A and F_B. *FEBS Lett. 338, 197-202.*

Mac M., Tang X.-S., Diner B. A., McCracken J., Babcock G. T. (1996). Identification of histidine as an axial ligand to $P700^+$. *Biochemistry 35, 13288-13293.*

Malkin R. (1986). On the function of two vitamin K_1 molecules in the PSI electron acceptor complex. *FEBS Lett. 208, 343-346.*

Maniatis, T., Frisch, E. F., Sambrook, J. (1989). *Molecular cloning: a laboratory manual. Cold Spring Harbour Laboratory Press, Cold Spring Harbour, NY.*

Mannan, R. M, Pakrasi H. M., Sonoike K. (1994). The PsaC protein is necessary for the stable association of the PsaD, PsaE, and PsaL proteins in the photosystem I complex: analysis of a cyanobacterial mutant strain. *Arch. Biochem. Biophys. 315, 68-73.*

Mansfield R. W. and Evans M. C. W. (1986). UV optical difference spectrum associated with the reduction of electron acceptor A_1 in photosystem I of higher plants. *FEBS Lett. 203, 225-229.*

Mansfield, R. W. and Evans, M. C. W. (1988). EPR characteristics of the electron acceptors A_0, A_1 and (iron-sulphur)$_X$ in digitonin and Triton X-100 solubilised pea photosystem I. *Isr. J. Chem. 28, 97-102.*

Markwell J. P., Thornber J. P., Boggs R. T. (1979). Higher plant chloroplasts: evidence that all the chlorophyll exists as chlorophyll-protein complexes. *Proc. Natl. Acad. Sci. USA 76, 1233-1235.*

Mathis P., Ikegami I., Sétif P. (1988). Nanosecond flash studies of the absorption spectrum of the photosystem I primary acceptor A_0. *Photosynth. Res. 16, 203-210.*

McDermott A. E., Yachandra V. K., Guiles R. D., Sauer K., Parret K. G., Golbeck J. H. (1989). An EXAFS structural study of F_X, the low potential Fe-S center in photosystem I. *Biochemistry 28, 8056-8059.*

Mehari T., Parret K. G., Warren P., Golbeck J. H. (1991). Reconstitution of the iron-sulphur clusters in the isolated F_A/F_B protein: ESR characterization of same-species and cross-species photosystem I complexes. *Biochim. Biophys. Acta 1056, 139-148.*

Mehari T., Qiao F., Scott M. P., Nellis D. F., Zhao J., Bryant D. A., Golbeck J. H. (1995). Modified ligands to F_A and F_B in photosystem I. I. Structural constraints for the formation of iron-sulphur clusters in free and rebound PsaC. *J. Biol. Chem. 270, 28108-28117.*

Miller A.-F. and Brudvig G. W. (1991). A guide to electron paramagnetic resonance spectroscopy of photosystem II membranes. *Biochim. Biophys. Acta 1056, 1-18.*

Mitchell P. (1961). Coupling of phosphorylation to electron and hydrogen transfer by a chemi-osmotic type of mechanism. *Nature 191, 144-148.*

Moënne-Loccoz P., Heathcote P., Maclachlan D. J., Berry M. C., Davis I. H., Evans M. C. W. (1994). Path of electron transfer in photosystem I: direct evidence of forward electron transfer fron A_1 to Fe-S_X. *Biochemistry 33, 10037-10042.*

Moulis J.-M., Davasse V., Gollinelli M.-P., Meyer J., Quinkal I. (1996). The coordination sphere of iron-sulphur clusters: lessons from site-directed mutagenesis experiments. *J. Bioinorg. Chem. 1, 2-14.*

Muhiuddin I., P., Rigby S. E. J., Evans M. C. W., Amesz J., Heathcote P. (1999). ENDOR and special TRIPLE resonance spectroscopy of photoaccumulated semiquinone electron acceptors in the reaction centres of green sulphur bacteria and heliobacteria. *In Press.*

Mühlenhoff U., Kruip J., Bryant D. A., Rögner M., Sétif P., Boekema E. (1996). Characterisation of a redox-active cross-linked complex between photosystem I and its physiological acceptor flavodoxin. *EMBO J. 15, 488-497.*

Naver H., Scott M. P., Golbeck J. H., Møller B. L., Scheller H. V. (1996). Reconstitution of barley photsystem I with modified PSI-C allows identification of domains interacting with PSI-D and PSI-A/B. *J. Biol. Chem. 271, 8996-9001.*

Nitschke W. and Rutherford W. (1991). Photosynthetic reaction centres: variations on a common theme?. *Trends Biochem. Sci. 16, 241-245.*

Nitschke W., Feiler U., Rutherford W. (1990a). Photosynthetic reaction centre of green sulphur bacteria studied by EPR. *Biochemistry 29, 3834-3842.*

Nitschke W., Sétif P., Liebl U., Feiler U., Rutherford A. W. (1990b). Reaction centre photochemistry of *Heliobacterium chlorum. Biochemistry 29, 11079-11088.*

Nugent J. H. A. (1996). Oxygenic photosynthesis: electron transfer in PSI and PSII. *Eur. J. Biochem. 237, 519-531.*

Nuijs A. M, van Dorssen R. J., Duysens L. N. M., Amesz J. (1985a). Excited states and primary photochemical reactions in the photosynthetic bacterium *Heliobacterium chlorum. Proc. Natl. Acad. Sci. USA 82, 6865-6868.*

Nuijs A. M., Vasmel H., Joppe H. L. P., Duysens L. N. M., Amesz J. (1985b). Excited states and primary charge separation in the pigment system of the green photosynthetic bacterium *Procochloris aestuarii* as studied by picosecond absorbance difference spectroscopy. *Biochim. Biophys. Acta 807, 24-34.*

Nuijs A. M., Shuvalov V. A., van Gorkom H. J., Plijter J. J., Duysens L. N. M. (1986). Picosecond absorbance difference spectroscopy on the primary reactions and the antenna-excited states in photosystem I particles. *Biochim. Biophys. Acta 850, 310-318.*

Oh-oka H., Takahashi Y., Kuriyama K., Saeki K., Matsubara H. (1988a). The protein responsible for centre A/B in spinach photosystem I: isolation with iron-sulphur cluster(s) and complete sequence analysis. *J. Biochem. 103, 962-968.*

Oh-oka H., Takahashi Y., Matsubara H., Itoh S. (1988b). EPR studies of a 9kDa polypeptide with an iron-sulphur cluster(s) isolated from photosystem I complex by *n*-butanol extraction. *FEBS Lett. 234, 291-294.*

Oh-oka H., Takahashi Y., Matsubara H. (1989). Topological considerations of the 9-kDa polypeptide which contains centers A and B, associated with the 14- and 19-kDa polypeptides in the photosystem I complex of spinach. *Plant Cell Physiol. 30, 869-875.*

Oh-oka H., Itoh S., Saeki K., Takahashi Y., Matsubara H. (1991). F_A/F_B protein from the spinach photosystem I complex: isolation in a native state and some properties of the iron-sulphur clusters. *Plant Cell Physiol. 32, 11-17.*

Parret K. G., Mehari T., Warren P., Golbeck J. H. (1989). Purification and properties of the intact P700 and F_X-containing photosystem I core protein. *Biochim. Biophys. Acta 973, 324-332.*

Parret K. G., Mehari T., Golbeck J. H. (1990). Resolution and reconstitution of the cyanobacterial photosystem I complex. *Biochim. Biophys. Acta 1015, 341-352.*

Patel V. (1996). Analysis of Photosystem I mutants in *Chlamydomonas reinhardtii. Ph.D Thesis, University College London.*

Petrouleas V., Brand J. J., Parret K. G., Golbeck J. H. (1989). A Mössbauer analysis of the low-potential iron-sulphur center in photosystem I. Spectroscopic evidence that F_X is a 4Fe-S cluster. *Biochemistry 28, 8980-8983.*

Przibilla E., Heiss S., Johanningmeier J., Trebst A. (1991). Site-specific mutagenesis of the D1 subunit of photosystem II in wild type *Chlamydomonas. Plant Cell 3, 169-174.*

Rigby S. E. J., Nugent J. H. A., O'Malley P. J. O. (1994). ENDOR and special triple resonance studies of chlorophyll cation radicals in photosystem 2. *Biochemistry 33, 10043-10050.*

Rigby S. E. J., Evans M. C. W., Heathcote P. (1996). ENDOR and special triple resonance spectroscopy of $A_1^{\cdot -}$ of photosystem I. *Biochemistry 35, 6651-6656.*

Rochaix J. D., Mayfield S., Goldschmidt-Clermont M., Erickson J. (1988). Molecular biology of *Chlamydomonas. Plant Molecular biology, A Practical Approach. Ed. C. H. Shaw. IRL Press of Oxford. pp.253-275.*

Rodday S. M., Sung-Soo J., Biggins J. (1993). Interaction of the F_A/F_B containing subunit with the photosystem I core heterodimer: evidence for the functional involvement of a domain containing arginine residues. *Photosynth. Res. 36, 1-9.*

Rodday S. M., Schultz R., McIntosh L., Biggins J. (1994). Structure-function studies on the interaction of PsaC with the PSI heterodimer. *Photosynth. Res. 42, 185-190.*

Rodday S. M., Weber A. N., Bingham S. E., Biggins J. (1995). Evidence that the F_X domain in PSI interacts with the subunits PsaC: site directed changes in PsaB destabilize the subunit interaction in *Chlamydomonas reinhardtii. Biochemistry 34, 6328-6334.*

Rodday S. M., Do L. T., Chynwat V., Frank H. A., Biggins J. (1996). Site-directed mutagenesis of the subunit PsaC establishes a surface-exposed domain interacting with the photosystem I core binding site. *Biochemistry 35, 11832-11838.*

Rousseau F., Sétif P., Lagoutte B. (1993). Evidence for the involvement of the PSI-E subunit in the reduction of ferredoxin by photosystem I. *EMBO J. 12, 1755-1765.*

Ruffle, S. V., Donnelly, D., Blundell, T. L., Nugent, J. H. A. (1992). A three-dimensional model of the photosystem II reaction centre of *Pisum sativum. Photosynth. Res. 34, 287-300.*

Rutherford A. W. and Sétif P. (1990). Orientation of P700, the primary electron donor of photosystem I. *Biochim. Biophys. Acta 1019, 128-132.*

Sakurai H., Inoue K., Fujii T., Mathis P. (1991). Effects of selective destruction of iron-sulfur center B on electron transfer and charge recombination in photosystem I. *Photosynth. Res. 27, 65-71.*

Scheller H. V., Naver H., Møller B. L. (1997). Molecular aspects of photosystem I. *Physiol. Plant. 100, 842-851.*

Schlodder E., Falkenberg, K., Gergeleit, M., Brettel, K. (1998). Temperature dependence of forward and reverse electron transfer from A_1^-, the reduced secondary electron acceptor in photosystem I. *Biochemistry 37, 9466-9476.*

Schluchter W. M., Shen G., Zhao J., Bryant D. A. (1996). Characterization of *psaI* and *psaL* mutants of *Synechococcus* sp. strain PCC 7002: A new model for state transitions in cyanobacteria. *Photochem. Photobiol. 64, 53-66.*

Schmidt C. L. and Malkin R. (1993). Low molecular weight subunits associated with the cytochrome b_6f complexes from spinach and *Chlamydomonas reinhardtii. Photosynth. Res. 38, 73-81.*

Sétif P, and Bottin H. (1989). Identification of electron-transfer reactions involving the acceptor A_1 of photosystem I at room temperature. *Biochemistry 28, 2689-2697.*

Shin M. (1973). Ferredoxin-NADP reductase from spinach. *Meth. Enzymol. 23, 440-447.*

Smart L. B., Warren P. V., Golbeck J. H., McIntosh L. (1993). Mutational analysis of the structure and biogenesis of the photosystem I reaction centre in the cyanobacterium *Synechocystis* sp. PCC6803. *Proc. Natl. Acad. Sci. USA 90, 1132-1136.*

Snyder L. B., Rustandi R. R., Biggins J., Norris J. R., Thurnauer M. C. (1991). Direct assignment of vitamin K_1 as the secondary acceptor A_1 of photosystem I. *Proc. Natl. Acad. Sci. USA 88, 9895-9896.*

Sonoike K., Hatanaka H., Katoh S. (1993). Small subunits of PSI reaction centre complexes from *Synechococcus elongatus* II. The *psaE* gene product has a role to promote interaction between terminal electron acceptor and ferredoxin. *Biochim. Biophys. Acta 1141, 52-57.*

Takahashi Y., Goldschmidt-Clermont M., Soen S.-Y., Franzén L. G., Rochaix J.-D. (1991). Directed chloroplast transformation in *Chlamydomonas reinhardtii*: insertional activation of the *psaC* gene encoding the iron sulfur protein destabilizes photosystem I. *EMBO J. 10, 2033-2040.*

Terashima I., Funayama S., Sonoike K. (1994). The site of photoinhibition in leaves of *Cucumis sativis* L. at low temperatures is photosystem I, not photosystem II. *Planta 193, 300-306.*

Thurnauer M. C., Bowman M. K., Norris J. R. (1979). Time-resolved electron spin echo spectroscopy applied to the study of photosynthesis. *FEBS Lett. 100, 390-312.*

Tjus S., E., Andersson B., (1991). Extrinsic polypeptides of spinach photosystem I. *Photosynth. Res. 27, 209-219.*

Trost J. T., Brune D. C., Blankenship R. E. (1992). Protein acceptor sequences and redox titrations indicate that the electron acceptors in reaction centres from heliobacteriaare similar to PSI. *Photosynth. Res. 32, 11-22.*

Van de Meent E. J., Kobayashi M., Erkelens C., van Veelen P. A., Amesz J., Watanabe T. (1991). Identification of 8′-hydroxy-chlorophyll *a* as a functional reaction centre pigment in heliobacteria. *Biochim. Biophys. Acta 1058, 356-362.*

Van de Meent E. J., Kobayashi M., Erkelens C., van Veelen P. A., Otte S. C. M., Amesz J. (1992). The nature of the primary electron acceptor in green sulphur bacteria. *Biochim. Biophys. Acta 1102, 371-378.*

Van der Est A., Bock C., Golbeck J., Brettel K., Sétif P., Stehlik D. (1994). Electron transfer from the acceptor A_1 to an iron-sulphur centers in photosystem I as studied by transient EPR spectroscopy. *Biochemistry 33, 11789-11797.*

Van der Est A., Prisner T., Bittl R., Fromme P., Lubitz W., Möbius K., Stehlik D. (1997). Time resolved X-, K-, and W-band EPR of the radical pair state $P700^{+}\cdot A1^{-}\cdot$ of photosystem I in comparison with $P865^{+}\cdot Q_A^{-}\cdot$ in bacterial reaction centres. *J. Phys. Chem 101, 1437-1443.*

Van Niel C. B. (1941). The bacterial photosyntheses and their importance for the general problem of photosynthesis. *Adv. Enzymol. 1, 263-328.*

Vassiliev I. R., Jung Y.-S., Smart L. B., Schulz R., McIntosh L., Golbeck J. H. (1995). A mixed-ligand iron-sulphur cluster ($C556S_{PsaB}$ or $C565S_{PsaB}$) in the F_X-binding site leads to a decreased quantum efficiency of electron transfer in photosystem I. *Biophys. J. 69, 1544-1553.*

Vassiliev I. R., Jung Y.-S., Yang F., Golbeck J. H. (1998). PsaC subunit of photosystem I is oriented with iron-sulphur cluster F_B as the immediate electron donor to ferredoxin and flavodoxin. *Biophys. J. 74, 2029-2035.*

Warren P. V., Parrett K. G., Warden J. T., Golbeck J. H. (1990). Characterisation of a photosystem I core containing P700 and intermediate electron acceptor A_1. *Biochemistry 29, 6545-6550.*

Warren P. V., Golbeck J. H., Warden J. T. (1993a). Charge recombination between $P700^+$ and A_1^- occurs directly to the ground state of P700 in a photosystem I core devoid of F_X, F_B and F_A. *Biochemistry 32, 849-857.*

Warren P. V., Smart L. B., McIntosh L., Golbeck J. H. (1993b). Site-directed conversion of cysteine-565 to serine in PsaB of photosystem I results in the assembly of [3Fe-4S] and [4Fe-4S] clusters in F_X. A mixed-ligand [4Fe-4S] cluster is capable of electron transfer to F_A and F_B. *Biochemistry 32, 4411-4419.*

Webber A. N. and Bingham S. E. (1998). Structure and function of photosystem I. *The Molecular Biology of Chloroplasts and Mitochondria in Chlamydomonas. Eds. J.-D. Rochaix, M. Goldschmidt-Clermont, S. Merchant. Kluwer Academic Publishers. pp. 323-348.*

Webber A. N., Gibbs P. B., Ward J. B., Bingham S. E. (1993). Site directed mutagenesis of the photosystem I reaction centre in chloroplasts. *J. Biol. Chem. 268, 12990-12995.*

Webber A. N., Su H., Bingham S. E., Käss H., Krabben L., Kuhn M., Jordan R., Schlodder E., Lubitz W. (1996). Site-directed mutations affecting the spectroscopic characteristics and midpoint potential of the primary donor in photosystem I. *Biochemistry 35, 12857-12863.*

Weber N. and Strotmann H. (1993). On the function of subunit PsaE in chloroplast Photosystem I. *Biochim. Biophys. Acta 1143, 204-210.*

Xu Q., Armbrust T. S., Guikenna J. A., Chitnis P. R. (1994a). Organisation of PSI polypeptides: a structural interaction between the PsaD and PsaL subunits. *Plant Physiol. 106, 1057-1063.*

Xu Q., Jung Y.-S., Chitnis V. P., Guikema J. A., Golbeck J. H., Chitnis P. R. (1994b). Mutational analysis of Photosystem I polypeptides in *Synechocystis* sp. PCC6803. Subunit requirements for reduction of $NADP^+$ mediated by ferredoxin and flavodoxin. *J. Biol. Chem. 269, 21512-21518.*

Yu L., Mühlenhoff U., Bryant D. A., Golbeck J. H. (1993). PsaE is required for in vivo cyclic electron flow around photosystem I in the cyanobacterium *Synechococcus* sp. PCC 7002. *Plant Physiol. 103, 171-180.*

Yu L., Smart L. B., Jung Y. S., Golbeck J., McIntosh M. (1995a). Absence of the PsaC subunit allows assembly of PSI core but prevents binding at PsaD and PsaE in *Synechocystis* sp. PCC6803. *Plant Mol. Biol. 29, 331-342.*

Yu L. A., Vassiliev I. R., Jung Y. S., Bryant D. A., Golbeck J. H. (1995b). Modified ligands to F_A and F_B in photosystem I. II. Characterisation of a mixed ligand 4Fe-4S cluster in the C51D mutant of PsaC upon rebinding to P700-F_X cores. *J. Biol. Chem. 270, 28118-28115.*

Zhao J., Warren P. V., Li N., Bryant D. A., Golbeck J. H. (1990). Reconstitution of electron transport in photosystem I with PsaC and PsaD proteins expressed in *Escherichia coli. FEBS Letts. 276, 175-180.*

Zhao J., Snyder W. B., Mühlenhoff U., Rhiel E., Warren P. V., Golbeck J. H., Bryant D. A. (1993). Cloning and characterisation of the *psaE* gene of the cyanobacterium *Synechococcus* sp. PCC 7002: characterisation of a *psaE* mutant and overproduction of the protein in *Escherichia coli. Mol. Microbiol. 9, 183-194.*

Ziegler K., Lockau W., Nitschke W. (1987). Bound electron acceptors of photosystem I. Evidence against the identity of redox center A_1 with phylloquinone. *FEBS Lett. 217, 16-20.*

Zilber A. L. and Malkin R. (1988). Ferredoxin cross-links to a 22kD subunit of photosystem I. *Plant Physiol. 88, 810-814.*